THE ROLE OF DOCOSAHEXAENOIC ACID IN REGULATION OF EPIDERMAL GROWTH FACTOR RECEPTOR ACTIVATION AND FUNCTION

A Dissertation

by

HARMONY FAITH TURK

Submitted to the Office of Graduate Studies of
Texas A&M University
in partial fulfillment of the requirements for the degree of

DOCTOR OF PHILOSOPHY

Approved by:

Chair of Committee,	Robert S. Chapkin
Committee Members,	Robert Burghardt
	Joanne Lupton
	Gonzalo Rivera
Intercollegiate Faculty Chair,	Jimmy Keeton

December 2012

Major Subject: Nutrition

Copyright 2012 Harmony Faith Turk

ABSTRACT

The epidermal growth factor receptor (EGFR) is a transmembrane receptor tyrosine kinase integral in regulating cell growth, survival, and migration. EGFR signaling, which is dependent on localization of the receptor within lipid rafts, is often hijacked during colon tumorigenesis. Previous work has found that docosahexaenoic acid (DHA) is protective against colon cancer. This fatty acid is proposed to function in part by perturbing lipid rafts and thereby altering cell signaling. The overall objective of this work was to determine whether DHA alters EGFR function and signaling.

We assessed EGFR localization and ligand-induced phosphorylation in YAMC cells treated with fatty acids. We found that DHA reduced the localization of EGFR to lipid rafts. Concomitant with altering receptor localization, DHA was found to increase EGFR phosphorylation. However, DHA paradoxically suppressed EGFR signal transduction. We found that DHA uniquely altered EGFR activity, and other long chain polyunsaturated fatty acid did not exert the same effect. We additionally observed similar effects on EGFR activation and signaling by feeding mice a diet enriched in fish oil (high in DHA), and this was attendant with reduced colon tumorigenesis.

We next probed the mechanism by which DHA enhances EGFR phosphorylation. We found that DHA facilitates receptor dimerization to increase phosphorylation. We additionally identified Ras activation as the site of perturbation of signal transduction. DHA suppressed signal transduction by both changing the

localization of EGFR within the plasma membrane and increasing receptor endocytosis and degradation.

Lastly, we extended our observations into a wounding model. Although DHA uniquely altered ligand-stimulated EGFR activity, both DHA and EPA altered EGFR transactivation and signaling upon injury. This culminated in reduced wound healing in DHA and EPA treated cells. In an animal model, we found that diets enriched in either DHA or EPA altered EGFR signaling in the colonocytes of wounded animals.

Overall, we found that DHA modifies EGFR signaling, which can be beneficial or detrimental for health depending on the disease state of an individual. These data help elucidate a mechanism by which DHA protects against colon cancer, as well as indicating a potential downside of n-3 PUFA therapy.

ACKNOWLEDGEMENTS

I would like to start by thanking my mentor, Robert Chapkin. He has been an inexhaustible source of knowledge, encouragement, and support. I will always be grateful for his guidance. I would likewise like to thank my committee members: Robert Burghardt, Joanne Lupton, and Gonzalo Rivera. Their insight and direction was indispensable in developing this body of work. I am also thankful for the aid of all of the members of the Chapkin lab. They were always willing to provide a helping hand when it was most needed.

I would also like to thank my husband, Joel Berry. I can never thank him enough for his love and understanding throughout this process. His assistance both in the lab and at home was integral in my success.

Lastly, I appreciate the love and support of my family. My parents have always inspired and encouraged me. I know that none of this would have been possible without them.

TABLE OF CONTENTS

LIST OF FIGURES

1. INTRODUCTION*

1.1 Colon cancer

Colon cancer is a major public health concern due to the high prevalence of the disease both globally and in the United States (Jemal et al., 2011). Colon cancer is third in cancer incidence in both men and women and the second leading overall cause of cancer mortality (Siegel et al., 2012), with incidence and death rates of colon cancer being higher in men than in women (Siegel et al., 2012). In the United States alone, approximately 140,000 new cases occur each year, with colon cancer causing the death of approximately 50,000 people every year (Jemal et al., 2010). Therefore, developing strategies for prevention and treatment of this pernicious disease is of the utmost importance. Both genetic and environmental factors have been indicated as mediators of colon cancer risk (Fernandez et al., 2004). Additionally, many modifiable factors, including diet, exercise, and smoking are suggested to play a role in more than 50% of colon cancer cases (Emmons et al., 2005; Lieberman et al., 2003).

1.1.1 Histological progression of colon cancer

Formation of colon cancer is hypothesized to be a multi-step process that results from a systematic accumulation of both genetic and epigenetic perturbations that cause normal colonic epithelial cells to transform and progress into cancer. Colonic transformation develops through multiple distinct histologically abnormal stages.

---

*Part of this chapter is reprinted with permission from "Membrane lipid raft organization is uniquely modified by n-3 polyunsaturated fatty acids" by Harmony F. Turk and Robert S. Chapkin, 2012. *Prostaglandins Leukotrienes and Essential Fatty Acids*,doi: 10.1016/j.plefa.2012.03.008, Copyright 2012 by Elsevier Ltd.

Aberrant crypts foci: Aberrant crypts foci (ACF), indicated as putative biomarkers of colonic carcinogenesis, are very early, microscopic lesions composed of hyperplastic epithelium(Takayama et al., 1998). It currently remains unclear whether ACF are precursors for colon cancer, but many studies have shown that ACF incidence increases with increased risk factors for colon cancer (Rudolph et al., 2005).

Polyps: Polyps are macroscopic growths of hyperplastic or dysplastic cells that can be observed in the colon (Kinzler and Vogelstein, 2002). Some polyps are innocuous, whereas others can develop into cancer. Polyps are classified as either hyperplastic, adenomatous, or serrated (Noffsinger, 2009). Hyperplastic polyps are traditionally classified as benign lesions. However, it has been clearly demonstrated that adenomatous polyps, or adenomas, can develop into carcinomas subsequent to a well-established accumulation of molecular alterations (Vogelstein et al., 1988; Vogelstein et al., 1989). Recently, it has been shown that serrated polyps can also serve as precursors to colon cancer. The molecular alterations that contribute to this pathway of tumorigenesis, termed the serrated neoplasia pathway, are distinct from those affiliated with the adenoma-to-carcinoma conversion (Noffsinger, 2009). Although some polyps serve as precursor for cancer, polyps are considered benign growths because they have not yet broken through the basement membrane.

Carcinoma: Once one of these abnormal growths breaches the basement membrane and begins innfiltrating the surrounding tissue, it is classified as a carcinoma and is considered malignant. The transformation from adenoma to carcinoma takes an average of eight to twelve years, but most adenomas are thought to never develop into

cancer (Saif and Chu, 2010). Colon carcinomas can penetrate into underlying stromal layers and smooth muscle and eventually metastasize to distal locales. The major site of colon cancer metastasis is the liver (Chambers et al., 2002).

1.1.2 Molecular basis of colon cancer

The multi-step process of carcinogenesis is hypothesized to include 3 major steps: initiation, promotion, and progression. Each of these stages arises due to specific molecular and genetic changes that occur. The molecular basis of colon cancer has been extensively researched. Three major molecular contributors to colon cancer are chromosomal instability, inactivation of tumor suppressor genes, and activation of oncogenes.

Genomic instability: Genomic instability has been found to be a major contributor to colon cancer. Genetic instability in colon cancer is often divided by researchers into two classes: microsatellite instability or chromosomal instability (Cancer Genome Atlas, 2012; Sugai et al., 2006). Chromosomal instability is most often the source of genomic instability in colon cancer (Lengauer et al., 1997). These two classes of genomic instability induce distinct perturbations to the genome. Microsatellite instability displays a high rate of alterations in short, tandemly repeated nucleotide sequences, whereas chromosomal instability manifests as major abnormalities in chromosome structure and number (Georgiades et al., 1999). Numerous genes which function to maintain genetic stability become inactivated in colonic epithelium to result in instability that leads to cancer (Barber et al., 2008). Specifically, many colon cancer patients have inactivated mismatch repair genes, including *MLH1* and *MSH2*

(Markowitz and Bertagnolli, 2009), and mismatch repair deficiency contributes to microsatellite instability (Lengauer et al., 1997). In contrast, chromosomal instability is often linked to loss of genes that function as critical mitotic checkpoints (Georgiades et al., 1999). Gene mutation and aberrant DNA methylation commonly drive the of inactivation of mismatch repair genes and mitotic checkpoint genes (Kondo and Issa, 2004). In fact, aberrant methylation has been clearly demonstrated to be a major mechanism of inactivation of *MLH1* (Young et al., 2001). Additionally, recent work assessing the colon cancer epigenome has shown that virtually all colon cancers have hundreds to thousands of abnormally methylated genes (Lao and Grady, 2011). Hypermethylation of promoter-associated CpG islands of genes leads to transcriptional silencing of genes. Widespread CpG island promoter methylation, known as the CpG island methylator phenotype (CIMP), is frequently present in colon cancer (Toyota et al., 1999). CIMP is most commonly observed in colon cancers with microsatellite instability (Hawkins et al., 2002; Toyota et al., 1999).

Inactivation of tumor suppressor genes: Genes that restrict the growth of cells are referred to as tumor suppressor genes. Inactivation of tumor suppressor genes unfetters cells from the constraints implemented by these genes, allowing for uncontrolled cell growth. Similarly to mismatch repair genes, many tumor suppressor genes are inactivated in colon cancer through genetic mutation or aberrant methylation. Major tumor suppressor genes known to be inactivated in colon cancer include *APC*, *TP53*, and *TGFBR2*. APC inhibits the nuclear localization of the oncoprotein β-catenin and targets it for proteolysis. A deficiency in APC results in constitutive activation of

the Wnt signaling cascade, which is an initiating event in colon cancer (Markowitz and Bertagnolli, 2009). Germ-line *APC* mutations lead to a predisposition for colon cancer, and somatic mutations and deletions of *APC* have been found to occur in most sporadic colon cancers (Goss and Groden, 2000). Mutation of *TP53* is also key in colon cancer. *TP53* encodes p53, which is central in controlling the cell cycle (Vazquez et al., 2008). *TP53* inactivation most often occurs at an intermediate stage in cancer development during the transition from adenoma to carcinoma (Markowitz and Bertagnolli, 2009). Moreover, approximately one in three colon cancers develops a mutation in *TGFBR2*, which encodes the receptor for TGF-β (Grady et al., 1999; Markowitz et al., 1995; Markowitz and Bertagnolli, 2009). TGF-β signaling is involved in regulation of multiple cellular processes, including cell cycle progression and apoptosis. In addition to mutations in *TGFBR2*, other components of the TGF-β pathway, including SMADs, are often mutated in colon cancer (Eppert et al., 1996; Wood et al., 2007). Similar to the p53 pathway, inactivation of the TGF-β pathway correlates with the transition from adenoma to carcinoma (Grady et al., 1998). However, TGF-β signaling plays a dichotomous role in human cancers. It can serve as a tumor promoter in the latter stages of colon cancer by inducing the epithelial-to-mesenchymal transition and enhancing tumor invasion and metastasis(Gatza et al., 2011). Overall, inactivation of tumor suppressor genes expedites tumorigenesis by enabling tumor cells to grow unchecked.

Activation and overexpression of oncogenes: In addition to inactivation of tumor suppressor genes, activation and/or overexpression of oncogenes plays a central role in colon tumorigenesis. In contrast to tumor suppressor genes, oncogenes potentiate cell

growth. Key oncogenes known to be mutated in colon cancer include *RAS, PIK3CA, BRAF,* and *EGFR.* Activating mutations of *RAS* have been found to occur in approximately 40% of colorectal cancers (Bos et al., 1987; Markowitz and Bertagnolli, 2009). *KRAS* is the Ras isoform that most often has been found to be mutated in colon cancer (Samowitz et al., 2000). *BRAF,* which encodes B-Raf, has also been found to be highly mutated in colon cancer (Davies et al., 2002). B-Raf is a downstream signaling partner of Ras, and the Ras-Raf signaling cascade is integral in activating cell proliferation. Another important signaling mediator, phosphatidylinositol 3-kinase (PI3K), is often hyperactivated in colon cancer. In fact, approximately one-third of colon cancers possess an activating mutation in *PIK3CA*, the catalytic subunit of PI3K (Samuels et al., 2004). PI3K leads to activation of Akt, which is important for inhibition of apoptosis. Additionally, the epidermal growth factor receptor (EGFR), which regulates signaling through both Ras and PI3K, is often overexpressed in colon cancer (Galizia et al., 2006; Jorissen et al., 2003; McKay et al., 2002; Quesnelle et al., 2007; Shia et al., 2005). Activating mutations of EGFR have been detected in some studies, but the rates of EGFR mutation have been found to be extremely low (Barber et al., 2004; Ogino et al., 2005). Higher rates of EGFR mutation were observed in a Japanese study (Nagahara et al., 2005), suggesting potential ethnic disparities in acquisition of EGFR mutations. However, the promotive role of EGFR in colon cancer is well-established. Consistent with the inactivation of tumor suppressor genes, overexpression and/or hyperactivation of these oncogenes are central for the hyperproliferative and anti-apoptotic phenotype of colon cancer.

1.1.3 Location of colon cancer

Colon cancer can arise in either the right side (proximal) or left side (distal) of the colon. Interestingly, research findings have implicated differing genetic alterations as the cause of colonic transformation in left-sided compared to right-sided colorectal cancers (Iacopetta, 2002; Meza et al., 2010; Sugai et al., 2006). Microsatellite instability has been shown to be primarily located in right-sided cancers (Cancer Genome Atlas, 2012), whereas chromosomal instability is more common in left-sided colon cancer (Lindblom, 2001). CIMP incidence most often occurs in right-sided colon cancers (Hawkins et al., 2002). Furthermore, mutations in *TP53* and *KRAS* genes occur predominantly in left-sided carcinomas (Bleeker et al., 2000; Sugai et al., 2006). The differences between left- and right-sided colon cancers provide evidence of different mechanisms contributing to colonic transformation.

1.2 Epidermal growth factor receptor

1.2.1 EGFR background

In the 1960s, a peptide that could stimulate proliferation of epithelial cells was discovered and termed the epidermal growth factor (EGF) (Cohen, 1962; Cohen, 1965). A decade later, the EGF receptor was identified (Carpenter et al., 1978; Carpenter et al., 1975). EGFR was subsequently reported to be a receptor tyrosine kinase (Ullrich et al., 1984). Since its discovery, numerous studies have been conducted on EGFR, and it is one of the most well understood receptor tyrosine kinases. EGFR is a member of the ErbB family of receptors, which is composed of EGFR/ErbB1, ErbB2/Neu/HER2,

ErbB3/HER3, and ErbB4/HER4 (Ferguson et al., 2003; Normanno et al., 2006; Yarden, 2001).

1.2.2 EGFR structure

EGFR is a transmembrane glycoprotein comprised of 1186 amino acids (Ullrich et al., 1984). EGFR consists of an extracellular ligand-binding domain, a single hydrophobic transmembrane region, and an intracellular domain (Olayioye et al., 2000). The 662 amino acid extracellular domain of EGFR is composed of four subdomains (I-IV) (Bajaj et al., 1987). Subdomains I and III are leucine rich regions that have been found to be integral in ligand binding. Subdomains II and IV are cysteine rich regions, and subdomain II possesses the dimerization loop to support direct receptor-receptor interactions. Prior to ligand binding, the extracellular domain of EGFR exists in a tethered conformation due to intramolecular interactions between subdomains II and IV. Following ligand binding, the receptor undergoes conformational changes allowing the dimerization loop to project from EGFR and facilitate interaction with another ligand bound EGFR. Additionally, EGFR can heterodimerize with other members of the ErbB family. When heterodimerizing, EGFR displays the highest affinity for ErbB2. Unlike EGFR, the extracellular domain of ErbB2 precludes the receptor from binding ligand, and therefore, ErbB2 always functions in heterodimers with other members of the ErbB family. ErbB3 also only functions in heterodimers because ErbB3 lacks an intracellular kinase domain. The alpha-helical transmembrane domain of EGFR forms a single pass through the plasma membrane (Wells, 1999). The final 542 amino acids of EGFR constitute the intracellular domain, which can be subdivided into three regions. The

juxtamembrane region (~50 amino acids) is a site for feedback attenuation by protein kinase C and mitogen-activated protein kinases (MAPKs), including extracellular signal-regulated kinases 1 and 2 (ERK1/2). There is evidence that this region may also associate with heterotrimeric G proteins (Sun et al., 1997). The next region, composed of ~250 amino acids, includes the tyrosine kinase domain (Wells, 1999). Lastly, the final 229 amino acids constitute the C-terminal tail. This region includes motifs for both autophosphorylation and transphosphorylation. The tail is also involved in receptor regulation due to its three internalization motifs, sites for proteolytic activation and degradation, and autoinhibitory function (Wells, 1999).

Classically, the inactive EGFR was thought to reside in the plasma membrane as a monomer prior to activation, which results in dimerization. However, recent evidence has suggested the existence of preformed, inactive EGFR oligomers (Clayton et al., 2005; Gadella and Jovin, 1995; Martin-Fernandez et al., 2002; Saffarian et al., 2007), although the majority of receptors are suggested to exist as monomers (Saffarian et al., 2007). The role that preformed oligomers play in EGFR function and signaling remains unclear.

1.2.3 EGFR ligands

EGFR has multiple ligands which can active EGFR in either an autocrine or paracrine manner. Binding specificity of EGFR ligands is conferred by an EGF-like domain which consists of three disulfide-bonded intramolecular groups (Yarden, 2001). These ligands also contain variable structural motifs, including glycosylation sites, immunoglobulin-like domains, and heparin-binding sites. Some of the ligands for EGFR,

including EGF, TGF-α, and amphiregulin bind specifically to EGFR, whereas others, including betacellulin, heparin-binding growth factor, and epiregulin, have dual specificity for EGFR and ErbB4. These ligands are translated with a plasma membrane tethering domain, and in response to certain stimuli, the ligands will undergo ectodomain cleavage, allowing them to activate EGFR. The multiple ligands for EGFR impart high specificity and an expanded repertoire of potential signaling responses.

1.2.4 EGFR activation

Following ligand binding and receptor dimerization, the conformational changes allow the EGFR intracellular kinase domain to become activated. It has been clearly shown that EGFR activation requires the formation of an asymmetric dimer of the kinase domains of an EGFR dimer (Zhang et al., 2006). Thus, the C-lobe of the kinase domain of one EGFR docks to the N-lobe of the kinase domain of the other EGFR to induce the active conformation of a key regulatory helix (Jura et al., 2009; Zhang et al., 2006). Activation of the EGFR kinase domain additionally requires repositioning of functional regions in the kinase domain, such as inducing the active conformation of the activation loop (Wood et al., 2004). These conformational changes culminate in activation of the kinase domain of one EGFR molecule within the dimer, which will phosphorylate tyrosine residues on the cytoplasmic C-terminal tail of the dimerization partner. The residues that are phosphorylated in response to ligand-induced activation of EGFR include Y992, Y1045, Y1068, Y1086, S1142, Y1148, and Y1173 (Guo et al., 2003).

Multiple signaling cascades can also lead to transactivation of EGFR. Some cytokines can activate Janus tyrosine kinase 2 (Jak2), which can phosphorylate EGFR on

specific tyrosine residues (Yamauchi et al., 1997). Additionally, many signaling cascades activate the tyrosine kinase Src, which can phosphorylate EGFR tyrosine residues to perpetuate EGFR signaling (Biscardi et al., 1999). Furthermore, stimulation of G-protein coupled receptors (GPCR) leads to activation of matrix metalloproteinases (MMPs), which cleave EGF ligands tethered to the plasma membrane, allowing these ligands to activate EGFR (Higashiyama and Nanba, 2005; Sahin et al., 2004).

1.2.5 EGFR function

Following receptor activation, the phosphorylated tyrosine residues on the C-terminal tail of EGFR serve as docking sites for downstream mediator and signaling proteins that contain Src homology 2 (SH2) domains and phosphotyrosine-binding (PTB) domains, such as Grb2, Shc, Crk, Nck, phospholipase C-γ1 (PLC-γ1), Src, PI3K, phosphatases (SHP1 and SHP2), and Cbl E3 ubiquitin ligase (Marmor and Yarden, 2004; Yaffe, 2002). EGFR mediates signaling through multiple canonical oncogenic signaling cascades, including the Ras/MAPK pathway, the PI3K/Akt pathway, and the signal transducer and activator of transcription (STAT) 3 pathway. These signaling cascades result in modulation of transcription and translation, which ultimately lead to cell proliferation, migration, angiogenesis, and inhibition of apoptosis. In addition to these kinase-dependent functions of EGFR, the receptor has been shown to have roles that are independent of its kinase activity. EGFR can mediate some cellular processes through its ability to interact with other proteins. One study has illustrated that EGFR stabilizes the sodium/glucose cotransporter 1 in the plasma membrane to facilitate uptake of glucose to sustain cell function and survival (Weihua et al., 2008).

Additionally, many mutagenesis experiments have shown that expression of a kinase-deficient EGFR mutant does not have nearly the detrimental effects on viability as knock-out of EGFR (Luetteke et al., 1994; Miettinen et al., 1995). It has been clearly demonstrated that kinase-dead EGFR retains the ability to activate DNA synthesis and promote survival (Coker et al., 1994; Deb et al., 2001; Ewald et al., 2003; Zhu et al., 2010). Central to both kinase-dependent and kinase-independent EGFR function is the localization of the receptor.

1.2.6 EGFR localization

EGFR resides in the plasma membrane of epithelial, stromal, and select glial and smooth muscle cells (Wells, 1999). Within the plasma membrane, EGFR is known to be localized to specific plasma membrane microdomains termed lipid rafts (described in further detail below). Following receptor activation, EGFR can be internalized through clathrin-dependent and clathrin-independent forms of endocytosis (Sigismund et al., 2008). Following endocytosis, EGFR can be trafficked through endosomes to lysosomes for proteolysis or recycled back to the plasma membrane. EGFR has been shown to retain the ability to activate some downstream signaling cascades from endosomes (Burke et al., 2001; Sadowski et al., 2009; Wiley and Burke, 2001). Additionally, EGFR can be translocated to the nucleus or mitochondria (Boerner et al., 2004; Lin et al., 2001). In the nucleus, EGFR has been shown to directly alter gene expression by binding to promoters alone or through interactions with transcription factors, including STAT3, E2F1, and STAT5 (Hanada et al., 2006; Hung et al., 2008; Lin et al., 2001; Lo et al., 2010; Lo et al., 2005). EGFR in the nucleus has been shown to regulate

expression of many important mediators of cell proliferation and survival, including cyclin D1 (Lin et al., 2001), inducible nitric oxide synthase (Lo et al., 2005), B-Myb (Hanada et al., 2006), cyclooxygenase-2 (Lo et al., 2010), aurora A (Hung et al., 2008), and c-Myc (Jaganathan et al., 2011). In the mitochondria, EGFR has been shown to decrease cytochrome c oxidase activity and ATP production (Boerner et al., 2004; Demory et al., 2009). This function of EGFR may aid cell survival by modulating cytochrome c oxidase dependent functions. Mitochondrial targeting of EGFR has been indicated in drug resistance(Cao et al., 2011).

1.2.7 EGFR in colon cancer

As briefly mentioned above, EGFR is a master signal involved in colonic transformation (Matveev and Smart, 2002; Pike, 2005; Ringerike et al., 2002). The EGFR signaling cascade is intimately linked with colon cancer. EGFR has been implicated in all stages of colon tumorigenesis. The early colonic abnormal lesions, ACF, have been shown to exhibit increased signaling through EGFR in humans (Cohen et al., 2006). EGFR signaling is also required for the formation of colonic adenomas in mice treated with carcinogen (Fichera et al., 2007). Furthermore, overexpression of EGFR has been reported in 30-85% of human colon cancer (Galizia et al., 2006; Jorissen et al., 2003; McKay et al., 2002; Quesnelle et al., 2007; Shia et al., 2005), and up to nearly 90% of cases of metastatic colon cancer overexpress EGFR (Arteaga, 2001). In addition, EGFR is overexpressed in a wide range of tumors and is involved in their growth and proliferation through various mechanisms. EGFR expression has recently found to vary based on colon tumor location (proximal versus distal; left- versus right-

sided) and stage (Papagiorgis et al., 2012). Expression of EGFR has been shown to correlate with a more aggressive disease (Coffey et al., 1992; Koretz et al., 1990; Yasui et al., 1988) resulting in poor prognosis (Lee et al., 2002; Mayer et al., 1993; Radinsky, 1995). In addition to EGFR expression, nuclear localization of EGFR has been linked to enhanced proliferation, inflammation, and drug resistance (Carpenter and Liao, 2009; Han and Lo, 2012; Lo, 2010; Wang et al., 2010). Several small molecule kinase inhibitors and therapeutic antibodies that target EGFR are FDA-approved to treat cancer patients. Cetuximab and Panitumumab are humanized monoclonal antibodies against EGFR that are currently being utilized in the treatment of metastatic colon cancer (Di Fiore et al., 2010; Han and Lo, 2012; Plesec and Hunt, 2009). Interestingly, it has been shown that the localization of EGFR to lipid rafts can alter the response of breast cancer cells to EGFR-targeted therapy (Irwin et al., 2010), and changing the localization of EGFR from lipid rafts into the bulk membrane domain is suggested to improve the efficacy of anti-EGFR therapies. Therefore, the following section will focus on the area of lipid raft research.

1.3 Lipid rafts

The lipid raft hypothesis was initially conceptualized to explain the aggregation of glycolipids at the apical membrane of epithelial cells (Simons and van Meer, 1988). This concept then developed further to encompass membrane subcompartmentalization. This hypothesis states that lateral heterogeneity, driven by affinity of membrane

components, functions in cellular signaling, endocytosis, membrane trafficking, and other membrane functions (Simons and Toomre, 2000).

1.3.1 Composition

Two types of membrane microdomains have been described: caveolae and lipid rafts. Caveolae are more fully defined because they have a distinct morphology. Caveolae are 50-70 nm flask-shaped pits in the plasma membrane enriched in caveolin-1 (Anderson, 1998; Parton, 1996). Lipid rafts are much less distinct, and they are much more difficult to define due to their small size and heterogeneity. The lipid raft hypothesis postulates that the size of lipid rafts can vary between 10 and 200 nm (Pike, 2006). Lipid rafts are further defined as dynamic plasma membrane domains enriched in cholesterol and sphingolipids (Pike, 2005). They are also described as highly-ordered lipid assemblies due to the interaction between cholesterol and sphingolipids, as well as the enrichment of saturated and long hydrocarbon chains and hydroxylated ceramide backbones (Brown and London, 2000; Simons and Sampaio, 2011). The composition of lipid rafts imparts upon them two distinct characteristics: detergent-resistance and low-buoyant density (Jacobson et al., 2007). These properties are highly exploited in studies on lipid rafts, which employ detergent extractions and gradient isolation of these domains. To avoid the intrinsic problem of isolating lipid rafts, many researchers are focusing on microscopy techniques to study their composition, organization, and function (Ianoul and Johnston, 2007; Kusumi et al., 2011; Loura and Prieto, 2007; Marquer et al., 2012). Lipid rafts are highly heterogeneous, and the structure of lipid

rafts is dynamic. Lipid rafts are constantly altering their composition of both lipids and proteins.

1.3.2 Proteins in lipid rafts

Several studies have clearly demonstrated that certain proteins are dynamically associated with lipid domains. Proteins can be targeted to lipid rafts through multiple mechanisms. The protein-targeting theory hypothesizes that proteins collect in membrane domains based on specific molecular addresses encoded in the protein that direct them to these locations (Anderson and Jacobson, 2002). It has also been shown that certain lipid modifications on proteins can target them to lipid rafts. Cysteine palmitoylation is one lipid modification that can target proteins to rafts, particularly intracellular proteins (Levental et al., 2010). It has been found that inhibition of protein palmitoylation can reduce the lipid raft localization of certain proteins (Webb et al., 2000). Additional raft-targeting lipid modifications include N-terminal myristic acid tails, isoprenylation, and the addition of C-terminal sterol moieties (Levental et al., 2010). In addition to lipid modifications, some proteins are hypothesized to be encased in a shell of cholesterol and sphingolipids which targets them to lipid rafts (Anderson and Jacobson, 2002). Secretory vesicles containing sphingolipids and sterols carry raft protein cargo from the trans-Golgi network to the plasma membrane, indicating that lipids are directly involved in the sorting process (Klemm et al., 2009). Furthermore, lipid rafts are enriched with specific proteins that contain cholesterol- or ganglioside-binding domains (Coskun and Simons, 2010), which allows them to bind to lipid raft components. Additionally, many glycosylphosphatidyl-inositol (GPI)-anchored proteins

localize to lipid rafts (Fiedler et al., 1993; van Zanten et al., 2009). There are likely many additional modes of targeting proteins to lipid raft domains that remain to be elucidated. The inclusion of proteins into lipid raft domains is contingent on raft lipid and protein composition (George and Wu, 2012).

1.3.3 Role in signal transduction

Membrane rafts play a fundamental role in mediating multiple cell functions, including signal transduction (Deans et al., 1998; Field et al., 1997; Simons and Toomre, 2000; Smart et al., 1999b; Staubach and Hanisch, 2011). Lipid rafts are thought to provide a platform in which signaling partners can accumulate to support highly efficient signal transduction. Additionally, small rafts can coalesce upon activation of membrane signaling to form larger and more stable platforms for signaling (Hofman et al., 2008; Kono et al., 2002). Extensive studies have been performed to elucidate the role of lipid rafts in the activation of T lymphocytes, which requires clustering of signaling components in a large, stable lipid raft domain at the immunological synapse (Alonso and Millan, 2001; Drbal et al., 2007). Extrinsic induction of apoptosis relies on signaling through lipid rafts, and the composition of lipid rafts has been shown to affect apoptotic responses (Algeciras-Schimnich et al., 2002; Bang et al., 2005; George and Wu, 2012). Many integral protein signaling components have been shown to localize to lipid rafts, including G-protein coupled receptors (GPCR), PDGF receptor, NGF receptor, VEGF receptor, and many more (Patel et al., 2008; Pike, 2005). In many cases, the function of proteins depends greatly on their association with lipid rafts

(George and Wu, 2012). The dynamics and heterogeneity of lipid rafts allow for a large number of signals to be transduced from the outer membrane to intracellular domains.

1.3.4 Lipid rafts in cancer

Recent evidence suggests that lipid rafts may modulate the malignant transformation process. In fact, the levels of lipid rafts are increased in many types of cancer (Hazarika et al., 2004; Li et al., 2006; Patra, 2008). Additionally, lipid rafts mediate cell signaling events that are often constitutively or hyper-activated in cancer (Fedida-Metula et al., 2012; Lasserre et al., 2008; Roy et al., 2008). There is also some evidence suggesting that disruption of lipid rafts in cancer can lead to increased responsiveness to anti-cancer therapies (Irwin et al., 2010). Additionally, some anti-cancer drugs have beneficial effects through alteration of the protein content of lipid rafts (George and Wu, 2012). In colon cancer, lipid rafts have been shown to function in cell death-mediated signaling (Lacour et al., 2004; Rebillard et al., 2007), entry of bioactive compounds (Adachi et al., 2007), and localization of key proteins involved in immune response (Bacso et al., 2002).

1.3.5 EGFR in lipid rafts

As mentioned above, the important signaling mediator EGFR is localized to lipid rafts. Localization of EGFR to lipid rafts has been associated with both N-glycosylation and the second cysteine rich region of the EGFR (Cummings et al., 1985; Yamabhai and Anderson, 2002). Extensive evidence suggests that the ability of EGFR to signal is dependent on its localization to lipid raft domains in the plasma membrane (Matveev and Smart, 2002; Pike, 2005; Ringerike et al., 2002; Roepstorff et al., 2002). Lipid rafts

have the ability to assemble the molecular machineries necessary for intracellular propagation of EGFR signals and receptor internalization (Mineo et al., 1996; Pike and Casey, 1996; Puri et al., 2005). Specifically, EGFR has been shown to colocalize with downstream signaling partners, including PI3K, Ras and c-Src in lipid rafts (Eisenberg and Henis, 2008; Irwin et al., 2010). Due to the importance of lipid rafts as signaling platforms, perturbation of these domains is predicted to significantly affect cell signaling. In fact, disruption of lipid rafts has been found to have significant effects on EGFR phosphorylation and downstream signaling. Raft disruption through cholesterol depletion increases EGFR clustering prior to simulation (Saffarian et al., 2007). Cholesterol depletion also increases ligand binding, dimerization, and phosphorylation but decreases EGF-stimulated signaling (Chen and Resh, 2002; Pike, 2005; Pike and Casey, 1996; Pike and Casey, 2002; Pike and Miller, 1998; Ringerike et al., 2002; Roepstorff et al., 2002). Furthermore, localization of EGFR to lipid rafts has been shown to affect the efficacy of EGFR-targeted chemotherapeutic agents. Cells with higher amounts of EGFR within lipid rafts were found to be less responsive to tyrosine kinase inhibitors used in the treatment of cancer (Irwin et al., 2010). Therefore, alteration of EGFR localization in lipid rafts is likely to result in modified EGFR signaling.

1.4 Docosahexaenoic acid

Docosahexaenoic acid (DHA) is a fatty acid composed of a 22-carbon chain with 6 cis double bonds. The first double bond from the methyl end of the fatty acid is

located at the third carbon, thereby classifying DHA as an omega-3, or n-3, polyunsaturated fatty acid (PUFA). DHA is found highly enriched in select tissues, including the brain (Breckenridge et al., 1972), sperm (Neill and Masters, 1973), and the retina (Stillwell and Wassall, 2003). In fact, DHA can approach 50 mol% of the phospholipid acyl chains in the membranes of these tissues (Simopoulos et al., 1986), and di-DHA phospholipid species have been isolated from these tissues (Bell et al., 1997). In most other tissues, DHA is not highly concentrated and often composes less than 5 mol% of the total phospholipid acyl chains (Simopoulos et al., 1986). DHA is primarily found in the sn-2 position of phospholipids in the membranes of these tissues (Anderson and Sperling, 1971). However, DHA content of these "unenriched" tissues can be increased 2-10 fold through dietary measures (Robinson et al., 1993; Simopoulos et al., 1986; VanMeter et al., 1994). Oily, cold water fish are the major dietary source of DHA. DHA can rapidly incorporate into a variety of membranes, mainly into the mitochondria (Stillwell et al., 1997; Tahin et al., 1981) and the plasma membrane (Zerouga et al., 1996). DHA is primarily incorporated into phosphatidylethanolamine and phosphatidylcholine (Robinson et al., 1993; Stubbs and Smith, 1984; Zerouga et al., 1996), but DHA-accumulation in specific phospholipids can be tissue specific (Knapp et al., 1994; Salem et al., 1986).

1.4.1 Effects of n-3 PUFA on colon cancer

Risk of colon cancer is directly linked with modifiable factors, including diet (Martínez and Jacobs, 2004). In fact, researchers have found over 180 dietary interventions and pharmacologic agents that reduce ACF in models of chemical-induced

colon carcinogenesis (Corpet and Tache, 2002). One major dietary component that has been indicated in the prevention of colon cancer is fish oil. Experimental, clinical, and epidemiological studies have strongly indicated a role for fish oil, and its most abundant bioactive dietary lipids eicosapentaenoic acid (EPA, 20:5 n-3) and DHA, in colon cancer prevention (Anti et al., 1994; Anti et al., 1992; Bartram et al., 1993; Caygill et al., 1996; Chang et al., 1998; Courtney et al., 2007; Geelen et al., 2007; Hall et al., 2008; Kim et al., 2010a; Pot et al., 2008) (Murff et al., 2012; Sasazuki et al., 2011). However, knowledge of the mechanism(s) by which fish oil confers chemoprotection is rudimentary. The current literature suggests multiple mechanisms to explain the anti-neoplastic activity of DHA and EPA. The suggested mechanisms include inhibition of cyclooxygenase (COX) activity (Calviello et al., 2004; Habbel et al., 2009; Swamy et al., 2004), reduction of inflammation (Angeles Puertollano et al., 2001; Bannenberg et al., 2007; Calviello et al., 2004; D'Ambola et al., 1991; Ibrahim et al., 2011; Rao et al., 2001; Yaqoob et al., 1994), fatty acid signaling through G protein coupled receptors (Arita et al., 2005; Arita et al., 2007; Im, 2012; Krishnamoorthy et al., 2010; Oh et al., 2010; Serhan et al., 2011), altered cellular oxidative stress (Benais-Pont et al., 2006; Chen and Istfan, 2000; Crnkovic et al., 2012; Dupertuis et al., 2007; Engel and Evens, 2006; Ng et al., 2005; Nomura et al., 1999; Wang et al., 2000), and alteration of membrane dynamics (discussed in detail below). Modification of cell membranes can have extensive effects on cellular function. DHA has been shown to have substantial effects on plasma membrane properties, including membrane fluidity, phase behavior, permeability, fusion, and flip-flop (Stillwell and Wassall, 2003; Wassall et al., 2004).

Recent evidence further suggests that DHA can perturb lipid rafts (Chapkin et al., 2008a; Kim et al., 2008; Shaikh et al., 2009b). DHA, due to its high degree of unsaturation, is sterically incompatible with cholesterol (Wassall et al., 2004), a major constituent of rafts. Additionally, DHA displays non-ideal mixing with sphingomyelin, another major component of lipid rafts, in model membranes (Shaikh et al., 2009a). Conceivably, disruption of lipid rafts could be caused by the lack of affinity of DHA for lipid raft components. As mentioned above, several important processes involve lipid rafts, including T-cell activation, signal transduction, and protein and lipid trafficking (Pike, 2005). Many of these lipid raft-mediated processes play an integral role in colon tumorigenesis. Signaling pathways emanating from lipid rafts, frequently exacerbated in cancer, mediate a variety of tumor-promoting activities, including cell proliferation, migration, and invasion (Patra, 2008). Additionally, chronic inflammation, central to the process of tumorigenesis (Ullman and Itzkowitz, 2011), involves excessive lipid raft-mediated T-cell activation. Numerous recent discoveries highlight the role of n-3 PUFA in the regulation of lipid rafts and lipid raft-mediated signaling.

1.4.2 n-3 PUFA alter lipid raft size

Lipid raft size is an important feature in lipid raft function that has been shown to be altered by n-3 PUFA (Nicolau et al., 2006). Lipid raft size is integral for dynamic lateral segregation of signaling proteins into microdomains. Partitioning of proteins into rafts can increase specific protein-protein collision rates to facilitate efficient signaling. However, to maximize this essential, biologically relevant function, rafts must be mobile and small, with a diameter up to 14 nm (Nicolau et al., 2006). The size of lipid rafts in

splenic T-cells from wild type and *fat-1* transgenic mice, which express n-3 fatty acid desaturase cloned from *C. elegans*, has been compared (Kang et al., 2004). This enzyme can catalyze the production of endogenous n-3 PUFA by introducing a double bond into fatty acyl chains. *Fat-1* mice are a useful tool for the assessment of the biological properties of n-3 PUFA without diet manipulation. *Fat-1* mice were shown to have T-cells that exhibited enhanced clustering of lipid rafts to form large raft domains (Kim et al., 2008). The poor affinity of cholesterol for n-3 PUFA likely causes a lipid-driven mechanism for lateral phase separation of cholesterol- and sphingolipid-rich lipid microdomains from n-3 PUFA. By increasing the size of lipid rafts, n-3 PUFA impair efficient functioning of lipid rafts in T-cells. This in turn suppresses T-cell activation (Kim et al., 2008), which is a potential mechanism by which n-3 PUFA function as anti-inflammatory agents. Similar results have been observed in HeLa cells, a human cancer cell line. HeLa cells treated with DHA exhibited enhanced clustering of lipid raft domains compared to untreated cells (Chapkin et al., 2008c). Consistent with these findings, work done by Rockett et al. in B cells illustrated that the effect of fish oil on lipid raft size is likely mediated specifically by DHA (Rockett et al., 2012). In breast cancer cells, DHA has been shown to increase the height of lipid rafts, while reducing the overall number of lipid rafts (Corsetto et al., 2012). Importantly, increasing lipid raft size has implications in the regulation of multiple signaling events associated with these microdomains.

1.4.3 n-3 PUFA alter lipid raft composition

In addition to lipid raft size, the composition of lipid rafts is important for lipid raft function. Lipid rafts provide a more ordered lipid environment than the bulk membrane due to interactions between cholesterol, sphingolipids, and phospholipids containing saturated fatty acyl chains (Brown and London, 2000). Extraction of certain lipids from raft microdomains, including cholesterol, has been shown to perturb their function (Ilangumaran and Hoessli, 1998; Pike and Casey, 2002; Pike and Miller, 1998; Westover et al., 2003; Zhuang et al., 2002). Therefore, the effect of n-3 PUFA on lipid composition of rafts in multiple cell types has been studied extensively. Upon feeding mice a diet enriched in n-3 PUFA, the cholesterol content of lipid rafts in colonocytes was reduced by 46% compared to mice fed a diet enriched in n-6 PUFA (Ma et al., 2004). Dietary n-3 PUFA also reduced lipid raft sphingolipid content by ~45% in mouse splenic T-cells (Fan et al., 2003a). Specifically, raft sphingomyelin content was decreased by 30% in T-cells from mice fed n-3 PUFA (Fan et al., 2004). n-3 PUFA have been shown to have similar effects in multiple cell types. Treatment of both endothelial and breast cancer cells with DHA was also found to reduce raft sphingomyelin and cholesterol content (Schley et al., 2007; Ye et al., 2010). These n-3 PUFA induced modifications of lipid raft composition are significant because cholesterol and sphingomyelin are major building blocks of lipid rafts that promote the formation of hydrophobic liquid-ordered molecular packing.

Furthermore, various proteins are known to be enriched in lipid rafts. Specifically, eminent signaling proteins, including receptors and G proteins, require raft

localization for proper functioning (Pike, 2003; Smart et al., 1999a). One such lipid raft sequestered protein is Ras. Ras is an important signaling mediator, and one of its major isoforms, H-Ras, is well known to localize to lipid raft domains (Prior et al., 2003). Activation of H-Ras and downstream signal transduction has been shown to be dependent on lipid raft localization (Eisenberg et al., 2006; Mineo et al., 1996; Prior et al., 2001). Feeding mice a diet enriched in n-3 PUFA and treating immortalized young adult mouse colonocytes (YAMC) with DHA decreased the localization of H-Ras to lipid raft domains in colonocytes (Ma et al., 2004). Furthermore, DHA has been shown to inhibit the plasma membrane targeting of lipidated proteins, including H-Ras (Seo et al., 2006). Src and Fyn are lipid raft localized signaling mediators, and DHA has been found to cause a redistribution of these proteins out of rafts in colon cancer cells (Duraisamy et al., 2007). n-3 PUFA have also been shown to alter lipid raft partitioning of key proteins involved in T-cell activation, including PKCθ, PLC-γ1, and F-actin. Dietary fish oil significantly suppressed the recruitment of PKCθ to lipid rafts following stimulation (Fan et al., 2004). In a complementary study, recruitment of PKCθ, PLC-γ1, and F-actin to lipid raft domains was suppressed in T-cells isolated from *fat-1* transgenic mice compared to wild-type mice (Kim et al., 2008). Treatment of T-cells with DHA has additionally been shown to displace IL-2R, JAK1, JAK3, and STAT5 from lipid raft domains (Li et al., 2005). In B-cells, DHA has been shown to reduce the recruitment of TLR4 to lipid raft domains (Wong et al., 2009). Overall, these data clearly demonstrate that n-3 PUFA modify the lipid raft microenvironment (Li et al., 2005). A proposed model for the effect of n-3 PUFA on lipid rafts is presented in Fig. 1.

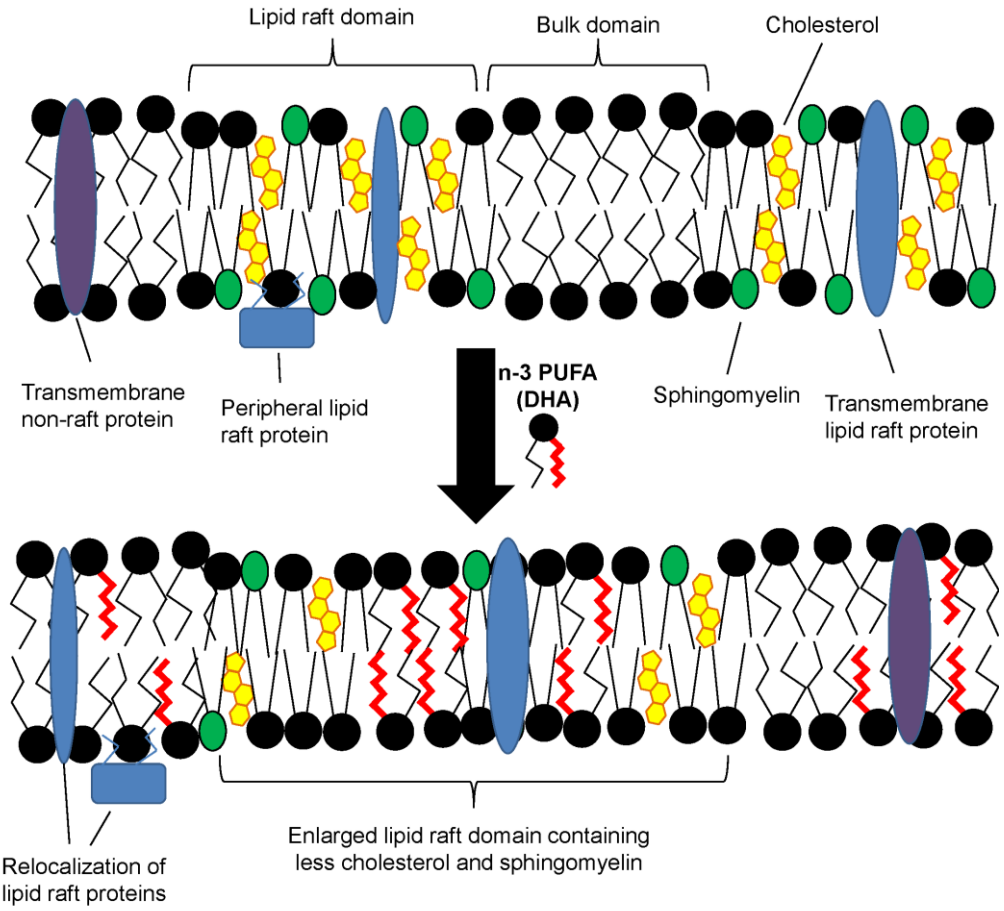

Figure 1. Putative model for the effect of n-3 PUFA on lipid rafts. Lipid rafts are nanoscale regions of the plasma membrane, enriched in cholesterol, sphingomyelin, and phospholipids containing saturated acyl chains. Both transmembrane and peripheral membrane proteins can be localized to lipid rafts. Upon treatment with a combination of n-3 PUFA or DHA alone, these PUFA are incorporated into phospholipids which are inserted into both raft and non-raft regions of the plasma membrane. This results in enhanced clustering of lipid raft regions, which are depleted of cholesterol and sphingomyelin. Additionally, many lipid raft associated proteins "mislocalize" to the bulk membrane domain. This results in a suppression of lipid raft mediated processes, including T-cell activation and downstream signal transduction.

1.4.4 n-3 PUFA perturb lipid raft regulated signaling

Observations on the effect of n-3 PUFA on lipid raft size and composition indicate that n-3 PUFA likely suppress lipid raft mediated cell signaling. Lipid rafts compartmentalize signal-transducing molecules to provide an environment conducive to signal transduction (Leitenberg et al., 2001). Many studies have addressed the effect of n-3 PUFA on signaling events that originate in rafts. n-3 PUFA feeding has been shown to suppress EGF-induced activation of H-Ras, but not K-Ras in colonocytes (Ma et al., 2004). Interestingly, H-Ras signaling has been shown to be sensitive to lipid raft perturbations, whereas K-Ras signaling is largely insensitive (Roy et al., 1999). Phosphorylation of PLC-γ1 is a lipid raft dependent process that occurs in the very early stages of T-cell activation (Zhang and Samelson, 2000). Stimulation-induced PLC-γ1 phosphorylation is inhibited in cells from *fat-1* transgenic mice compared to wild-type mice (Kim et al., 2008). Additionally, lipid rafts have been shown to both integrate and amplify signaling processes that lead to activation of transcription factors, including AP-1 and NF-κB in T-cells. Activation of NF-κB and AP-1 has been shown to be essential for induction of responses to immune and inflammatory challenges (Ben-Neriah and Karin, 2011; Hess et al., 2004). Therefore, the effect of n-3 PUFA on receptor-induced activation of these important pathway modifiers has been studied. Both fish oil and purified DHA suppress the binding activity of AP-1 and NF-κB (Fan et al., 2004). TLR4 activation in lipid rafts is important in B-cell mediated events, and TLR4 activation has been shown suppressed by DHA (Wong et al., 2009). Together, these

findings are consistent with the hypothesis that changes in membrane composition induced by n-3 PUFA have functional consequences with regard to cell signaling.

1.4.5 n-3 PUFA suppress lipid raft-mediated cell function

Lipid raft mediated cell signaling ultimately mediates numerous cell functions. T-cell activation requires lipid raft coalescence and translocation of key proteins, ultimately leading to the production of cytokines and cell cycle progression. IL-2 functions in both a paracrine and autocrine manner to induce T-cell proliferation. Feeding a diet enriched in n-3 PUFA has been shown to inhibit activation-induced production of IL-2 and thereby suppress T-cell proliferation (Fan et al., 2004). Additionally, T-cell proliferation in response to multiple stimuli is suppressed in *fat-1* mice (Kim et al., 2008). Fish oil feeding also suppressed lipid-raft mediated B-cell stimulation of CD4+ T-cells (Rockett et al., 2012). n-3 PUFA have additionally been found to reduce levels of the lipid raft localized lipid, phosphatidylinositol-4,5-bisphosphate (PIP_2), in T-cells, which results in suppression of actin-remodeling (Hou et al., 2012). In epithelial cells, DHA-induced disruption of lipid rafts was found to reduce cell proliferation and increase apoptosis (Corsetto et al., 2012; Ravacci et al., 2012). DHA has additionally been shown to decrease oxidative-stress induced calcium influx, a lipid raft-mediated process, in endothelial cells (Ye et al., 2010). These data signify the implicit role of n-3 PUFA in regulation of lipid raft mediated cell processes.

1.4.6 Effects of DHA on EGFR

Two initial studies have assessed the effects of n-3 PUFA on EGFR localization and signaling. Initially, a combination of EPA and DHA was shown to alter the

localization of EGFR within the plasma membrane of a breast cancer cell line. The altered localization was concurrent with increased ligand-induced EGFR phosphorylation and downstream activation of p38MAPK (Schley et al., 2007). The second study utilized DHA alone, and similarly reported an alteration in EGFR localization in lung and breast cancer cell lines (Rogers et al., 2010). Although EGFR phosphorylation and downstream signaling was only investigated under basal conditions, the increase in EGFR phosphorylation was associated with a suppression of Ras and ERK1/2 activation upon DHA treatment. These initial observations, although intriguing, did not directly address how n-3 PUFA impact EGFR functionality since receptor activation was never examined within the context of a ligand specific for the EGFR. Therefore, the molecular mechanisms leading to the suppressive effects of DHA treatment on EGFR-dependent signaling remain undetermined. Additionally, these studies only assessed a single downstream cascade emanating from EGFR.

1.5 Current study

The major objective of this research is to determine the effects of the long chain n-3 PUFA DHA on the activation and signaling axis of EGFR. The evidence discussed here strongly suggests that DHA alters EGFR localization and thereby profoundly suppresses EGFR function. Therefore, this study specifically addresses the effects of n-3 PUFA on EGFR localization in the plasma membrane and downstream signaling. In addition, we have assessed the effects of this class of dietary lipid on EGFR-mediated processes including cell proliferation and wound healing. This study is intended to

elucidate the mechanism by which DHA functions in chemoprevention. This work can bolster efforts aimed at determining ideal candidates for n-3 PUFA-mediated therapies targeting epithelial cells.

2. EFFECT OF DHA ON EGFR LOCALIZATION AND SIGNALING*

2.1 Introduction

Colon cancer prevention is an open frontier for cancer research. Many leaders in the field agree that significant efforts should be made to further research in chemoprevention. Dietary manipulation can have a major impact on colon cancer risk. Sundry dietary agents have been found to either protect against or promote cancer. One such dietary component is DHA. Significant research suggests that DHA is protective against colon tumorigenesis. However, in the United States, consumption of DHA is extremely low, with the average intake reported to be less than 0.2 g/day (Conquer and Holub, 1998; Kris-Etherton et al., 2000). If conclusive data shows that DHA can protect against colon tumorigenesis, it would be manageable for at risk populations to increase their consumption of this fatty acid. However, the exact mechanism(s) of action of DHA remains elusive. It is imperative to understand the mechanism of action of a chemoprotective agent in order to determine optimal dosing and timing, as well as identifying people who are most likely to benefit from a particular intervention.

Research suggests that one potential mechanism of action of DHA is to perturb lipid rafts (Chapkin et al., 2008c). This lipid raft disrupting effect of DHA has since been shown to occur in multiple cell types, including colonocytes. Many critical signaling events involved in cell proliferation and migration originate in lipid rafts (Staubach and Hanisch, 2011). Therefore, DHA is hypothesized to protect against colon

*Part of this chapter is reprinted with permission from "Alteration of EGFR spatiotemporal dynamics suppresses signal transduction" by Harmony F. Turk, Rola Barhoumi, and Robert S. Chapkin, 2012. *PLoS ONE*, 7,e39682, Copyright 2012 by Harmony F. Turk.

cancer by suppressing oncogenic cell signaling that emanates from lipid rafts. However, it remains unclear which molecular mechanism are modulated by DHA.

A major oncogenic protein known to localize to lipid rafts is EGFR. As mentioned above, EGFR plays an important role in colon tumorigenesis. Lipid rafts serve to facilitate EGFR signaling, as well as to partially constrain receptor activation (Ringerike et al., 2002). EGFR signals through ERK1/2, STAT3, Akt, and mammalian target of rapamycin (mTOR) to stimulate cell proliferation and inhibit cell death. ERK1/2 (also known as p44/42 MAPK) are serine/threonine kinases. ERK1/2 activation is rapidly stimulated by EGF, and ERK1/2 activation is integral for the G_1- to S-phase transition of the cell cycle (Cargnello and Roux, 2011). ERK1/2 regulate gene transcription by activating or stabilizing transcription factors, including Elk-1 and c-Fos. STAT3 is a transcription factor that homodimerizes upon activation, enters the nucleus, and activates genes required for cell survival (Bcl-X, survivin, caspases) and cell proliferation (c-Myc, p21, cyclin D1) (Klampfer, 2008). Similar to ERK1/2, Akt is a serine/threonine protein kinase. Akt phosphorylates numerous proteins involved in cell survival (BAD, CREB, Iκ-B kinase, Procaspase-9) and cell cycle progression (GSK-3, $p21^{WAF1}$) (Nicholson and Anderson, 2002). mTOR is also a serine/threonine kinase. EGF-induced stimulation of both Akt and ERK1/2 can lead to activation of a protein complex containing mTOR, i.e., mTORC1 (Laplante and Sabatini, 2012). EGF can also induce activation of mTORC2, another mTOR-containing protein complex. mTORC1 regulates protein synthesis by activating ribosomal S6 kinase (S6K) and inhibiting 4E-BP1 and Maf1 (Laplante and Sabatini, 2012). mTORC2 is integral in regulating cell

survival by activating Akt and SGK1, and this complex is also important for activating cytoskeletal organization (Laplante and Sabatini, 2012). EGFR also activates a multitude of other signaling mediators that regulate other cellular functions, including migration, adhesion, invasion, and angiogenesis (Yarden, 2001). Precise signaling of EGFR has been intimately linked to its lipid raft localization (Chen and Resh, 2002; Pike and Casey, 1996; Roepstorff et al., 2002). DHA has been shown to redistribute some lipid raft localized proteins into the bulk domain (Duraisamy et al., 2007; Kim et al., 2008), which affects protein function. Consequently, we propose that DHA could alter the lipid raft localization of EGFR and thereby modify receptor function.

Our first aim was to assess the effect of DHA on EGFR localization and signaling in young adult mouse colonocytes (YAMC), a non-malignant transformed cell line. Specifically, we evaluated the membrane distribution of EGFR in cells left untreated or treated with DHA or the control fatty acid linoleic acid, LA 18:2n-6. We then analyzed the effect of the localization of EGFR on the ability of the receptor to autophosphorylate and activate downstream signaling through ERK1/2, STAT3, Akt, and mTOR. We also compared the effects of DHA and EPA on EGFR phosphorylation. Lastly, we determined the effect of DHA on cell viability, including cell proliferation and overall cellular death.

2.2 Materials and methods

2.2.1 Cell culture

Young adult mouse colonic (YAMC) cells, conditionally immortalized colonocytes, were originally obtained from R.H. Whitehead, Ludwig Cancer Institute (Melbourne, Australia). Both wild-type and $EGFR^{-/-}$ isotype YAMC cells were utilized. YAMC cells (passages 12–17) were cultured under permissive conditions, 33°C and 5% CO_2 in RPMI 1640 media (Mediatech, Manassas, VA) supplemented with 5% fetal bovine serum (FBS; Hyclone, Logan, UT), 2 mM GlutaMax (Gibco, Grand Island, NY), 5 µg/mL insulin, 5 µg/mL transferrin, 5 ng/mL selenious acid (Collaborative Biomedical Products, Bedford, MA), and 5 IU/mL of murine interferon-γ (Roche, Mannheim, Germany). Select cultures were treated for 72 h with 50 µM fatty acid [DHA, linoleic acid (LA, 18:2n-6), arachidonic acid (AA, 20:4n-6), or eicosapentaenoic acid (EPA, 20:5n-3); NuChek, Elysian, MN] complexed with bovine serum albumin (BSA). Where indicated, DHA treated cultures were washed three times with PBS followed by incubation with untreated media or LA for an additional 40 h. In select cultures, for the final 16-18 h, complete media was replaced with low-serum (0.5% FBS) media. Cells were then stimulated with 0-25 ng/mL recombinant mouse EGF (Sigma, St. Louis, MO) and harvested.

2.2.2 Lipid raft isolation

To determine the localization of EGFR within the plasma membrane, YAMC cells were treated with fatty acid and serum starved as above. Detergent-free lipid raft-enriched fractions were isolated as previously described (Ma et al., 2004; Smart et al.,

1995). All steps were performed at 4°C. YAMC cells grown in 12 T-175 flasks per treatment were harvested with trypsin-EDTA (Gibco) and pelleted at 200 x *g* for 5 min. The pellets were resuspended in Buffer A (250 mM sucrose, 1 mM EDTA, 20 mM Tricine, 100 µM activated sodium orthovanadate, 40 µL/mL protease cocktail, pH 7.8) at 1 x 10^7 cell/mL. Cells from each treatment were pooled and lysed by two rounds of rapid freeze (-80^{o}C) and thaw (37^{o}C). Cell lysates were then centrifuged at 1000 x *g* for 10 min, and the supernatants were retained. Cell pellets were resuspended in Buffer A and homogenized as above, and the centrifugation step was repeated. The resulting supernatants were pooled into a post-nuclear supernatant (PNS). The PNS was layered on top of 30% Percoll (Amersham, Pittsburg, PA) in Buffer A and centrifuged at 84,000 x *g* for 30 min in a Beckman SW28 rotor. The plasma membrane fraction was collected and sonicated 3 times (50-J bursts) with 2 rapid pulses each time. The samples were then mixed with OptiPrep (Accurate Chemical and Scientific Corp, Westbury, NY) in Buffer A (final concentration 23%), overlaid with a 6 mL linear 20 to 10% OptiPrep gradient, and centrifuged in a Beckman SW41Ti rotor at 52,000 x *g* for 90 min. The top 5 mL of the gradient was collected and combined with 4 mL of 50% OptiPrep in Buffer A. An aliquot of the denser membrane band was also collected. The 9 mL fraction was overlaid with 1 mL of 15% Optiprep in Buffer A and 0.5 mL of 5% Optiprep in Buffer A and was centrifuged at 52,000*g* for 90 min in a Beckman SW41Ti rotor. A lipid raft/caveolae-enriched membrane fraction was collected from the 5/15% interface, and a membrane fraction defined as the intermediate fraction was collected at the bottom of the 15% layer. Slide-a-lyser cassettes (Pierce, Rockford, IL) were used to dialyze

samples overnight in dialysis buffer (1 mM EDTA, 20 mM tricine, pH 7.8). Samples were placed into 1.5 mL Eppendorf tubes and centrifuged in a SpeedVac System to 1/3 the original volume to concentrate. Protein concentration was measured with Coomassie Plus Protein assay (Pierce), and fractions were subjected to SDS-PAGE and western blotting as described above.

2.2.3 Colocalization

The plasmid containing RFP conjugated with a truncated H-Ras composed of the C-terminal 9 amino acid targeting domain (RFP-tH) was a generous gift from Ian Prior, Univ. of Liverpool (Apolloni et al., 2000). The plasmid containing full length human EGFR fused to GFP containing a point mutation of A206K in the GFP sequence to prevent GFP dimerization (EGFR-mGFP) was a kind gift from Hung-Jun Liao, Vanderbilt University (Liao and Carpenter, 2007). Cells were seeded at a density of 1.0 x 10^5 cells per well into Lab-Tek II 2-well chambered coverglass slides (Nalge Nunc, Rochester, NY) 24 h prior to transfection and cultured in complete RPMI media containing 50 µM fatty acid. Cells were cotransfected with 0.3 µg RFP-tH and 1.5 µg EGFR-mGFP using Effectene (Qiagen, Valencia, CA) in media without fatty acid according to the manufacturer's instructions. Transfection conditions were optimized to minimize the amount of DNA and lipofection reagent used to avoid nonspecific cytotoxicity. Four h after transfection, cells were washed and the media was replaced and supplemented with 50 µM fatty acid for 48 h. Cells were incubated in serum-starvation media (0.5% FBS) with fatty acid for the final 16-18h prior to imaging. Cells were imaged 48 h after transfection. Prior to imaging, cultures were washed with

Leibovitz's L-15 medium (Gibco) followed by addition of 1 mL of Leibovitz's media (without serum) per well. Images were collected with a Zeiss 510 META NLO Multiphoton Microscope System consisting of an Axiovert 200 MOT microscope (Carl Zeiss Microimaging, Thornwood, NY) equipped with argon and helium-neo lasers, PMT, and LSM software. For EGFR-mGFP and RFP-tH, excitation wavelengths of 488 nm and 543 nm were used, and fluorescence emission was monitored at 530 nm and 590 nm, respectively. Images were collected in confocal mode with the pinhole set at 1 AU using a 40X objective (1.3 NA oil immersion lens) at room temperature. Identical acquisition parameters were used for all images within the experiment. Colocalization at the plasma membrane was analyzed by quantifying Mander's colocalization coefficient for green (EGFR-mGFP) with red (RFP-tH) using Nikon Elements AR 3.2. Analysis was performed on background-subtracted 16-bit images.

2.2.4 Western blotting

For western blotting, cells were homogenized in ice-cold homogenization buffer (50 mM Tris-HCl, pH 7.2, 250 mM sucrose, 2 mM EDTA, 1 mM EGTA, 50 mM sodium fluoride, 100 mM sodium orthovanadate, 1%Triton X-100, 100 µM activated sodium orthovanadate, 10 mM β-mercaptoethanol, and protease inhibitor cocktail) as previously described (Davidson et al., 1999). Following homogenization, lysates were sheared using a 29G needle, incubated on ice for 30 min, and centrifuged at 16,000 x *g* for 20 min. The supernatant was collected and protein concentration was assessed using Coomassie Plus Protein assay (Pierce). Lysates were treated with 1X pyronin sample buffer and subjected to SDS polyacrylamide gel electrophoresis (PAGE) in precast 4–

20% Tris-glycine mini gels (Invitrogen). After electrophoresis, proteins were electroblotted onto a polyvinylidene fluoride membrane with the use of a Hoefer Mighty Small Transphor unit at 400 mA for 90 min. Following transfer, the membrane was incubated in 5% BSA (Roche) and 0.1% Tween 20 in TBS (TBST) at room temperature for 1 h with shaking, followed by incubation with shaking overnight at 4^{o}C with primary antibody diluted in 5% BSA in TBST. Membranes were washed with TBST and incubated with peroxidase conjugated secondary antibody as per manufacturer's instructions. Bands were developed using Pierce SuperSignal West Femto^{TM} maximum sensitivity substrate. Blots were scanned using a Fluor-S Max MultiImager system (Bio-Rad, Hercules, CA). Quantification of bands was performed using Quantity One software (Bio-Rad). Monoclonal rabbit anti-EGFR, phospho-EGFR (Tyr1068), Akt, phospho-Akt (Ser473), ERK1/2, p-ERK1/2, STAT3, phospho-STAT3 (Tyr705), p70 S6kinase, and phospho-p70 S6kinase (Thr389) and monoclonal mouse phospho-tyrosine were purchased from Cell Signaling (Danvers, MA). Affinity purified mouse anti-clathrin heavy chain and purified mouse anti-caveolin 1 were purchased from BD Transduction Laboratories (Bedford, MA). Peroxidase conjugated goat anti-rabbit IgG was purchased from Kirkegaard and Perry Laboratories (Gaithersburg, MD), and peroxidase conjugated goat anti-mouse IgG was purchased from Jackson ImmunoResearch (West Grove, PA). For detection of ganglioside GM-1, peroxidase conjugated cholera toxin B subunit was purchased from Sigma.

2.2.5 Immunoprecipitation

Cell lysates were incubated with rotation purified polyclonal rabbit anti-EGFR antibody (Millipore, Billerica, MA) overnight. The protein-antibody conjugates were then pulled down using protein-G conjugated Dynabeads (Invitrogen). Protein was eluted from the Dynabeads using 2X pyronin buffer, and equal volumes of the samples were run on SDS-PAGE and western blotted for EGFR, phospho-tyrosine, or ubiquitin. Lysates analyzed for ubiquitination of EGFR were treated with 5 mM N-ethylmaleimide to prevent post lysis deubiquitination of EGFR (Gan et al., 2010).

2.2.6 Cell proliferation and viability

YAMC cells (both wild-type and $EGFR^{-/-}$) were treated with fatty acids for 24 h prior to being seeded into a 96-well plate at a density of 1.0×10^5 cells per well. Cells were cultured in complete media supplemented with fatty acids for an additional 48 h. Cells were then washed with PBS and cell proliferation was measured using CyQuant cell proliferation assay (Molecular Probes, Grand Island, NY) according to the manufacturer's instructions. Cell viability was assessed using Trypan blue (Invitrogen). YAMC cells were grown in T-175 flasks and untreated or treated with fatty acids (DHA or LA) for 72 hours. Cells were then trypsinized and placed into a conical tube. Trypsin activity was neutralized using complete RPMI-1640 media. A 0.4% trypan blue solution in PBS was prepared, and a cell suspension to trypan blue solution was prepared at a ratio of 10:1. This preparation was then loaded onto a hemocytometer, and the number of blue (dead) and total cells was counted.

2.2.7 Mice

Female C57BL/6 wild-type mice were used. All procedures followed guidelines approved by the U.S. Public Health Service and the Institutional Animal Care and Use Committee at Texas A&M University. This study and all animal protocols and procedures were approved by the Institutional Animal Care and Use Committee at Texas A&M University (Permit number: AUP2010-079). All efforts were made to minimize suffering. Mice were maintained under barrier conditions and initially consumed a Teklad commercial mouse non-purified diet (Harlan, Indianapolis, IN) ad libitum. Mice were maintained for 15 weeks on a semi-purified defined diet that was adequate in all nutrients, containing 320 (g/kg diet) sucrose, 200 casein, 220 corn starch, 3 DL-methionine, 35 AIN 76 salt mix, 10 AIN 76 mineral mix, 2 choline chloride, 60 cellulose (Bio-Serv, Frenchtown, NJ), 150 corn oil (CO) (Dyets, Bethlehem, PA) or 115 vacuum-deodorized Menhaden fish oil (FO) (Omega Protein, Houston, TX) plus 35 CO. The animals were provided the defined diet 2 weeks prior to an injection of azoxymethane (AOM; 7.5 mg/kg body weight). One week after the AOM injection, mice were exposed to 3 cycles of 1% dextran sulfate sodium (DSS) for 4 d followed by 17 d of recovery. Mice were sacrificed 6 weeks after the last DSS treatment (13 weeks post AOM injection) by CO_2 asphyxiation. Colon lesions were mapped and excised prior to colonic mucosa isolation by scraping, and the mucosa was snap frozen in liquid nitrogen and stored at -80°C until homogenization. Lesions were fixed in 4% paraformaldehyde, embedded in paraffin, stained with hematoxylin-eosin, and evaluated in a blinded manner by a board-certified pathologist. For immunoblotting, mucosa was homogenized

in ice-cold homogenization buffer as described above. For immunoprecipitation, mucosa was homogenized using Pierce Classic™ IP lysis buffer according to the manufacturer's instructions. Following homogenization, lysates were sheared using a 29G needle, incubated on ice for 30 min, and then centrifuged at 16,000 x *g* for 20 min. The supernatant was collected. Protein concentration was determined using Coomassie Protein Plus assay (Pierce).

2.2.8 Statistics

The effect of 2 independent variables (treatment effects) was assessed using Student's t-test. The effect of more than 2 independent variables (treatment effects) was assessed using the one-way analysis of variance test (ANOVA), and differences among means were evaluated using Tukey's post-hoc test of contrast. P values <0.05 were considered to be statistically significant.

2.3 Results

2.3.1 DHA reduces partitioning of EGFR into lipid raft domains

Lateral organization of EGFR within the plasma membrane is directly linked to receptor function. Previous reports have shown that n-3 PUFA can alter the localization of EGFR within the plasma membrane of lung and breast cancer cells (Rogers et al., 2010; Schley et al., 2007). Therefore, we first determined the effect of DHA on localization of EGFR within the plasma membrane of colonocytes. Experiments were conducted using the YAMC cell line, originally described by Whitehead and colleagues (Whitehead et al., 1993). We employed two complementary, established methods to

investigate the localization of EGFR. First, a detergent-free method of plasma membrane fractionation to isolate lipid raft enriched domains was utilized (Ma et al., 2004). We chose to use a detergent-free method due to strong evidence suggesting that detergent-based methods of extraction can lead to artifacts (Smart et al., 1995). Cells were either untreated (control; no fatty acid) or incubated with 50 μM DHA or LA (control fatty acid) for 72 h. We utilized this dose of fatty acid because we have previously found that it can recapitulate similar results as feeding a fish-oil enriched diet to experimental animal models(Fan et al., 2003b). Additionally, consumption of an n-3 PUFA enriched diet can result in circulating levels of DHA in excess of 50 μM (Kim et al., 2010b). Furthermore, we treat our cell cultures with BSA-complexed fatty acids, which resemble the non-esterified fatty acids that are bound to albumin *in vivo.* For the final 16-18 h of fatty acid treatment, cells were serum starved (0.5% FBS) prior to harvesting because EGFR has been shown to be localized to lipid rafts prior to activation. The bulk plasma membrane was isolated and fractionated on density gradients into three fractions, and each fraction was analyzed for EGFR using western blotting. The lowest density fraction from each treatment was enriched with caveolin and GM-1, which served as lipid raft markers, and depleted of clathrin, which is excluded from lipid rafts, indicating that this fraction is enriched with lipid rafts. In control and LA treated cells, EGFR was highly concentrated in the lipid raft enriched (LR) fraction of the plasma membrane (Fig. 2). This fraction exhibited a more than three-fold enrichment in EGFR compared to the intermediate density membrane (IDM) and high density membrane (HDM) fractions. However, in DHA treated cells, EGFR

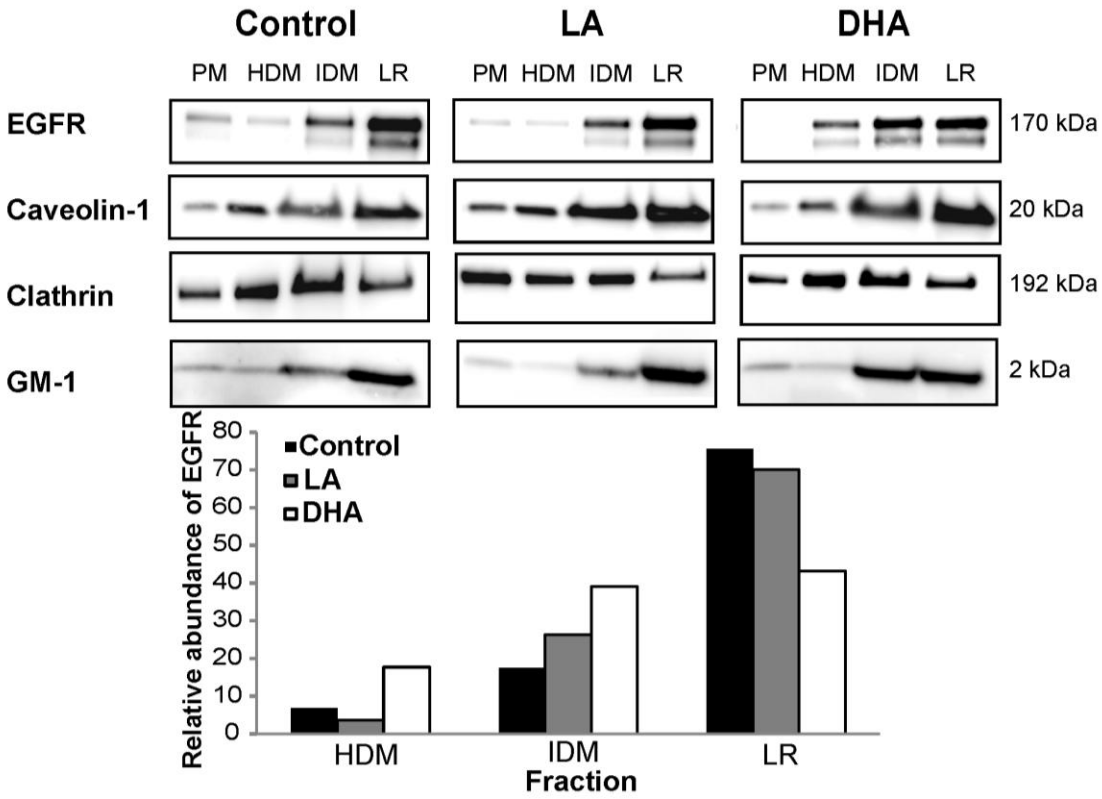

Figure 2. DHA reduces the localization of EGFR to lipid rafts. YAMC cells were treated with 50 μM BSA-complexed fatty acids for 72 h (12 flasks per treatment). For the final 16-18 h, cells were serum starved (0.5% FBS) with the same concentration of fatty acids. Cells were harvested from each flask, pooled (n=12), and the plasma membrane (PM) was isolated. Following isolation, the plasma membrane was fractionated into 3 distinct fractions, high density membrane (HDM), intermediate density membrane (IDM), and lipid raft enriched membrane (LR) by gradient ultracentrifugation. Fractions were collected and an equal amount of protein from each fraction was analyzed by western blotting using antibodies against EGFR, caveolin-1, and clathrin or using peroxidase conjugated cholera toxin B subunit (for GM-1). Quantification of band intensity was performed, and data are presented as the relative amount of EGFR in each fraction, with the sum of each fraction equaling 100. Western blots are representative of 2 independent experiments. C, control; LA, linoleic acid; DHA, docosahexaenoic acid; PM, plasma membrane; HDM, high density membrane; IDM, intermediate density membrane; LR, lipid raft enriched membrane.

displayed a more even distribution across all plasma membrane fractions. In fact, we observed equal enrichment of EGFR in the LR and IDM fractions in DHA treated cells. These results indicate a change in EGFR localization within the plasma membrane upon treatment with DHA.

To corroborate our initial results, confocal fluorescence microscopy was also used to determine localization of EGFR. Control and fatty acid treated cells were co-transfected by means of lipofection with plasmids encoding monomeric GFP-tagged EGFR (EGFR-mGFP) and RFP-tagged truncated H-Ras (RFP-tH). RFP-tH, which is targeted by a CAAX motif that is both palmitoylated and farnesylated, is a well-established lipid raft marker that is localized exclusively to low density fractions on sucrose gradients (Prior et al., 2001). It additionally has been clearly demonstrated to form cholesterol dependent nanoclusters on the inner leaflet of the plasma membrane (Plowman et al., 2005; Prior et al., 2003). RFP and GFP are ideal for colocalization studies because they do not have overlapping excitation and emission peaks. Colocalization was quantified by calculating Mander's colocalization coefficient at the plasma membrane. In control and LA treated cells, plasma membrane EGFR-mGFP strongly colocalized with RFP-tH (Fig. 3). This colocalization was significantly decreased by treatment with DHA. These results are intriguing and indicate that DHA altered the localization of EGFR, RFP-tH, or both within the membrane. However, interpretation of these results in regards to lipid rafts is limited due to the fact that rafts are below the limit of resolution (~200 nm) using confocal microscopy. Interestingly, in many of the DHA treated cells, EGFR-GFP and RFP-tH formed patches in the

membrane that were localized in close proximity to each other, but not overlapping. Additionally, the overall localization of the lipid raft marker, RFP-tH, was altered by treatment with DHA, which is in agreement with a plethora of data suggesting that DHA alters lipid rafts (Chapkin et al., 2008c; Kim et al., 2008; Shaikh et al., 2009b). Lastly, whereas EGFR was primarily localized to the plasma membrane in control and LA treated cells, a substantial proportion of EGFR in the DHA-treated cells was localized intracellularly. This allows us to conclude that DHA altered the cellular localization of EGFR. Overall, these complementary datasets strongly indicate that DHA treatment altered the plasma membrane organization of EGFR within colonocytes, which is consistent with previous observations in breast and lung cells (Rogers et al., 2010; Schley et al., 2007).

2.3.2 DHA increases EGFR phosphorylation

Due to the role that lipid rafts play in the regulation of EGFR activation and downstream signaling, we next investigated the effects of DHA on EGFR activation status and signaling in YAMC cells. Untreated and fatty acid treated cells were serum-starved (0.5% FBS) overnight in order to reduce signaling from growth factors within the serum. Subsequently, cells were stimulated with 25 ng/mL EGF for 10 min followed by isolation of cell lysates. To assess the effects of fatty acid treatment on EGF-induced EGFR phosphorylation, lysates were probed for EGFR phosphorylated on Tyr1068, one of the major sites of EGFR phosphorylation that is involved in activation of downstream signaling. EGF stimulated EGFR phosphorylation in all treatment groups (Fig. 4).

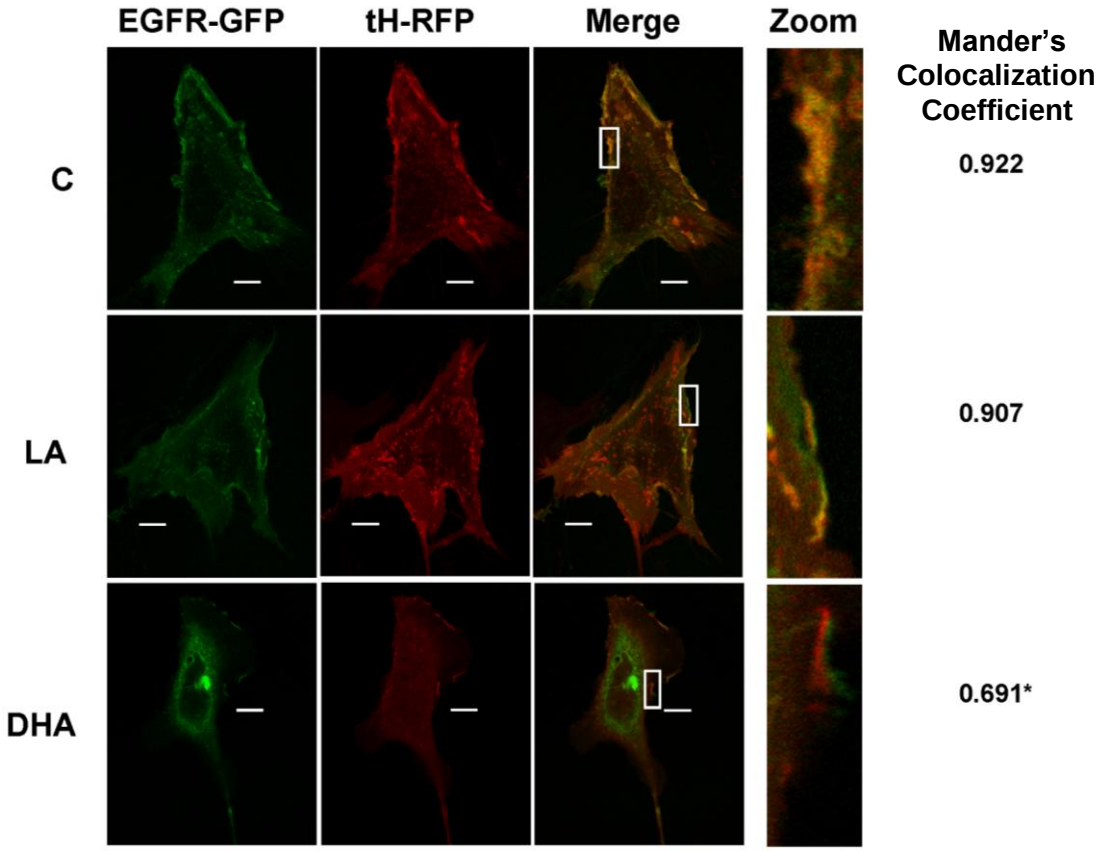

Figure 3. DHA reduces colocalization of EGFR with the lipid raft marker, tH. YAMC cells were treated with 50 μM BSA-complexed fatty acids for 72 h. Twenty-four h after initiating fatty acid treatment, cells were co-transfected with RFP-tH and EGFR-mGFP. Approximately 32 h after transfection, cells were incubated in serum starvation media (0.5% FBS) overnight prior to imaging. Images are representative of 4 independent experiments. Whole cell images of each individual channel and the merged images are shown on the left. High magnification images of the plasma membrane are shown on the right. Mander's colocalization coefficient was calculated at the plasma membrane for the amount of EGFR-mGFP (green) colocalizing with tH-RFP (red) using Nikon Elements AR 3.2. The coefficient is the mean of n=30-40 cells per treatment. Statistical significance between treatments (*P<0.05) was determined using ANOVA and Tukey's test of contrast. Bars,10 μm.

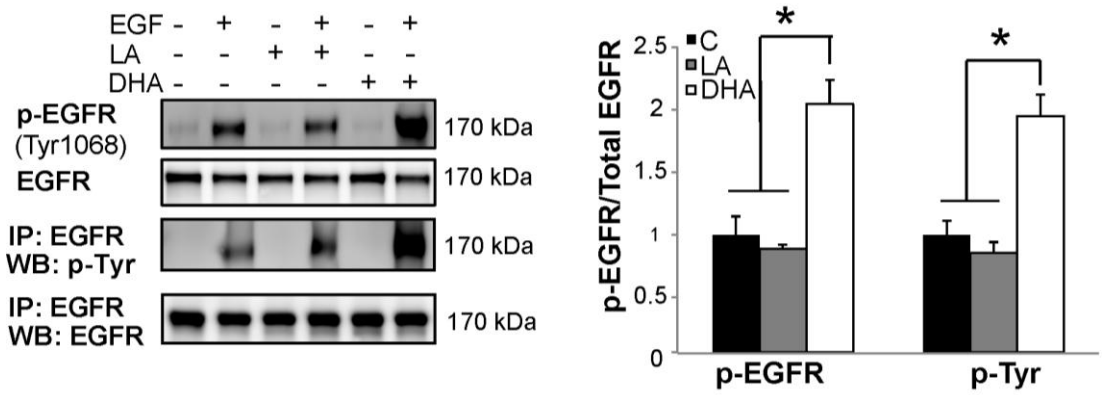

Figure 4. **DHA enhances ligand-induced phosphorylation of EGFR.** YAMC cells were treated with BSA-complexed fatty acids for 72 h. For the final 16-18 h, cells were incubated in serum starvation (0.5% FBS) with the same concentration of fatty acids. Cells were either unstimulated or stimulated for 10 min with 25 ng/mL EGF and subsequently harvested. A) Equal amounts of protein from whole cell lysates were western blotted for total and phosphorylated (Tyr1068) EGFR. Additionally, EGFR was immunoprecipitated from total cellular lysates prior to western blotting for EGFR and phosphorylated tyrosine resides. Quantification of band volume was performed and data are presented as mean ± SEM normalized to control (n=3-4 experiments per treatment). Data are expressed as the ratio of the phosphorylated receptor to total receptor and normalized to control. Statistical significance between treatments (*P<0.05) was determined using ANOVA and Tukey's test of contrast. C, control; LA, linoleic acid; DHA, docosahexaenoic acid

However, DHA treatment resulted in a greater than two-fold increase in EGFR phosphorylation compared to untreated control or LA treated cells. EGFR was also immunoprecipitated from cell lysates followed by immunoblotting for total phosphorylated tyrosine residues. Consistent with the results for Tyr1068, DHA enhanced total EGFR tyrosine phosphorylation by greater than two-fold (Fig. 4). We additionally determined if higher doses of DHA could further increase EGFR phosphorylation. YAMC cells were treated with 50, 75, and 100 μM DHA for 72 h and stimulated with EGF. We found that all doses lead to an increase in EGFR phosphorylation, but there was no further increase in EGFR phosphorylation at higher doses of DHA (Fig. 5). Therefore, we continued using the physiologically relevant dose of 50 μM DHA for future experiments.

Since DHA and EPA are both long chain omega-3 fatty acids that have been shown to reduce colon tumor development, we examined whether each of these fatty acids cause an increase in EGFR phosphorylation or if the effect is specific to DHA. We also assessed the effects of arachidonic acid (AA; 20:4 n-6) on EGFR phosphorylation as a control, long-chain n-6 PUFA. This allows us to compare the effects of fatty acids with 4, 5, and 6 double bonds. Cells were treated with fatty acids, serum-starved, and stimulated with EGF as in previous experiments. Cell lysates were probed for phosphorylated EGFR. Neither AA nor EPA treatment resulted in an increase in EGFR phosphorylation compared to control (Fig. 6). Only DHA treatment increased the phosphorylation status of EGFR, indicating a unique property of this fatty acid.

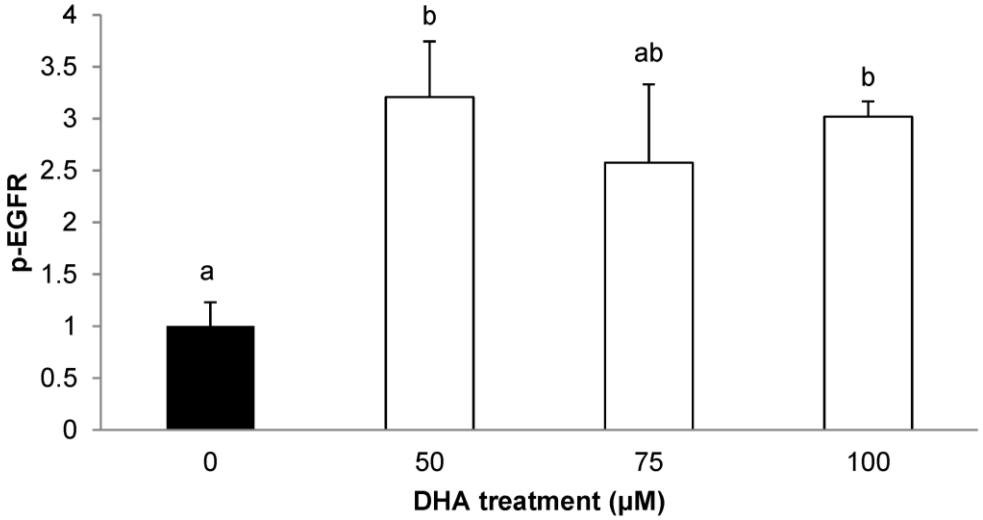

Figure 5. **Low doses of DHA are effective for enhancing EGFR phosphorylation.** YAMC cells were treated with varying concentrations of BSA-complexed DHA (0, 50, 75, or 100 μM) for 72 h. For the final 16-18 h, cells were incubated in low serum media (0.5% FBS) with the same concentration of fatty acid. Cells were then stimulated for 10 min with 25 ng/mL EGF and subsequently harvested. Equal amounts of protein from whole cell lysates were western blotted for phosphorylated (Tyr1068) EGFR. Quantification of band volume was performed and data are presented as mean ± SEM normalized to control (n=3 experiments per treatment). Data are expressed as the ratio of the phosphorylated receptor to total receptor and normalized to control. Statistical significance between treatments (represented by different letters, $P<0.05$) was determined using ANOVA and Tukey's test of contrast. DHA, docosahexaenoic acid

We postulated that if the DHA-induced phosphorylation of EGFR is a result of membrane enrichment causing disruption of lipid rafts, then the effect should be reversible by depleting the cells of DHA. To test this hypothesis, cells were treated with DHA, followed by a washout period wherein the cells were either left untreated or treated with LA. We have previously shown that this wash-out period is sufficient to reduce the amount of DHA in the plasma membrane (Seo et al., 2006). Following the wash-out period in DHA treated cells, ligand-induced EGFR phosphorylation was normalized back to the same level as control (Fig. 7). These data indicate that the

inhibition of EGFR signaling by DHA is dependent on its presence in the plasma membrane.

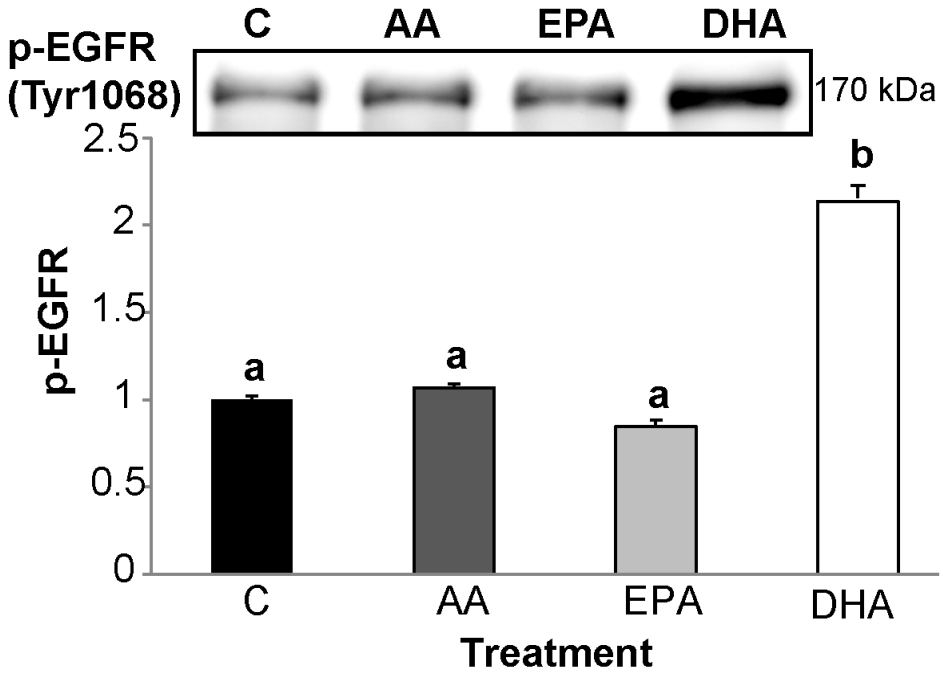

Figure 6. DHA uniquely modifies EGFR phosphorylation. YAMC cells were treated with BSA-complexed fatty acids for 72 h. For the final 16-18 h, cells were incubated in serum starvation (0.5% FBS) with the same concentration of fatty acids. Cells were either unstimulated or stimulated for 10 min with 25 ng/mL EGF and subsequently harvested. Lysates were assessed by western blotting for phosphorylated EGFR (Tyr1068). The blot is representative of 3 independent experiments. Data are presented as mean ± SEM of phosphorylated EGFR, normalized to control. Statistical significance between treatments as indicated by different letters ($P<0.05$) was determined using ANOVA and Tukey's test of contrast. C, control; AA, arachidonic acid; EPA, eicosapentaenoic acid; DHA, docosahexaenoic acid; LA, linoleic acid.

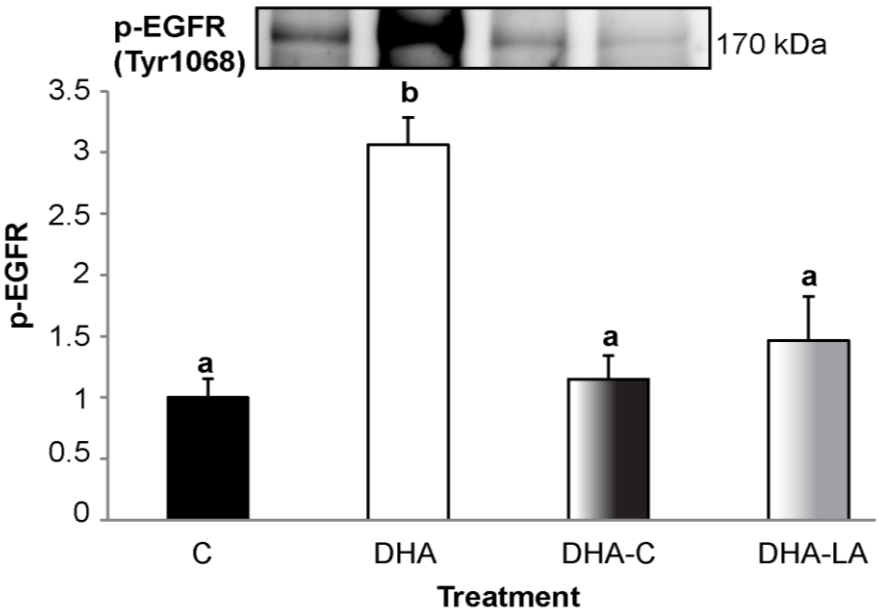

Figure 7. Washout of DHA from the plasma membrane reverses the effect of DHA on EGFR phosphorylation. YAMC cells were either untreated or treated with 50 µM DHA for 72 h. Select DHA treated cultures were then washed and incubated for an additional 40 h with either untreated media or 50 µM LA. For the final 16-18 h, cells were serum starved (0.5% FBS) followed by stimulation with 25 ng/mL EGF then harvested. Lysates were assessed by western blotting for phosphorylated EGFR (Tyr1068). The blot is representative of 3 independent experiments. Data are presented as mean ± SEM of phosphorylated EGFR, normalized to control. Statistical significance between treatments as indicated by different letters (P<0.05) was determined using ANOVA and Tukey's test of contrast. C, control; DHA, docosahexaenoic acid; LA, linoleic acid.

2.3.3 DHA suppresses activation of downstream mediators of EGFR signaling

Since EGFR phosphorylation is characteristically associated with activation of downstream signaling, we probed cell lysates for phosphorylation of downstream effector proteins, including ERK1/2, STAT3, and Akt. In cells treated with DHA, there was a ~50% reduction in the EGF-stimulated activation of ERK1/2 and STAT3

compared to untreated control and LA treated cells (Fig. 8). DHA had no effect on Akt phosphorylation at Ser473 (Fig. 8). However, Akt phosphorylation at this site was not significantly induced by EGF stimulation in any of the treatment groups. To assess mTORC1 activity, we measured phosphorylation of S6K, a kinase that is directly phosphorylated by mTOR at Thr389. We found that DHA significantly suppressed EGF-induced phosphorylation of S6K, indicating reduced activation of mTOR (Fig. 8). Together, these data suggest that DHA disrupts the EGFR signaling cascade in colonocytes.

We further investigated the effect of DHA on EGFR phosphorylation and signaling at multiple time points. Untreated control and DHA treated cells were stimulated with 25 ng/mL EGF for 0-30 min. Consistent with initial results, EGFR phosphorylation was significantly increased by DHA treatment at 2, 5, and 10 min following stimulation (Fig. 9 A). EGFR phosphorylation peaked in DHA treated cells at 5 min and started decreasing, whereas EGFR phosphorylation was highest at 10 min in control samples, suggesting a dynamic alteration in EGFR regulation. Downstream signaling from EGFR through ERK1/2 and STAT3 was suppressed by DHA at each time point assessed (Fig. 9, B and C).

2.3.4 Suppression of cell proliferation by DHA

In order to document a functional endpoint of the DHA-induced decrease in EGFR signaling, we chose to measure cell proliferation, which is regulated in part by signaling through EGFR. DHA treatment of wild-type YAMC cells resulted in an approximately 40% decrease in cell proliferation compared to control and LA treated

cells (Fig. 10). Additionally, the effect of DHA on proliferation of an isogenic cell line that does not express EGFR ($EGFR^{-/-}$) was assessed. Interestingly, DHA treatment had no effect on cell proliferation in $EGFR^{-/-}$ YAMC cells compared to control. Together, these data demonstrate that DHA suppresses cell proliferation in an EGFR-dependent manner. Additionally, LA was found to increase cell proliferation in both wild-type and $EGFR^{-/-}$ cells, suggesting that this effect is EGFR-independent.

To verify that the DHA-mediated reduction in cell number is a direct result of decreased cell proliferation and not caused by an increase in cell death, we additionally assessed cell viability in control, LA, and DHA treated YAMC cells. Cell viability was assessed using the trypan blue assay. DHA had no effect on cell viability compared to control and LA treated cells (Fig. 11). This corroborates previously reported data that DHA does not increase apoptosis in the YAMC cell line (Kolar et al., 2007). These results confirm that the reduction in cell number mediated by DHA is a result of suppressed cell proliferation and not an induction of cell death.

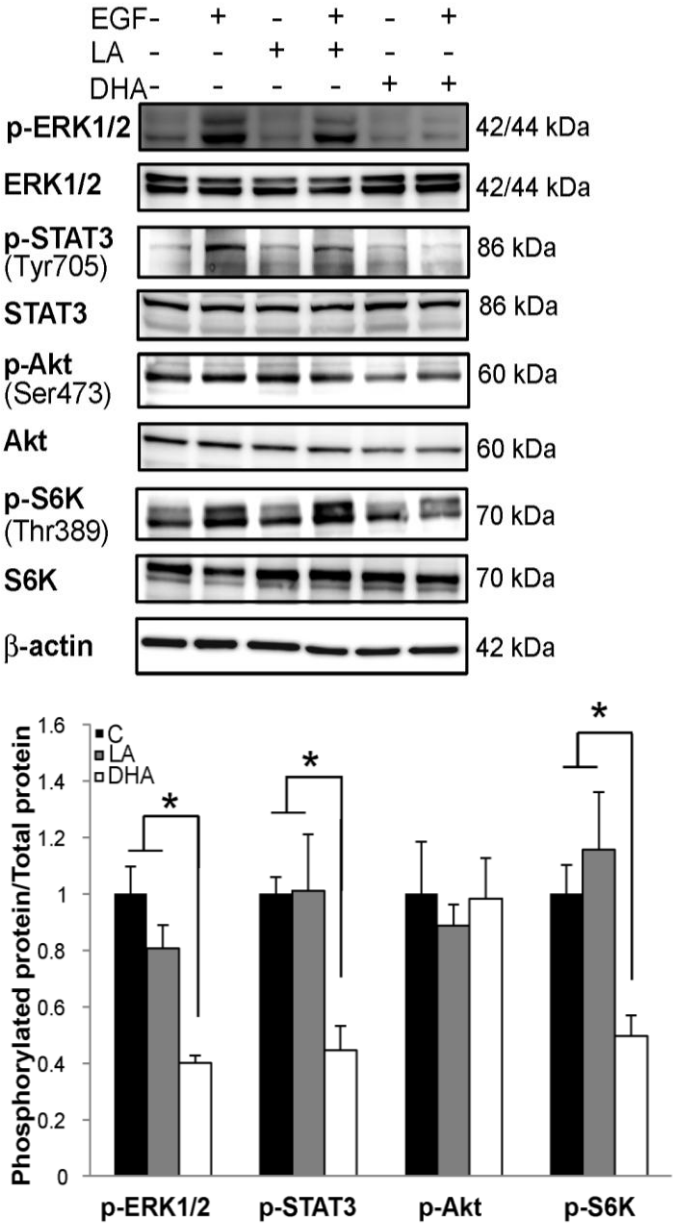

Figure 8. DHA reduces the EGF-induced activation of ERK1/2, STAT3, and S6K. Whole cell lysates were analyzed by western blotting for total and phosphorylated downstream mediators of EGFR signaling, including ERK1/2, STAT3, S6K, and Akt. Each blot is representative of 3-4 independent experiments with 3 replicates per treatment. Band quantification was performed, and data are presented as mean ± SEM normalized to control (n=3-4 experiments per treatment). Data are expressed as the ratio of the phosphorylated receptor to total receptor and normalized to control. Statistical significance between treatments (**P*<0.05) was determined using ANOVA and Tukey's test of contrast. C, control; LA, linoleic acid; DHA, docosahexaenoic acid.

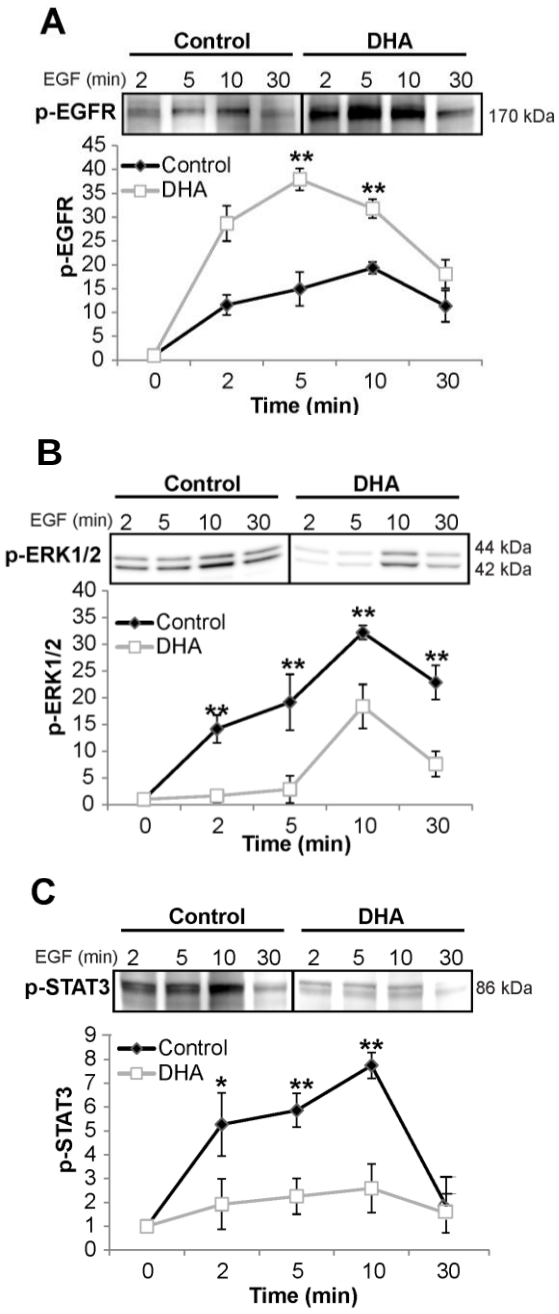

Figure 9. DHA alters the kinetics of EGFR activation and signaling. YAMC cells were treated with control or BSA-complexed DHA for 72 h. For the final 16-18 h, cells were incubated in low serum media (0.5% FBS) with the same concentration of fatty acids. Cells were stimulated for 0-30 min with 25 ng/mL EGF and subsequently harvested. Equal concentrations of protein from the whole cell lysates were analyzed by western blotting for (A) phosphorylated EGFR, (B) phosphorylated ERK1/2, and (C) phosphorylated STAT3. Each immunoblot is representative of 3 independent experiments. Quantification of band volume was performed and data are presented as mean ± SEM and normalized to time 0 (n=3). Statistical significance between treatments (**P*<0.05; ***P*<0.01) was determined using Student's *t*-test.

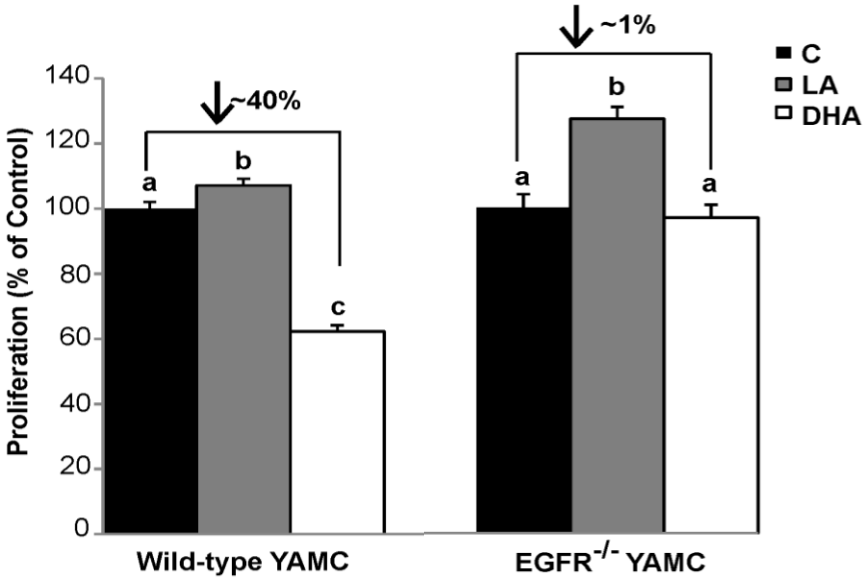

Figure 10. DHA reduces cell proliferation in an EGFR-dependent manner. Wild-type and EGFR$^{-/-}$ YAMC cells were treated with 50 μM BSA-complexed fatty acid for 24 h. Following the initial treatment, cells were seeded at an equal density into a 96-well plate, and cultured under the same treatment conditions for an additional 48 h. Cell proliferation was measured using CyQUANT cell proliferation assay. Results are representative of 3 independent experiments. Data are expressed as mean ± SEM (n=6 samples per treatment). Statistical significance between treatments as indicated by different letters (P<0.05) was determined using ANOVA and Tukey's test of contrast. No comparisons were made between proliferation of wild-type and EGFR$^{-/-}$ cells.

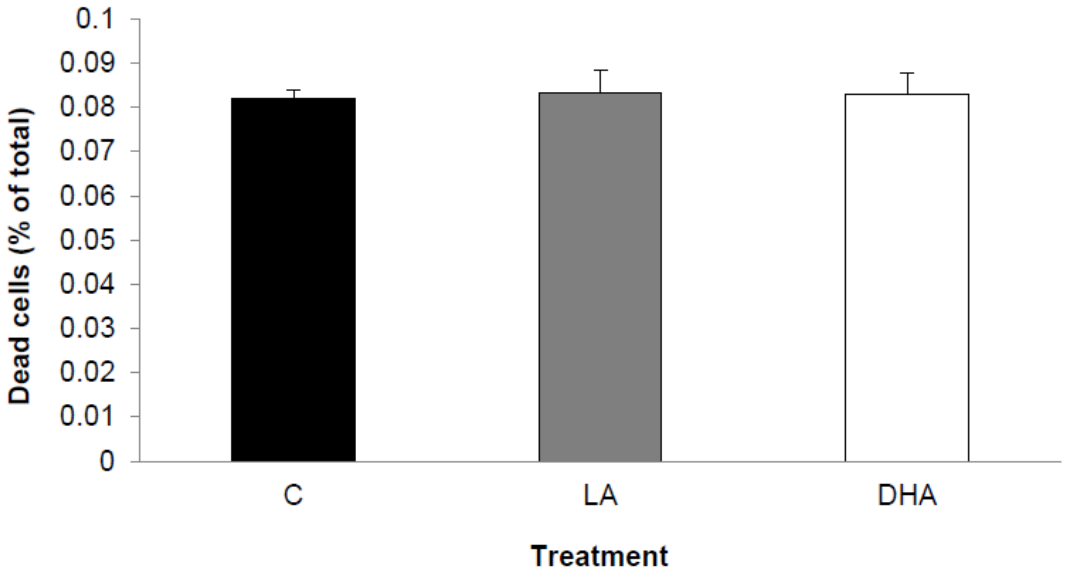

Figure 11. DHA does not induce cell death. YAMC cells were treated with control or BSA-complexed fatty acids (LA or DHA) for 72 h. Cells were trypsinized and stained with Trypan blue. The number of dead and total cells was counted using a hemocytometer. Data are presented as the mean of the number of dead cells/total number of cells ± SEM. No statistical significance between treatments (P<0.05) was observed as calculated using ANOVA and Tukey's test of contrast.

2.3.5 Effect of fish oil on EGFR phosphorylation

The *in vitro* data clearly demonstrating the capacity of DHA to alter EGFR signaling prompted us to test the effect of feeding a fish oil diet to mice on EGFR signaling and tumor development in the colon. We utilized an established model for colon cancer induction in mice. This model consists of a single injection of the carcinogen azoxymethane (AOM) and multiple rounds of inflammation that are induced with dextran sodium sulfate (DSS). AOM forms DNA adducts, and the repeated rounds of DSS and recovery mimic the active and inactive inflammation experienced by humans. This combination of AOM and DSS results in both flat and polypoid lesions

similar to those seen in humans with the disease, as well as the nuclear translocation of β-catenin that is often observed in human colon cancer (Clapper et al., 2007). We evaluated the status of total and phosphorylated EGFR in colonic mucosa from AOM-injected, DSS-treated C57BL/6 mice fed diets enriched in fish oil (containing DHA) or corn oil (control, contains primarily LA and no n-3 polyunsaturated fatty acids). Protein lysates from the uninvolved colonic mucosa were harvested and western blotted for total and phosphorylated EGFR (Tyr1068) or immunoprecipitated for EGFR followed by western blotting for phosphorylated tyrosine residues. Consistent with the cell culture data, phosphorylation of EGFR increased approximately two-fold in mice fed a fish oil diet compared to mice fed a corn oil diet, while no difference in the total expression of EGFR was observed (Fig. 12).

2.3.6 Effect of fish oil on EGFR signaling

We further probed tissue lysates for phosphorylation of ERK1/2, STAT3, and Akt. Similar to Fig. 8 data, phosphorylation of ERK1/2 and STAT3 decreased by approximately 40% and 50%, respectively, in fish oil fed mice compared to corn oil fed mice with no difference in phosphorylation of Akt between diets (Fig. 13). Overall, these data indicate a role for dietary fish oil in regulation of EGFR signal transduction.

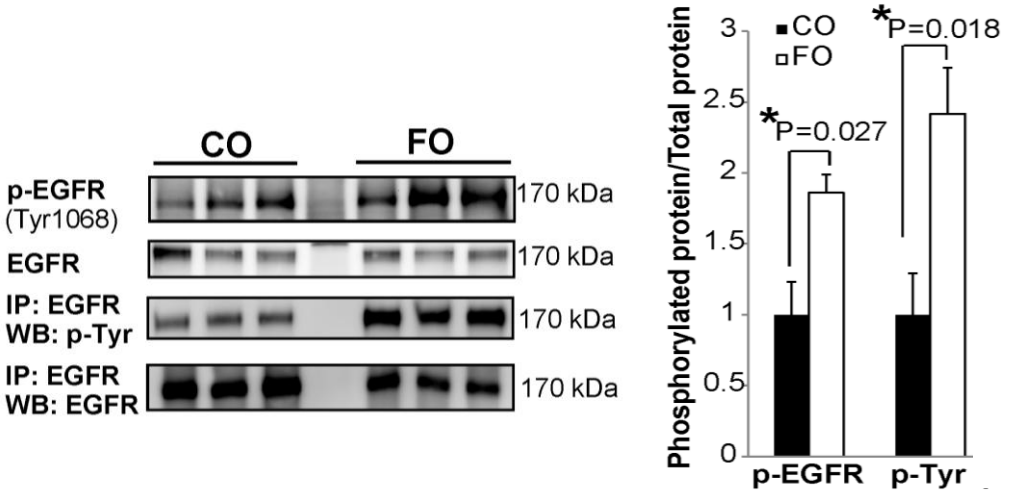

Figure 12. Fish oil feeding increases EGFR phosphorylation. Carcinogen (AOM) and DSS-treated mice were fed a diet enriched in fish oil or corn oil (contains no DHA) for a total of 15 weeks. Whole cell lysates were isolated from scraped colonic mucosa. Equal concentrations of protein were assessed by western blotting for total and phosphorylated EGFR (Tyr1068). Additionally, EGFR was immunoprecipitated from mucosal lysates and western blotted for phosphorylated tyrosine residues and EGFR. Each lane represents a different mouse (total n=12 mice per diet). Statistical significance between diets was determined using Student's *t*-test. CO, corn oil; FO, fish oil.

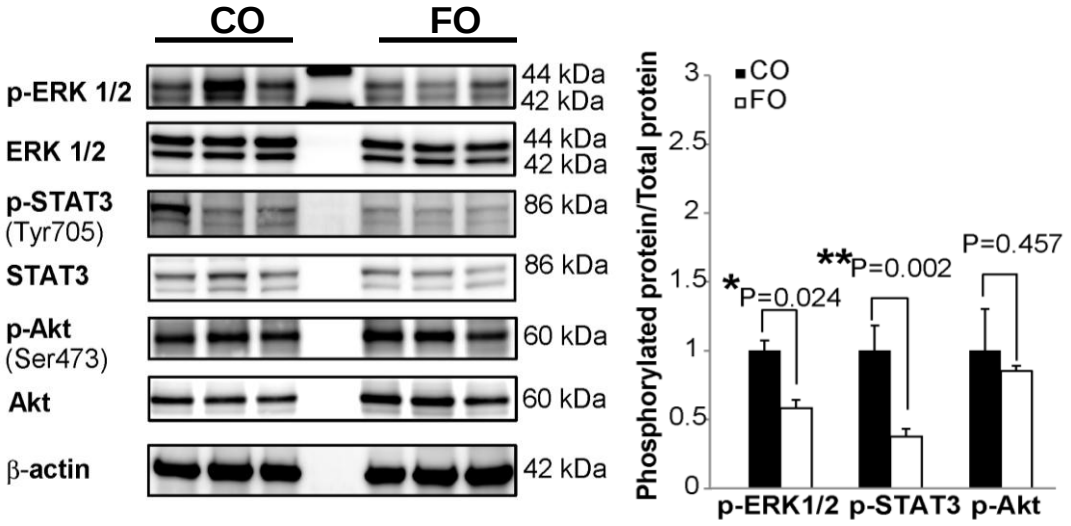

Figure 13. Fish oil feeding inhibits activation of downstream mediators of EGFR signaling. Carcinogen (AOM) and DSS-treated mice were fed a diet enriched in fish oil or corn oil (contains no DHA) for a total of 15 weeks. Whole cell lysates were isolated from scraped colonic mucosa and probed by western blotting for total and phosphorylated downstream mediators of EGFR signaling, including ERK1/2, STAT3, and Akt. Each lane represents a protein sample from a different mouse (total n=12 mice per diet). Quantification of band volume was performed and data are presented as mean ± SEM of the ratio of phosphorylated protein to total protein and normalized to CO. Statistical significance between diets was determined using Student's *t*-test. CO, corn oil; FO, fish oil.

2.3.7 Effect of fish oil on tumor formation

Ultimately, for a chemoprotective agent to be considered effective, it must be shown to prevent or reduce the formation of tumors in the tissue of interest. Therefore, we assessed the effect of fish oil feeding on tumor formation in the colon. At the time of sacrifice, colonic tumors from the animals were removed, followed by staining and typing. We found tumor formation in animals on both diets. Interestingly, fish oil fed animals developed fewer tumors compared to animals fed a corn oil diet (Fig. 14). Additionally, more fish oil fed animals (13 of 25) did not develop any tumors compared to corn oil fed animals (4 of 22). This indicates that fish oil contains chemoprotective properties.

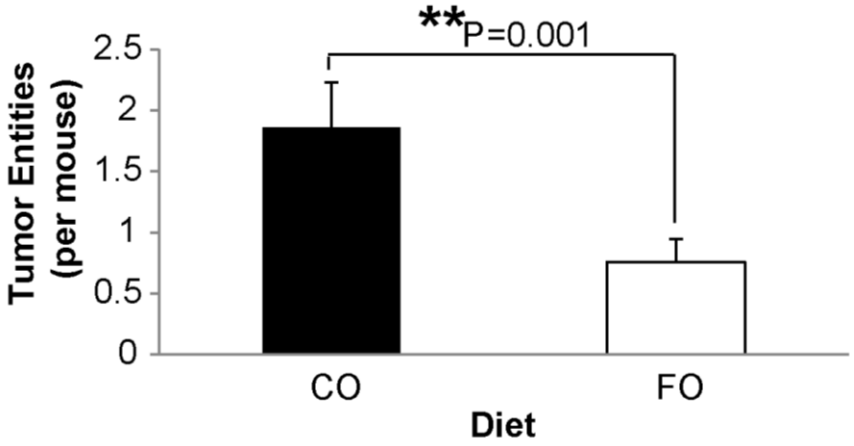

Figure 14. Fish oil reduces colon tumor multiplicity. Carcinogen (AOM) and DSS-treated mice were fed a diet enriched in fish oil or corn oil (contains no DHA) for a total of 15 weeks. Colon lesions were removed and fixed in 4% paraformaldehyde, embedded in paraffin, sectioned and stained with hematoxylin-eosin, and then evaluated. The mean colon tumor entity number, including adenomas and adenocarcinomas, per mouse in each diet treatment is presented, n=22-25 mice per diet. Statistical significance between diets was determined using Student's *t*-test. CO, corn oil; FO, fish oil.

2.4 Discussion

EGFR is a transmembrane receptor tyrosine kinase involved in transmitting external cues to the intestinal epithelium, thereby modulating cell proliferation, migration, and survival. Recent evidence suggests that the membrane lipid microenvironment can significantly modulate EGFR localization and function (Coskun et al., 2011). Here, we report that membrane incorporation of DHA alters the lateral organization of EGFR (Figs. 2 and 3). The lateral organization of the receptor has been shown to directly regulate ligand binding and receptor phosphorylation (Chen and Resh, 2002; Ringerike et al., 2002; Roepstorff et al., 2002). Consistent with these observations, we demonstrated that DHA treatment resulted in increased ligand-stimulated EGFR phosphorylation (Fig. 4). Therefore, the DHA-induced shift of EGFR localization within the plasma membrane alters the ability of the receptor to transphosphorylate. These findings favor a model in which receptor modulation by fatty acids is mediated by effects on the plasma membrane.

The differential effects of DHA and EPA, the two n-3 PUFAs enriched in fish oil, are often overlooked and underappreciated. Therefore, we assessed whether EPA had the same effect as DHA on EGFR phosphorylation. Interestingly, in contrast to DHA, neither EPA nor AA, another long-chain PUFA, exerted an effect on EGFR phosphorylation (Fig. 6). This is consistent with a previous study showing that DHA, but not EPA, suppressed EGF-stimulated activation of AP-1 (Liu et al., 2001). Collectively, these results highlight the uniqueness of DHA, which has been shown to significantly alter numerous membrane properties (Stillwell and Wassall, 2003; Wassall

and Stillwell, 2008). The effects of DHA on EGFR signaling are reversible when supplementation with DHA is discontinued and the fatty acid is washed out of the plasma membrane (Fig. 7). This is consistent with our hypothesis that DHA enrichment in the plasma membrane directly modulates EGFR signaling. DHA is a structurally unique fatty acid. It is slightly polar due to its six double bonds, and it rapidly reorients through multiple conformational states (Wassall and Stillwell, 2008). This flexible structure renders DHA incompatible with ordered saturated acyl chains and cholesterol, two major constituents of lipid rafts. Multiple biophysical studies utilizing model membranes and molecular dynamic simulations have shown that DHA acyl chains do not pack efficiently with cholesterol and saturated acyl chains (Rosetti and Pastorino, 2011; Soni et al., 2008). Although, the exact effect that DHA has on lipid rafts remains to be fully elucidated, an abundance of data clearly demonstrate that DHA can impede lipid raft mediated processes and alter lipid raft composition (Fan et al., 2004; Schley et al., 2007).

Lipid rafts are involved in sundry cellular processes, which require diversity in the composition of membrane domains (Pike, 2004). Both lipid-protein and lipid-lipid associations have the potential to organize features of the membrane, resulting in a heterogeneous population of lipid rafts. This heterogeneity is likely to result in differential effects of n-3 PUFA on lipid rafts. Therefore, the role of n-3 PUFA in the regulation of processes emanating from different types of lipid rafts is poorly understood and requires further investigation. Functional raft-based membrane heterogeneity is dependent upon both lipid and protein physical parameters (Lingwood et al., 2009), and

we have observed that n-3 PUFA can alter lipid raft composition of both lipids and proteins. Based on the interactions within certain raft domains, n-3 PUFA could be expected to perturb the function of some lipid raft domains while leaving others unaffected. Future research should be directed toward discerning the effects of n-3 PUFA on different types of lipid rafts.

According to the canonical process of signal transduction, the observed increase in EGFR phosphorylation upon treatment with DHA is expected to be correlated with enhanced downstream signaling. Two previous studies have observed that DHA increases EGFR phosphorylation, but they reported conflicting results regarding downstream signaling (Rogers et al., 2010; Schley et al., 2007). However, one of these studies did not directly stimulate cells with a ligand specific for EGFR, which renders the results difficult to interpret. Therefore, in our study, we evaluated the effect of DHA on EGF-stimulated activation of multiple signaling cascades in the colonic epithelium. Although DHA was found to increase EGFR phosphorylation, we noted that this fatty acid uniquely inhibited EGF-stimulated activation of downstream signaling from EGFR through ERK1/2, STAT3, and mTOR/S6K (Fig. 8). A substantial body of work has documented the central role of lateral membrane organization in mediating EGFR signal transduction (Lingwood and Simons, 2010). Integral to EGFR signaling is its localization to lipid raft domains due to the ability of these specialized membrane domains to assemble the molecular machineries necessary for intracellular propagation of EGFR signaling. Stimulation with EGF induces coalescence of lipid raft domains, promoting the formation of these signaling platforms, which suggests a central role for

these domains in EGFR signal propagation (Hofman et al., 2008). Our data suggest that by altering the plasma membrane localization of EGFR, DHA causes a paradoxical increase in EGFR phosphorylation and suppression of EGFR signal transduction. Studies have indicated that within the lipid raft, EGFR is slightly confined which partially restricts receptor activation (Ringerike et al., 2002). We hypothesize that the reduced partitioning of EGFR to lipid rafts upon DHA treatment is what facilitates the enhanced receptor phosphorylation. However, localization of EGFR within lipid rafts expedites interactions between EGFR and its downstream signaling partners. We therefore extrapolate that the altered localization of EGFR in DHA treated cells diminishes signal transduction by reducing the interactions of EGFR and its signaling partners. This attenuation of EGFR signaling then results in a diminution of cell proliferation (Fig. 10). Due to the reliance of cancer cells on overwhelming cell proliferation, this action of DHA likely contributes to its chemoprotective properties.

Phosphorylation of EGFR has previously been considered a marker for activation of downstream signaling. In contrast, our data describe a mechanism whereby DHA unfetters EGFR from the constraints of lipid rafts to increase phosphorylation, but this altered plasma membrane localization reduced colocalization of EGFR and its downstream signaling partners to suppress signal transduction. Further understanding of the relationship between plasma membrane composition and receptor organization is required to fully elucidate the regulation of cell signaling.

3. MECHANISMS OF ACTION OF DHA ON EGFR FUNCTION*

3.1 Introduction

The initial observations of the paradoxical effect of DHA on EGFR laid the groundwork for further investigation. Canonically, stimulation of EGFR with its ligand results in conformational changes that facilitate receptor dimerization. Receptor dimerization elicits activation of the tyrosine kinase domain, which then phosphorylates tyrosine residues on the C-terminal tail of dimerization partner. These phosphorylated tyrosine residues function as docking sites for downstream signaling mediators, and these mediators then activate multiple signaling cascades. Our data demonstrate that DHA increases the phosphorylation of EGFR while decreasing the activation of downstream signaling pathways. However, the molecular mechanisms underlying the enigmatic effects of DHA on EGFR function remain undetermined.

First, we wanted to clarify the mechanism by which DHA induces an increase in EGFR phosphorylation. Previous studies have suggested a number of possible contributing mechanisms. One potential mechanism is that by perturbing signal transduction DHA reduces feedback inhibition of EGFR phosphorylation. The activation status of EGFR is partially regulated by a feedback loop from downstream signaling events (Avraham and Yarden, 2011). Specifically, ERK1/2 activation modulates EGFR phosphorylation, and inhibition of ERK1/2 activation has been shown to result in increased EGFR phosphorylation (Gan et al., 2010). We have shown that

*Part of this chapter is reprinted with permission from "Alteration of EGFR spatiotemporal dynamics suppresses signal transduction" by Harmony F. Turk, Rola Barhoumi, and Robert S. Chapkin, 2012. *PLoS ONE,* 7, e39682, Copyright 2012 by Harmony F. Turk.

treatment with DHA reduces activation of ERK1/2, which could reduce feedback inhibition and lead to receptor hyperphosphorylation. Additionally, EGFR activation can also be significantly impacted by the environment in which the receptor resides. As detailed previously, the plasma membrane localization of EGFR considerably affects receptor activity. Redistribution of EGFR from lipid rafts to the bulk domain results in an increase in ligand-dependent and ligand-independent receptor phosphorylation (Chen and Resh, 2002; Lambert et al., 2006; Pike and Casey, 2002). EGFR localization to lipid raft domains restricts the receptor to some extent (Matveev and Smart, 2002), but the underlying cause of this remains unknown. One potential mechanism was presented by Coskun et al., who demonstrated that the lipid environment can directly influence EGFR dimerization, resulting in altered EGFR phosphorylation (Coskun et al., 2011). Therefore, by shifting EGFR from lipid rafts and altering the lipid environment of the receptor, DHA could potentiate EGFR dimerization and in so doing enhance receptor phosphorylation.

In addition to teasing out the mechanism of DHA-mediated increased EGFR phosphorylation, we also aimed to elucidate the process by which DHA reduces EGFR signal transduction. This required the identification of the specific step of signal transduction that is interrupted. We determined that EGF-induced activation of ERK1/2, STAT3, and mTOR is inhibited by DHA. Of these pathways, activation of ERK1/2 downstream of EGFR is the most direct and straightforward. The immediate proximal event in signal transduction following EGFR phosphorylation is recruitment of a cytosolic complex of Grb2 and son of sevenless (SOS) to the plasma membrane (Holt et

al., 1996). Grb2 is a 23-kDa adapter protein consisting of a single SH2 domain flanked by two SH3 domains (Lowenstein et al., 1992). Following EGFR phosphorylation, Grb2 traffics to EGFR and directly binds to the receptor at Tyr1068 and to a lesser extent Tyr1086 via its SH2 domain (Batzer et al., 1994). Grb2 can also indirectly link to EGFR through interaction with Shc, another SH2 domain containing adapter protein that can bind to phosphorylated EGFR at Tyr1173 and Tyr992 (Batzer et al., 1994). Binding of the Grb2-Sos complex to EGFR brings SOS into close proximity with its substrate, Ras. SOS is a guanylnucleotide exchange factor that activates the exchange of GDP for GTP on Ras, resulting in Ras activation (Chardin et al., 1993). GTP-bound Ras then recruits Raf to the membrane where it is activated. Raf activation results from phosphorylation that is dependent on both Ras and Src-family tyrosine kinase (Marais et al., 1995; Marais et al., 1997; Mason et al., 1999). Raf is a serine/threonine kinase that phosphorylates MEK1 and MEK2. MEK1/2 are dual-specificity protein kinases that facilitate the activation of ERK1/2 by phosphorylating them on tyrosine then threonine residues (Roskoski, 2012). Activation of each step in this signaling cascade is simple to assess, which will allow us to pinpoint the site of disruption in signal transduction.

The extent and duration of receptor signaling is regulated by receptor endocytosis and degradation. Many signaling mediators also function to facilitate receptor endocytosis. For example, in addition to leading to the activation of the Ras, Grb2 recruitment to EGFR is required for receptor endocytosis and degradation as well as (Jiang et al., 2003). EGFR endocytosis can also be affected by the plasma membrane localization of the receptor. EGFR endocytosis can occur through lipid raft-dependent

or –independent processes (Puri et al., 2005; Sigismund et al., 2008). The principal two endpoints of receptor endocytosis are receptor recycling back to the plasma membrane or targeting of the receptor for degradation. Receptor ubiquitination, which is mediated by Grb2-dependent recruitment of c-Cbl, ensures sorting of EGFR to lysosomes (Umebayashi et al., 2008). Receptor internalization and ubiquitination are major mechanisms of signal attenuation, although it is well-established that EGFR is able to continue signaling from early endosomes (Sadowski et al., 2009; Sorkin et al., 2000; Wiley and Burke, 2001). Therefore, it is necessary to assess the effects of DHA on EGFR endocytosis and degradation to fully understand the role of DHA in modulating EGFR function.

The aim of this research was to thoroughly probe the mechanism by which DHA regulates EGFR signaling. We tested two hypotheses to determine how DHA increases EGFR phosphorylation. Then, we sequentially evaluated each step in the EGFR-Ras-ERK1/2 signaling cascade in order to pinpoint the exact break point in signal transduction. By locating the site of signal perturbation, we have been able to further understand the mechanism by which DHA suppresses signal transduction.

3.2 Materials and methods

3.2.1 Cell culture

Young adult mouse colonic (YAMC) cells, conditionally immortalized colonocytes, were originally obtained from R.H. Whitehead, Ludwig Cancer Institute (Melbourne, Australia). YAMC cells (passages 12–17) were cultured under permissive

conditions, 33°C and 5% CO_2 in RPMI 1640 media (Mediatech, Manassas, VA) supplemented with 5% fetal bovine serum (FBS; Hyclone, Logan, UT), 2 mM GlutaMax (Gibco, Grand Island, NY), 5 µg/mL insulin, 5 µg/mL transferrin, 5 ng/mL selenious acid (Collaborative Biomedical Products, Bedford, MA), and 5 IU/mL of murine interferon-γ (Roche, Mannheim, Germany). Select cultures were treated for 72 h with 50 µM fatty acid [DHA, linoleic acid (LA, 18:2n-6), arachidonic acid (AA, 20:4n-6), or eicosapentaenoic acid (EPA, 20:5n-3); NuChek, Elysian, MN] complexed with bovine serum albumin (BSA). In select cultures, for the final 16-18 h, complete media was replaced with low-serum (0.5% FBS) media. Cells were then stimulated with 0-25 ng/mL recombinant mouse EGF (Sigma, St. Louis, MO) and harvested. In select cultures, cells were incubated with the ERK1/2 inhibitor U0126 (Invitrogen, Grand Island, NY) at 10 µM for 2 h prior to stimulation with EGF.

3.2.2 Receptor dimerization

To assess EGFR dimerization, cells were treated as above. Following serum-starvation, cells were washed with ice-cold PBS prior to incubation with 0 or 25 ng/mL EGF on ice for 1 h. Cells were then washed with ice-cold PBS followed by incubation on ice for 20 min with 3 mM bis(sulfosuccinimidyl) suberate (BS^3, Pierce), a non-permeable crosslinking reagent. In all experiments, a freshly prepared solution of BS^3 was used. The crosslinking reaction was quenched by adding 250 mM glycine in PBS and further incubation on ice for 5 min. Cells were washed with PBS and homogenized as above. Protein concentration was measured and lysates were assessed by western blotting for EGFR as described above.

3.2.3 Western blotting

For western blotting, cells were homogenized in ice-cold homogenization buffer (50 mM Tris-HCl, pH 7.2, 250 mM sucrose, 2 mM EDTA, 1 mM EGTA, 50 mM sodium fluoride, 100 mM sodium orthovanadate, 1% Triton X-100, 100 µM activated sodium orthovanadate, 10 mM β-mercaptoethanol, and protease inhibitor cocktail) as previously described (Davidson et al., 1999). Following homogenization, lysates were sheared using a 29G needle, incubated on ice for 30 min, and centrifuged at 16,000 x *g* for 20 min. The supernatant was collected and protein concentration was assessed using Coomassie Plus Protein assay (Pierce). Lysates were treated with 1X pyronin sample buffer and subjected to SDS polyacrylamide gel electrophoresis (PAGE) in precast 4–20% Tris-glycine mini gels (Invitrogen). After electrophoresis, proteins were electroblotted onto a polyvinylidene fluoride membrane with the use of a Hoefer Mighty Small Transphor unit at 400 mA for 90 min. Following transfer, the membrane was incubated in 5% BSA (Roche) and 0.1% Tween 20 in TBS (TBST) at room temperature for 1 h with shaking, followed by incubation with shaking overnight at 4^{o}C with primary antibody diluted in 5% BSA in TBST. Membranes were washed with TBST and incubated with peroxidase conjugated secondary antibody as per manufacturer's instructions. Bands were developed using Pierce SuperSignal West Femto^{TM} maximum sensitivity substrate. Blots were scanned using a Fluor-S Max MultiImager system (Bio-Rad, Hercules, CA). Quantification of bands was performed using Quantity One software (Bio-Rad). Monoclonal rabbit anti-EGFR was purchased from Cell Signaling (Danvers, MA). Monoclonal mouse anti-ubiquitin and polyclonal rabbit anti-K, H, and

N-Ras were purchased from Santa Cruz (Santa Cruz, CA). Peroxidase conjugated goat anti-rabbit IgG was purchased from Kirkegaard and Perry Laboratories (Gaithersburg, MD), and peroxidase conjugated goat anti-mouse IgG was purchased from Jackson ImmunoResearch (West Grove, PA).

3.2.4 Total internal reflection fluorescence (TIRF) microscopy

A plasmid containing the SH2 domain of Grb2 conjugated to YFP (Grb2-YFP) was generously provided by Alexander Sorkin, University of Colorado (Sorkin et al., 2000). For TIRF experiments, cells were treated with fatty acids for 24 h prior to transfection. Cells were transfected using Amaxa nucleofection kit L (Amaxa, Basel, Switzerland) with 2.0 µg Grb2-YFP. Following transfection, cells were seeded at a density of 25,000 cells/well into MatTek (Ashland, MA) glass bottom 35 mm dishes in the presence of fatty acid. Approximately 32 h after transfection, cells were incubated in serum starvation media (0.5% FBS) containing fatty acid for 16-18 h prior to imaging. Images were acquired on a Zeiss TIRF3 Microscope system consisting of a Zeiss AxioObserver Z1 microscope (Carl Zeiss) equipped with a high resolution AxioCam MRm camera, argon laser, and AxioVision 4 software. An excitation wavelength of 514 nm was used, and emission was monitored at 537 nm. All images were collected using a 100X objective (1.4 NA oil immersion) at 37°C and 5% CO_2. To observe the translocation of Grb2-YFP to the plasma membrane, cells were stimulated with 100 ng/mL EGF, and images were collected every 5 sec. Images were collected using identical image acquisition parameters for all images within the experiment. Whole cell

fluorescence intensity was performed on background-subtracted 16-bit images using Nikon Elements AR 3.2.

3.2.5 Ras activation assay

To assess the activation status of Ras, YAMC cells were treated for 72 h with fatty acid and serum starved for the final 16-18 h. Cells were stimulated with 25 ng/mL EGF for 2 min, then harvested using Pierce cell lysis buffer. Activated (GTP-bound) Ras was subsequently isolated and assessed by western blotting using the Pierce Active Ras Pull-Down and Detection™ kit according to the manufacturer's instructions. Additionally, Ras isoforms were detected by western blotting the isolated GTP-bound Ras using isoform specific antibodies as described above.

3.2.6 Cell proliferation assay

YAMC cells were treated with fatty acids for 24 h, followed by transfection using nucleofection (Amaxa kit L) with a constitutively active form of H-Ras (H-RasG12V-GTP), provided by Dr. Ian Prior (Rotblat et al., 2004), prior to being seeded into a 96 well plate at a density of 1.0×10^5 cells per well and cultured for 48 h. Cells were cultured in complete media supplemented with fatty acids for an additional 48 h. Cells were then washed with PBS and cell proliferation was measured using CyQuant cell proliferation assay (Molecular Probes, Grand Island, NY) according to the manufacturer's instructions.

3.2.7 Biotinylation

To assess cell surface EGFR and receptor internalization, cells were treated with fatty acids, serum starved and surface biotinylated using thiol-cleavable EZ-Link Sulfo-

NHS-SS-Biotin (Pierce), 0.5 mg/mL, dissolved in PBS for 30 min on ice. Labeled cells were then rinsed two times with ice-cold PBS, and excess biotin was quenched with 60 mM iodoacetamide in PBS buffer for 5 min at 4°C. Select cultures were harvested at this step in order to quantify cell surface expression of EGFR. Cells were then washed three times with ice-cold PBS, followed by incubation at 33°C in prewarmed serum-free RPMI media for 5 min followed by stimulation with 25 ng/mL EGF for 0-30 min. Biotin groups remaining on the cell surface were then cleaved off by three 20 min washes with buffer containing reducing agent [100 mM MESNA (sodium-2-mercaptoethane sulfonate), 50 mM Tris (pH 8.6), 100 mM NaCl, 1 mM EDTA, and 0.2% BSA] at 4°C. Cells were then washed three times in ice-cold PBS and lysed in RIPA buffer (20 mM Tris, 150 mM NaCl, 2 mM EDTA, 2 mM EGTA, 1% sodium deoxycholate, 1% SDS, and 1% Triton X-100) containing protease and phosphatase inhibitors. The lysates were clarified by centrifugation at 16,000 x *g* for 20 min. Protein concentration was assessed using BCA protein assay (Pierce). Biotinylated EGFR was captured on streptavidin ELISA plates (Nunc Immobilizer Streptavidin C8) from the cell lysates diluted to 5 µg/mL total protein in PBS containing 0.5% Tween 20, pH 7.3 (PBST), during a 2 h incubation at room temperature on a shaker. Plates were then washed three times with PBST, incubated with anti-EGFR antibody (Santa Cruz) (2 µg/mL) for 2 h at room temperature, washed, and incubated with horseradish peroxidase-conjugated secondary antibody for 1 h at room temperature. The plates were subsequently washed three times in PBST before adding color substrate (R&D Systems,

Minneapolis, MN) for 5-10 min. Color development was stopped by addition of an equal amount of 4 M H_2SO_4 and analyzed at 450 nm.

3.2.8 Statistics

The effect of 2 independent variables (treatment effects) was assessed using Student's t-test. The effect of more than 2 independent variables (treatment effects) was assessed using the one-way analysis of variance test (ANOVA), and differences among means were evaluated using Tukey's post-hoc test of contrast. P values <0.05 were considered to be statistically significant.

3.3 Results

3.3.1 Mechanism of DHA-induced increase in EGFR phosphorylation

EGFR phosphorylation is controlled by a variety of factors. Therefore, we next determined the mechanism by which DHA increases EGFR phosphorylation. Since we demonstrated that DHA both alters the membrane environment of EGFR and suppresses ERK1/2 phosphorylation, we assessed whether either of these two mechanisms contributed to the observed DHA-induced increase in EGFR phosphorylation. First, we utilized a specific inhibitor of ERK1/2, U0126, to recapitulate the suppressive effect of DHA on ERK1/2 activation. We then assessed the effect of this inhibitor on EGFR activation status. We found that treatment of cells with 10 μM U0126 for 2 h prior to stimulation completely inhibited EGF-induced activation of ERK1/2 (Fig. 15 A). However, this inhibition had no effect on overall EGFR phosphorylation, suggesting that a downstream feedback-mediated increase in EGFR phosphorylation induced by

ERK1/2 suppression is not a mechanism by which DHA enhances EGFR phosphorylation.

We subsequently measured the effect of DHA on EGFR dimerization. Following stimulation with EGF, EGFR dimers were linked using bis(sulfosuccinimidyl) suberate (BS^3), a non-permeable crosslinking reagent. DHA treated cells exhibited a greater than three-fold increase in dimerization compared to control and LA treated cells (Fig. 15 B). This is consistent with previous studies indicating that the lipid environment affects EGFR dimerization (Coskun et al., 2011), suggesting that the effect of DHA on EGFR is due to the alteration in the lipid environment of the receptor, resulting in increased EGFR dimerization and, therefore, phosphorylation.

3.3.2 DHA inhibits EGF-stimulated Ras GTP-binding

Due to the fact that DHA treatment increased EGFR phosphorylation while concurrently suppressing activation of downstream mediators, we attempted to pinpoint the site of perturbation in the signaling cascade. Since the EGFR-Ras-ERK1/2 pathway is well documented, we examined the components of this pathway downstream of the receptor. Following EGF stimulation, growth receptor-bound protein 2 (Grb2) is recruited to the plasma membrane and binds to phosphorylated tyrosine residues of EGFR (Y1068 and Y1086). To assess recruitment of this immediate proximal signal downstream of EGFR phosphorylation, cells were transfected with fluorescently-tagged SH2 domain of Grb2 (Grb2-YFP), capable of binding to the phosphorylated tyrosine residues of EGFR. Cells were subsequently imaged using TIRF microscopy to assess Grb2-YFP translocation to the plasma membrane in response to EGFR activation.

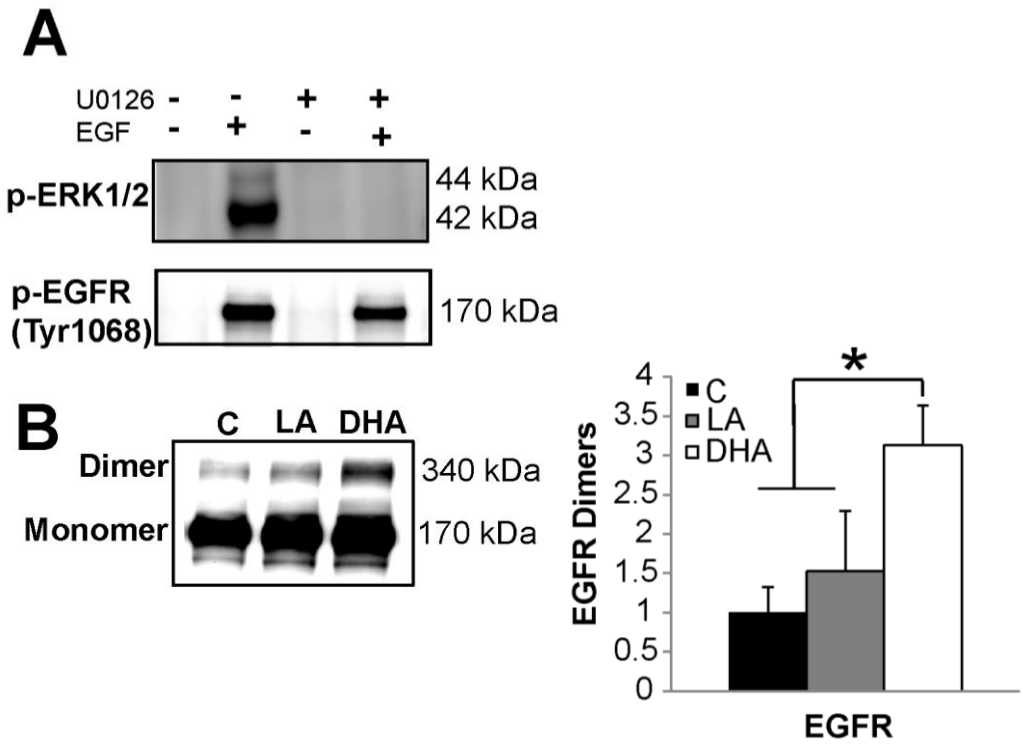

Figure 15. DHA facilitates EGFR dimerization to enhance receptor phosphorylation. (A) Control treated YAMC cells were incubated with low serum media overnight. Select cultures were then treated with 10 µM U0126 for 2 h followed by stimulation with 25 ng/mL EGF. Cell lysates were assessed by western blotting for phosphorylated ERK1/2 and EGFR. (B) Following stimulation with EGF, cells were subjected to chemical crosslinking prior to harvesting cell lysates. Cell lysate was assessed by western blotting for EGFR. EGFR dimers were identified as bands with twice the molecular weight of EGFR monomers. Data are presented as mean ± SEM of dimerized EGFR, normalized to control. Statistical significance between treatments (**P*<0.05) was determined using ANOVA and Tukey's test of contrast. C, control; DHA, docosahexaenoic acid; LA, linoleic acid.

Following stimulation with EGF, Grb2-YFP was rapidly recruited to the plasma membrane (Fig. 16). We observed a significant increase in EGF-stimulated Grb2-YFP plasma membrane translocation in DHA treated cells compared to control and LA treated cells.

Grb2 recruits Sos, a guanine nucleotide exchange factor (GEF), to activate Ras. Therefore, we assessed Ras activation status by pulling-down GTP-bound Ras followed by western blotting for Ras. DHA-treated cells had significantly lower levels of GTP-bound Ras compared to control and LA-treated cells (Fig. 17). This observation indicates that the DHA-induced perturbation in the EGFR-Ras-ERK1/2 pathway occurs at the site of Ras activation. Ras is comprised of three distinct isoforms, including H-Ras, K-Ras, and N-Ras. Isoform-specific signaling is regulated by differential compartmentalization within cell surface microdomains and intracellular compartments (Prior et al., 2003). H-Ras is enriched in lipid rafts, both caveolar and noncaveolar, whereas K-Ras is exclusively located in the bulk membrane (Prior et al., 2001; Prior et al., 2003). Additionally, N-Ras is mainly segregated into noncaveolar lipid rafts (Matallanas et al., 2003). Furthermore, Ras proteins have been shown to signal from the Golgi complex, the endoplasmic reticulum, and endomembranes, e.g., endosomes (9, 26, 32). The effect of this distinctive segregation on the signals generated by Ras remains to be determined. Therefore, we assessed the effect of DHA on activation of each Ras isoform to provide further clarity into the mechanism by which DHA suppressed EGF-induced Ras activation. We found that DHA suppressed activation of all three isoforms of Ras (Fig. 17), indicating a common mechanism by which DHA suppresses EGF-

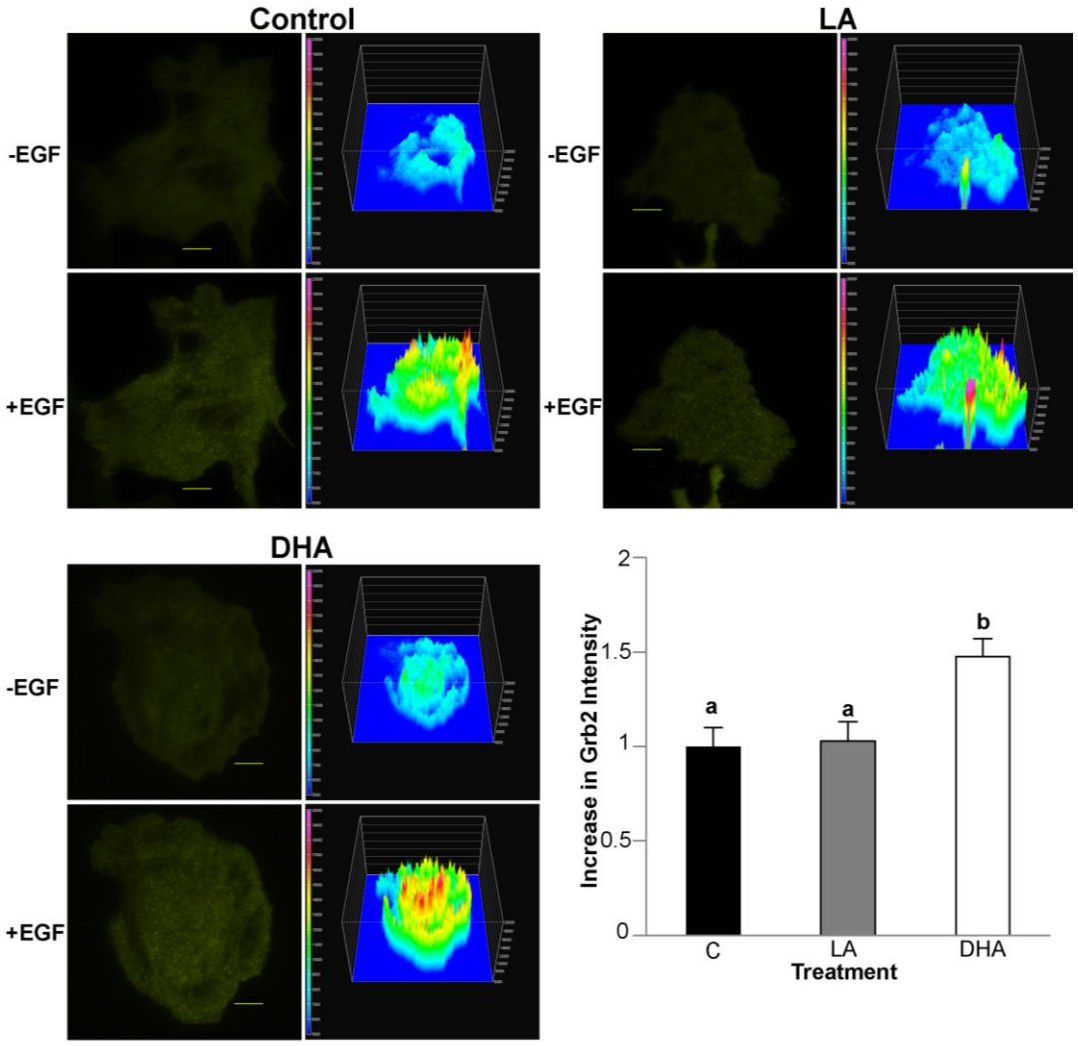

Figure 16. DHA increases EGF-stimulated recruitment of Grb2 to the plasma membrane. YAMC cells were treated with 50 µM BSA-complexed fatty acids for 72 h. Twenty-four h after initiating fatty acid treatment, cells were transfected with Grb2-YFP. For the final 16-18 h, cells were incubated with low serum (0.5% FBS) with the same concentration of fatty acids and imaged using TIRF microscopy. Cells were stimulated with 100 ng/mL EGF and imaged every 5 sec. Images are representative of 4 independent experiments (n=22-25 cells/treatment). Changes in total surface intensity were quantified using Nikon Elements AR 3.2. Fluorescence images and the respective surface intensity plots are shown. Surface intensity plots were generated in Nikon Elements AR 3.2; the scale is from blue (lowest intensity) to red/pink (highest intensity). Data are presented as mean ± SEM normalized to control. Bars, 10 µM. Statistical significance between treatments (P<0.05) as indicated by different letters was determined using ANOVA and Tukey's test of contrast. C, control; LA, linoleic acid; DHA, docosahexaenoic acid.

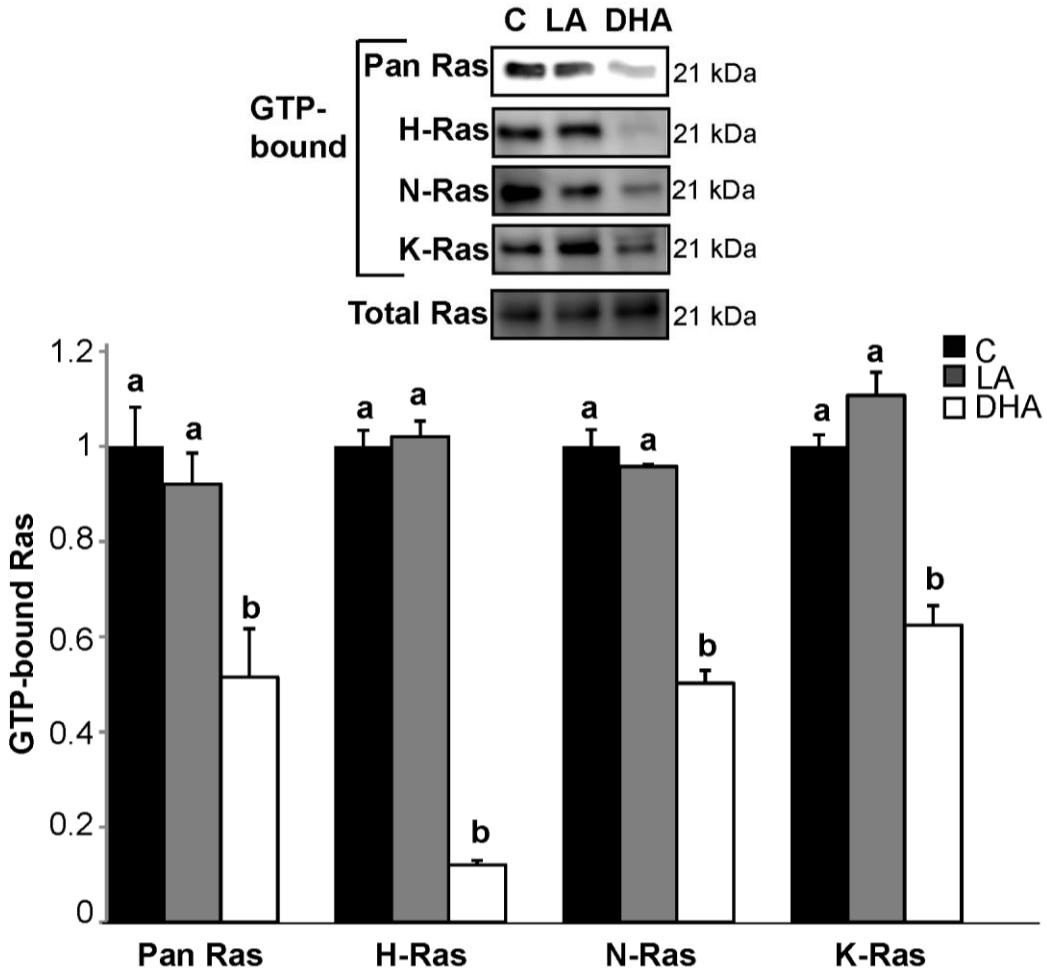

Figure 17. DHA inhibits EGF-stimulated activation of all Ras isoforms. YAMC cells were treated with 50 μM BSA-complexed fatty acids for 72 h. For the final 16-18 h, cells were incubated with low serum media (0.5% FBS) with the same concentration of fatty acids. Cells were stimulated with 25 ng/mL EGF for 2 min and harvested. GTP-bound Ras was isolated using a GST pull-down assay. Isolated GTP-bound Ras was then analyzed by western blotting for pan Ras. Isolated GTP-bound Ras was additionally analyzed by western blotting for H, K, and N-Ras. Blots are representative of 3 independent experiments. Quantification of band volume was performed. Data are expressed as mean ± SEM (n=3), normalized to control. Statistical significance between treatments (P<0.05) as indicated by different letters was determined using ANOVA and Tukey's test of contrast. C, control; LA, linoleic acid; DHA, docosahexaenoic acid.

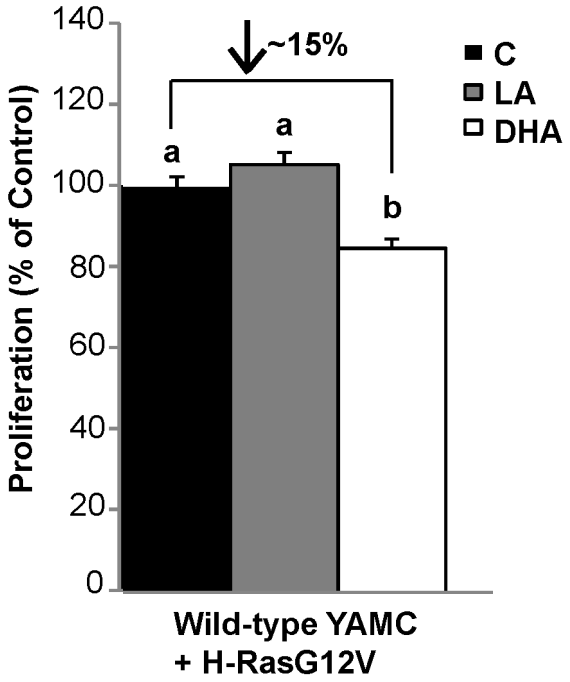

Figure 18. Expression of constitutively active H-Ras partially rescues cells from DHA-mediated reduction of cell proliferation. Wild-type YAMC cells were treated with 50 μM BSA-complexed fatty acid for 24 h. Cells were then transfected using nucleofection with GFP-H-RasG12V and seeded at an equal density into a 96-well plate, and cultured under the same treatment conditions for an additional 48 h. Cell proliferation was measured using CyQUANT cell proliferation assay. Data are expressed as mean ± SEM (n=9 samples per treatment). Statistical significance between treatments as indicated by different letters ($P<0.05$) was determined using ANOVA and Tukey's test of contrast.

induced activation of Ras. Furthermore, activation of H-Ras was almost entirely inhibited by DHA, suggesting a distinct mechanism of regulation for this specific isoform.

We additionally assessed whether expression of a constitutively active form of H-Ras (GFP-H-RasG12V) could rescue the DHA-induced suppression of cell proliferation. We found that DHA-treated cells expressing constitutively activated H-Ras recovered partially from the DHA-induced suppression of cell proliferation but still exhibited approximately a 15% decrease in cell proliferation compared to control cells expressing GFP-H-RasG12V (Fig. 18).

3.3.3 DHA induces increased EGFR internalization and degradation

Since DHA suppressed activation of each of the isoforms of Ras, this suggested a potential lipid raft-independent mechanism of action. Endocytosis is a major mechanism of EGFR signal attenuation by targeting the activated receptor for lysosomal proteolysis (Polo and Di Fiore, 2006). Recent evidence suggests that lipid rafts may play a role in mediating EGFR endocytosis (Puri et al., 2005; Sigismund et al., 2008). Additionally, EGFR phosphorylation and Grb2 recruitment to EGFR are intimately linked to EGFR internalization (Burke et al., 2001; Goh et al., 2010; Jiang et al., 2003; Yamazaki et al., 2002). Therefore, we next assessed the effect of DHA on EGFR endocytosis using a surface biotinylation assay. Interestingly, internalization of EGFR occurred more rapidly in DHA treated cells compared to untreated (control) cells (Fig. 19 A). In addition, consistent with data in Figs. 2 and 3, DHA reduced the steady-state plasma membrane localization of EGFR in unstimulated cells (Fig. 19 B).

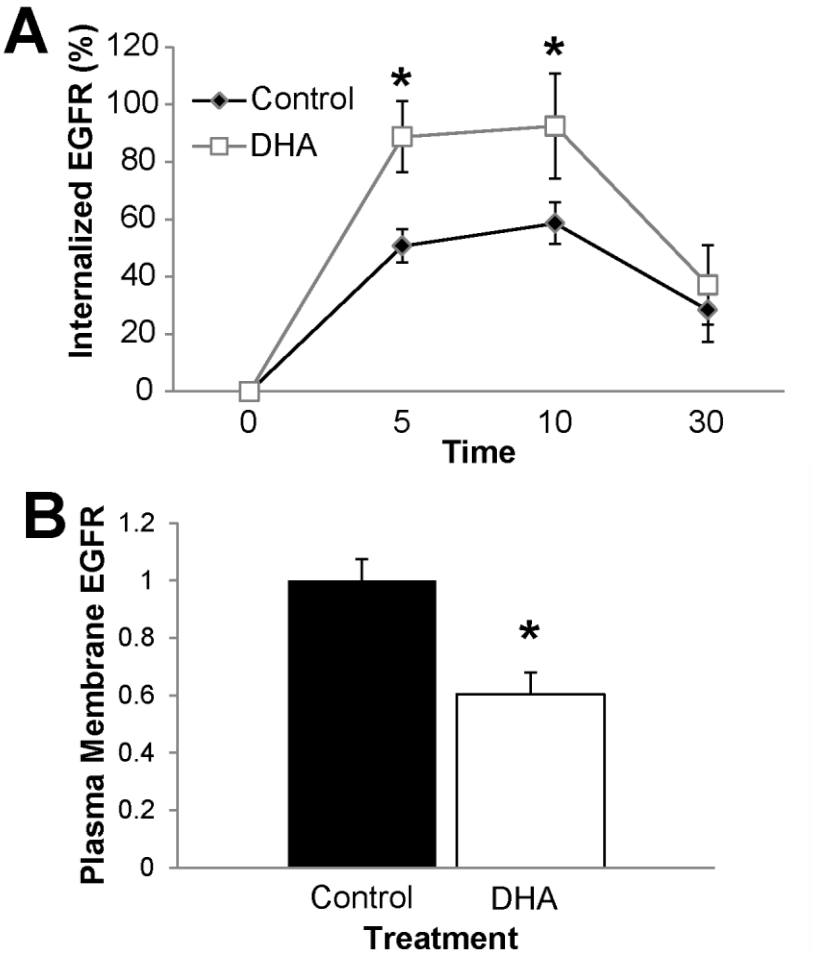

Figure 19. **DHA increases EGF-stimulated EGFR internalization and reduces resting state levels of EGFR at the plasma membrane.** YAMC cells were incubated with untreated media or media supplemented with 50 µM BSA-complexed DHA for a total of 72 h. For the final 16-18 h, cells were incubated in low serum (0.5% FBS). (A) Cell surface proteins were labeled with EZ-Link Sulfo-NHS-SS-Biotin followed by stimulation with 25 ng/mL EGF for 0-30 min. After stimulation, cells were washed and biotin remaining on the cell surface was cleaved. Cell lysates were harvested, and biotinylated EGFR was quantified by ELISA using streptavidin coated plates and anti-EGFR antibody. (B) Cell surface EGFR was assessed by treating cells the same as in A, and harvesting without stimulating with EGF or cleaving cell surface biotin. . Data represent mean ± SEM. In (A), data are normalized to time 0. In (B), data are normalized to control (no fatty acid). Statistical significance between treatments (**P*<0.05) was determined using Student's *t*-test. C, control; DHA, docosahexaenoic acid.

Following internalization, EGFR can either be recycled back to the cell surface or be targeted to the lysosome for degradation. Ubiquitin acts as a sorting signal to down-regulate the functions of plasma membrane proteins. EGFR internalization and degradation are facilitated by ubiquitin (Eden et al., 2011). Receptor endocytosis stimulated by ubiquitination is considered to be crucial to prevent oncogenesis because it sorts the receptor to the lumen of multivesicular bodies and terminates growth factor signaling (Umebayashi et al., 2008). This is especially crucial for EGFR since it has been shown to continue to signal from endosomes after it is internalized (Burke et al., 2001). Therefore, we assessed ubiquitination of the receptor in order to determine whether the DHA-induced increase in EGFR internalization was associated with increased receptor ubiquitination and degradation. Immunoprecipitation of EGFR followed by western blotting for ubiquitin to assess EGFR ubiquitination was utilized. We found that EGFR ubiquitination was significantly increased by DHA treatment (Fig. 20). Additionally, EGFR expression was reduced in DHA treated cells 30 min after stimulation. Together, these data suggest that DHA further regulates EGFR signaling capacity by increasing EGFR internalization and degradation.

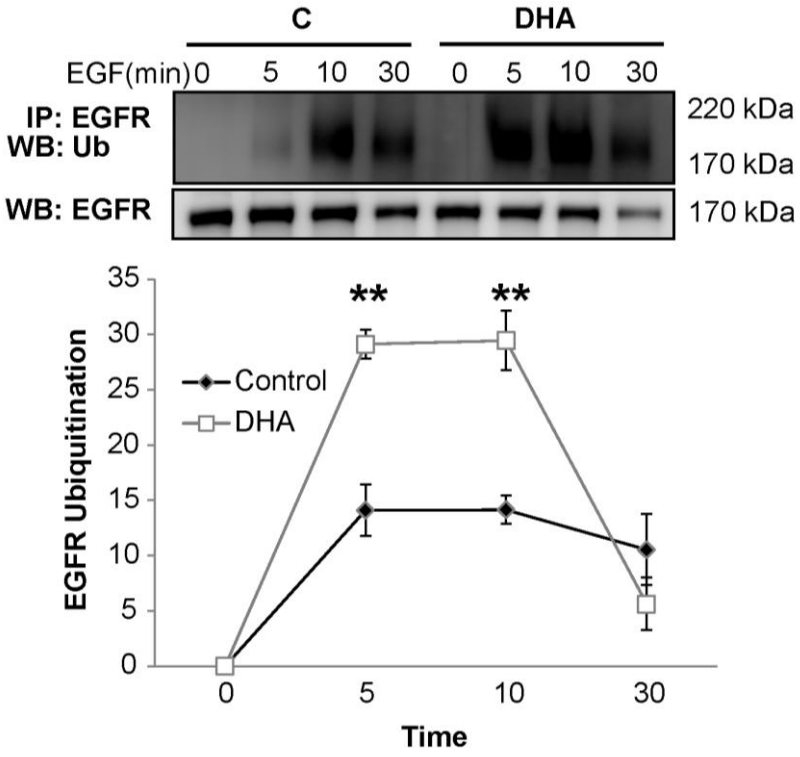

Figure 20. DHA increases EGFR ubiquitination. Cells were stimulated with 25 ng/mL EGF for 0-30 min and harvested. EGFR was immunoprecipitated from the total cell lysate, assessed by western blotting for ubiquitin, and quantification of band intensity was performed. All results are representative of at least 3 independent experiments. Data represent mean ± SEM. Data are normalized to time 0. Statistical significance between treatments (**P<0.01) was determined using Student's t-test. C, control; DHA, docosahexaenoic acid.

3.4 Discussion

Our initial observations regarding the role of DHA in regulating EGFR signaling opened numerous avenues for continued research. Here, we further probed the mechanism by which DHA alters EGFR function. We found that DHA enhances EGFR phosphorylation by increasing receptor dimerization. This is consistent with previous observations on the effect of altered EGFR plasma membrane localization on EGFR activation (Chen and Resh, 2002; Ringerike et al., 2002; Roepstorff et al., 2002). Many of these studies showed that cholesterol altered both receptor dimerization and ligand binding. Therefore, research on the effect of DHA on ligand binding is required for full understanding of the role of DHA in control of EGFR function.

To further understand the mechanism by which DHA suppresses EGFR signal transduction, we attempted to identify the exact locus of the DHA-induced perturbation in EGFR signal transduction. Therefore, we assessed the individual components of the EGFR-Ras-ERK1/2 signaling axis. Grb2 is an immediate proximal downstream mediator of EGFR signaling and directly binds to phosphorylated tyrosine residues of EGFR, including Tyr1068, which we showed here to be increased by DHA treatment. Grb2 mediates multiple responses to EGFR phosphorylation, including propagation of intracellular signaling and receptor endocytosis. We observed that DHA treatment increased the EGF-stimulated recruitment of Grb2 to the plasma membrane (Fig. 16), indicating that DHA does not affect the ability of phosphorylated EGFR to recruit intracellular signaling mediators. We subsequently demonstrated that the “breakpoint” in the DHA-mediated suppression of EGFR signaling was at the level of Ras activation

(Fig. 17). Our laboratory has previously shown that DHA suppresses the levels of activated GTP-bound Ras under basal conditions (Collett et al., 2001). We have extended these observations by demonstrating that EGF-stimulated activation of all three isoforms of Ras was suppressed by DHA. In addition, DHA had the strongest inhibitory effect on activation of H-Ras. This is intriguing due to the fact that both H-Ras and EGFR are localized to lipid rafts (Prior et al., 2001), and that EGF-stimulated interactions between Ras and its downstream partner Raf-1 have been shown to occur in lipid rafts (Mineo et al., 1996). A potential explanation for the observed DHA-induced suppression of activation of Ras, specifically H-Ras, is based on the altered localization of EGFR within the plasma membrane. Convincing evidence illustrates the importance of lateral segregation of signaling cascades on the plasma membrane. Indeed, for signal transduction to occur, phosphorylated EGFR must form a transient complex with Grb2, Sos, and Ras (Buday and Downward, 1993). Due to the altered plasma membrane localization of EGFR upon treatment with DHA, this could result in a spatial abrogation of signal transduction by reducing the formation of these transient complexes.

In addition to our previous observations that DHA regulated the localization of EGFR within the plasma membrane, we illustrated here that DHA also altered the subcellular distribution of EGFR. Under unstimulated conditions, DHA treated cells contained significantly less EGFR at the plasma membrane (Fig. 19 B). Additionally, concomitant with increased EGFR phosphorylation, DHA treated cells exhibited enhanced EGFR endocytosis following receptor stimulation (Fig. 19 A). Because a majority of signaling cascades are activated by EGFR at the plasma membrane, receptor

endocytosis and degradation play an important role in terminating EGFR signaling. Therefore, the DHA-induced enhancement of EGFR internalization is an additional mechanism by which DHA can suppress the ability of EGFR to activate downstream signaling. Once internalized, EGFR can continue signaling from endosomes, recycle back to the plasma membrane, or traffic for degradation. This is noteworthy because DHA increased EGFR ubiquitination and degradation (Fig. 20). Interestingly, although DHA treatment did not affect the steady-state levels of EGFR, following ligand-induced activation, it significantly increased EGFR ubiquitination and degradation. Since receptor endocytosis and degradation can function to mitigate signal transduction, we propose that this is an additional mode by which DHA modulates the signaling capacity of EGFR.

Since DHA antagonizes the activation of all Ras isoforms regardless of their plasma membrane localization, it is likely that an additional mechanism mediates the suppression of EGFR signal transduction by DHA. Therefore, we hypothesize that the observed increased endocytosis of the receptor contributes to the suppressive phenotype. The majority of activation of Ras by EGFR has been shown to occur at the plasma membrane (Augsten et al., 2006). Therefore, the observed DHA-induced increase in EGFR internalization likely contributes to the reduced activation of all Ras isoforms. We are currently determining whether the altered plasma membrane localization of EGFR and/or enhanced EGFR endocytosis is responsible for the suppression of downstream signaling. Additionally, further work is required to determine how the altered plasma membrane localization of EGFR contributes to enhanced receptor

internalization and degradation. Previous work by Sigismund et al. indicates that high levels of EGFR phosphorylation can lead to activation of additional forms of EGFR endocytosis which sort EGFR for degradation instead of recycling (Sigismund et al., 2008). Therefore, it is possible that DHA could function by altering EGFR plasma membrane localization, resulting in higher levels of EGFR phosphorylation and activation of a non-canonical form of receptor endocytosis that sorts the receptor for degradation as opposed to recycling. Current studies in our lab are focused on testing this hypothesis.

These results have substantial biological relevance because Ras plays a central role in the development of human colon cancer and is commonly hyperactivated by somatic mutation or signaling through growth factor receptors (Lievre et al., 2010). Hence, by suppressing EGF-stimulated activation of Ras, DHA can provide protection against colonic transformation. In addition to suppressing activation of the Ras-ERK1/2 pathway, DHA suppressed EGF-induced activation of STAT3. STAT3 can be activated downstream of EGFR by several pathways, and Ras signaling has been shown to be intimately linked to STAT3 activation (Corcoran et al., 2011; Plaza-Menacho et al., 2007; Yeh et al., 2009). Therefore, the reduction in STAT3 activation could be a direct result of reduced activation of Ras. Additionally, lipid rafts have been shown to play a central role in the activation of STAT3 (Sehgal et al., 2002), which may explain the DHA-induced suppression of EGF-induced STAT3 activation. Clearly, further studies are required to determine the exact mechanism of action. Additionally, expression of a constitutively active form of H-Ras partially rescued the DHA-induced suppression of

cell proliferation. The limited ability of GFP-H-RasG12V was likely due to the effect that DHA has on other downstream pathways from EGFR that are independent of Ras signaling.

Overall, these results further clarify the mechanism of action by which DHA perturbs EGFR function. Based on our findings, we have created a putative model depicting the effect of DHA on EGFR (Fig. 21). This model illustrates that DHA alters EGFR localization, which contributes to the increase in EGFR dimerization and phosphorylation. However, the altered localization of EGFR causes a lateral break in signal transduction that is dependent on lipid rafts. Additionally, the increased EGFR phosphorylation, and potentially other unknown processes, stimulates increased receptor endocytosis, which impedes signaling events that emanate from the plasma membrane. The enhanced receptor degradation subsequently subdues endosomal signaling. All of this culminates in an abrogation of signal transduction to hamper cell proliferation.

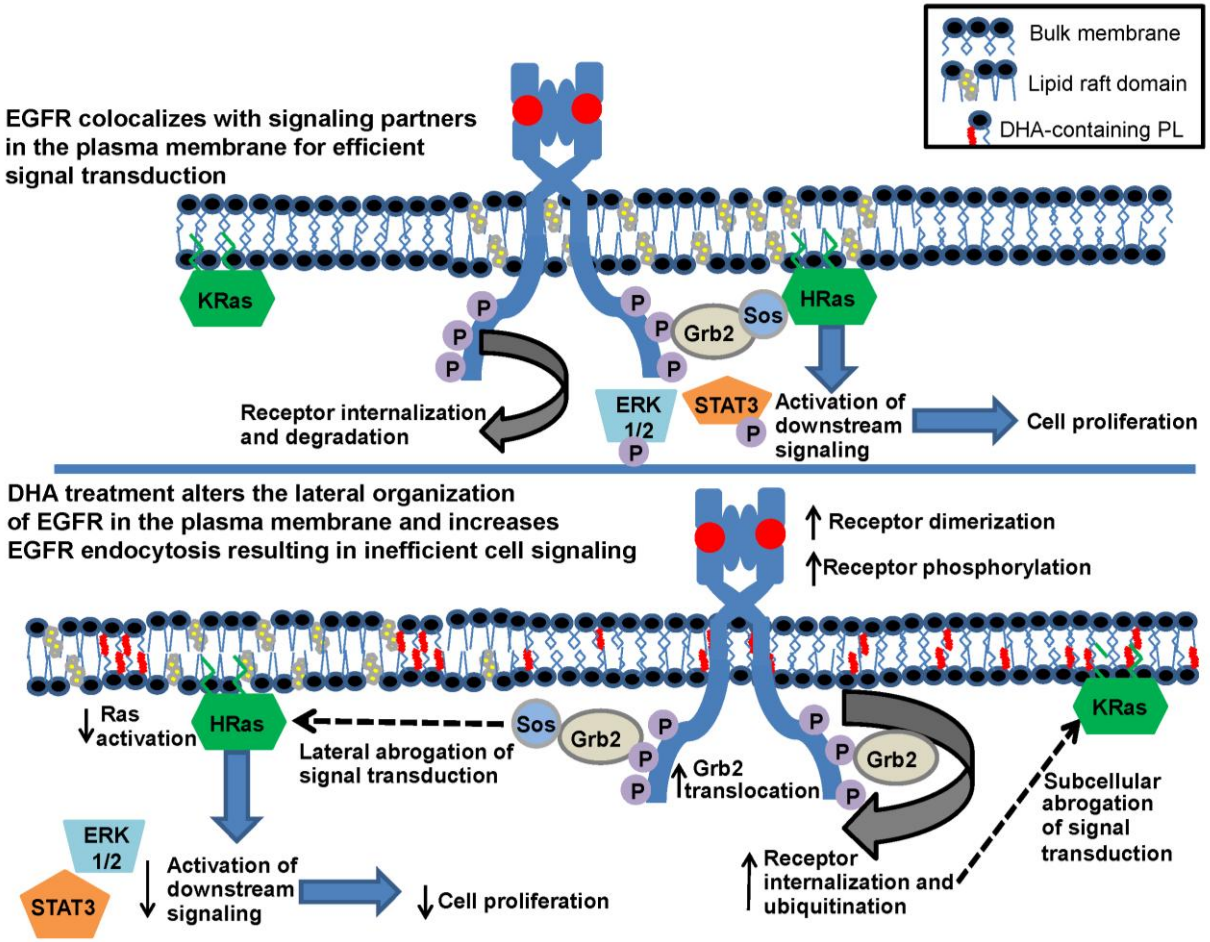

Figure 21. Proposed model for the effect of DHA on EGFR localization and signaling. Under control conditions, EGFR is enriched in liquid ordered lipid raft domains of the cell. Upon stimulation, ligand bound receptors dimerize and transphosphorylate. Signaling events are initiated from the phosphorylated tyrosine residues, and signaling is efficient due to the lateral organization of EGFR and downstream signaling partners. Upon fatty acid treatment, the cell incorporates DHA into plasma membrane phospholipids, which redistributes EGFR in the membrane. Ligand-induced receptor dimerization and phosphorylation is increased, along with receptor ubiquitination, internalization, and degradation. The altered lateral and subcellular organization of EGFR results in inefficient cell signaling.. This results in altered cellular function, including a reduction of cell proliferation.

4. EFFECT OF DHA ON COLONIC WOUND HEALING

4.1 Introduction

Intestinal wound healing requires a delicate balance of migration, proliferation, and differentiation of epithelial cells (Moyer et al., 2007). The first step of wound healing is epithelial restitution, in which epithelial cells adjacent to the wound rapidly migrate into the wounded area (Dignass and Podolsky, 1993; Dise et al., 2008; Sturm and Dignass, 2008). Restitution begins quickly following injury, within minutes to hours, and this process has been shown to be independent of cell proliferation (Dignass and Podolsky, 1993; Sturm and Dignass, 2008). The next step of wound healing, which begins hours to days after injury, requires proliferation of the mucosal epithelium to increase the number of enterocytes available to repopulate the injured area (Dignass and Podolsky, 1993; Iizuka and Konno, 2011). The final stage of wound healing requires maturation and differentiation of epithelial cells to restore and maintain intestinal function (Sturm and Dignass, 2008).

Many pathways that are hijacked by cancer cells are integral in the process of wound healing. Central amongst these pathways is the EGFR pathway. EGFR signaling is involved in all of the stages of intestinal wound healing, including restitution, proliferation, and differentiation. It has been clearly demonstrated that treatment with EGFR ligands, including EGF, HB-EGF, and TGF-α, promotes intestinal wound healing (El-Assal and Besner, 2005; Goke et al., 1998). In response to a wounding event, EGFR becomes activated. This activation is regulated in part by G-protein coupled receptors,

which signal to activate matrix metalloproteinases (Yin and Yu, 2009). These serve to cleave EGFR ligands from the plasma membrane so they can bind to their receptor. Src family tyrosine kinases have also been shown to play a central role in wound-induced transactivation of EGFR (Xu et al., 2006). In addition, ERK1/2 can mediate ligand shedding in response to wounds (Yin and Yu, 2009).

Multiple downstream signaling pathways from EGFR are central in regulating distinct stages of wound healing. Restitution requires extensive reorganization of the actin cytoskeleton through activation of Rho family small GTPases, including Rac1 and Cdc42 (Hall, 1998; Hopkins et al., 2007). Rho-GTPases alternate between an active GTP-bound form and an inactive GDP-bound form. Activation of Rho-GTPases promotes their translocation to the plasma membrane where they amplify signaling pathways involved in modification of the actin cytoskeleton. Activation of Rac1 and Cdc42 facilitates actin polymerization by inducing activation of WAVE and WASP/N-WASP nucleation factors, which then serve to activate the actin Arp2/3 complex (Eden et al., 2002; Rohatgi et al., 1999). Activation of different Rho GTPases correlates with formation of different cytoskeletal projections. Specifically, Rac1 activation is classically associated with the formation of lamellipodia, whereas Cdc42 is correlated with filopodia formation (Nobes and Hall, 1995a; Nobes and Hall, 1995b). It has been clearly demonstrated that EGFR activates Rac1 and Cdc42 through multiple downstream signaling cascades, including PI3K and Src (Dise et al., 2008; El-Sibai et al., 2007), and EGFR-mediated activation of these mediators is imperative for wound healing. PLC-γ1 is another downstream signaling partner of EGFR that mediates intestinal epithelial cell

migration (Li et al., 2009; Polk, 1998). PLC-γ1 contains an SH2 domain that allows it to directly bind to EGFR (Anderson et al., 1990; Meisenhelder et al., 1989). Binding to EGFR results in phosphorylation of tyrosine residues on PLC-γ1, which increases its enzymatic activity (Kamat and Carpenter, 1997). PLC-γ1 also contains two pleckstrin homology (PH) domains, which allow it to bind to phosphatidylinositol lipids in the plasma membrane. PLC-γ1 catalyzes the hydrolysis of phosphatidylinositol-4,5-bis-phosphate (PIP_2) into two second messengers, inositol 1,4,5-trisphophate and diacylglycerol (DAG). It has been shown that PLC-γ1 and Rac1 directly interact to co-regulate cytoskeletal remodeling and cell migration in response to EGF (Li et al., 2009). In addition to these early processes that enhance restitution, EGFR is integral in mediating the cell proliferation stage of wound healing by activating multiple downstream signaling cascades, including Ras-ERK1/2 and STAT3.

We have previously demonstrated that the n-3 PUFA, DHA, inhibits ligand-induced signaling through EGFR in colonocytes, which ultimately results in a suppression of cell proliferation. Based on the ability of DHA to suppress aspects of EGFR signaling and the central role of EGFR-mediated signaling in wound healing, we hypothesize that DHA is inimical with respect to intestinal wound healing. Furthermore, DHA affects multiple lipid raft mediated events, and lipid rafts have been shown to play a central role in EGFR-mediated cell migration (Murai, 2012). The postulate that DHA is detrimental for intestinal wound healing is supported by recent data generated by our laboratory, e.g., mice fed a diet enriched in fish oil, high in DHA, exhibited reduced overall survival and increased wounding following treatment with dextran sodium

sulfate (DSS)(Jia et al., 2008). An additional study conducted in humans demonstrated that wound healing of the skin is delayed in patients dosed with a combination EPA and DHA (McDaniel et al., 2008). Conversely, some studies have demonstrated a beneficial effect of n-3 PUFA in response to injury (Gravaghi et al., 2011; Hudert et al., 2006). These conflicting data are interesting and warrant further probing of the mechanisms by which n-3 PUFA affect wound healing. Since DHA, but not EPA, alters EGFR signaling (Fig. 6), we hypothesized that the differential effects of these two dietary lipids could explain the discrepancy in the n-3 PUFA and wound healing literature. Therefore, we probed the effects of fatty acids on EGFR signaling and wound healing.

4.2 Materials and methods

4.2.1 Cell culture

Young adult mouse colonic (YAMC) cells, conditionally immortalized colonocytes, were originally obtained from R.H. Whitehead, Ludwig Cancer Institute (Melbourne, Australia). YAMC cells (passages 12–17) were cultured under permissive conditions, 33°C and 5% CO_2 in RPMI 1640 media (Mediatech, Manassas, VA) supplemented with 5% fetal bovine serum (FBS; Hyclone, Logan, UT), 2 mM GlutaMax (Gibco, Grand Island, NY), 5 µg/mL insulin, 5 µg/mL transferrin, 5 ng/mL selenious acid (Collaborative Biomedical Products, Bedford, MA), and 5 IU/mL of murine interferon-γ (Roche, Mannheim, Germany). Select cultures were treated for 72 h with 50 µM fatty acid [DHA, LA, or EPA; NuChek, Elysian, MN] complexed with bovine serum albumin (BSA). In select cultures, for the final 16-18 h, complete media was

replaced with low-serum (0.5% FBS) media. Cells were then stimulated with 0-25 ng/mL recombinant mouse EGF (Sigma, St. Louis, MO) and harvested. To prepare whole cell extracts of wounded cells, cells were grown to confluence in 150-mm dishes. The monolayer was cross-scraped 25 times in all directions (100 scrapes total) with a 1-mL pipette tip as previously described (Egan et al., 2003). The monolayer was then gently washed with ice-cold PBS three times and harvested.

4.2.2 Western blotting

For western blotting, cells were homogenized in ice-cold homogenization buffer (50 mM Tris-HCl, pH 7.2, 250 mM sucrose, 2 mM EDTA, 1 mM EGTA, 50 mM sodium fluoride, 100 mM sodium orthovanadate, 1%Triton X-100, 100 µM activated sodium orthovanadate, 10 mM β-mercaptoethanol, and protease inhibitor cocktail) as previously described (Davidson et al., 1999). Following homogenization, lysates were sheared using a 29G needle, incubated on ice for 30 min, and centrifuged at 16,000 x *g* for 20 min. The supernatant was collected and protein concentration was assessed using Coomassie Plus Protein assay (Pierce). Lysates were treated with 1X pyronin sample buffer and subjected to SDS polyacrylamide gel electrophoresis (PAGE) in precast 4–20% Tris-glycine mini gels (Invitrogen). After electrophoresis, proteins were electroblotted onto a polyvinylidene fluoride membrane with the use of a Hoefer Mighty Small Transphor unit at 400 mA for 90 min. Following transfer, the membrane was incubated in 5% BSA (Roche) and 0.1% Tween 20 in TBS (TBST) at room temperature for 1 h with shaking, followed by incubation with shaking overnight at 4^{o}C with primary antibody diluted in 5% BSA in TBST. Membranes were washed with TBST and

incubated with peroxidase conjugated secondary antibody as per manufacturer's instructions. Bands were developed using Pierce SuperSignal West Femto^{TM} maximum sensitivity substrate. Blots were scanned using a Fluor-S Max MultiImager system (Bio-Rad, Hercules, CA). Quantification of bands was performed using Quantity One software (Bio-Rad). Monoclonal rabbit anti-EGFR, anti-phosphorylated (Tyr1068) EGFR, anti-PLC-γ1, and anti-phosphorylated (Tyr783) PLC-γ1 were purchased from Cell Signaling (Danvers, MA). Peroxidase conjugated goat anti-rabbit IgG was purchased from Kirkegaard and Perry Laboratories (Gaithersburg, MD).

4.2.3 Small Rho-GTPase activity assay

Activation of Cdc42 and Rac1 was assessed using kits from Cytoskeleton (Denver, CO). Samples for these assays were harvested as detailed above using the lysis buffer provided with the kits and supplemented with protease and phosphatase inhibitors (Sigma). Activation of Cdc42 was analyzed using the G-LISA Cdc42 Activation Assay Biochem Kit in the colorimetric format. Activation of Rac1 was assessed using the Rac1 G-LISA Activation Assay in the colorimetric format. The assays were performed using 25 μg of protein according to the manufacturer's instructions. Absorbance was measured on a SpectraMax 190 Microplate Reader (Molecular Devices, Sunnyvale, CA).

4.2.4 Scratch assay

YAMC cells in T-75 flasks were either untreated or treated with 50 μM fatty acid (LA, DHA, or EPA) for 24 hours. Cells were then trypsinized and seeded at a density of 100,000 cells/mL into 35-mm glass bottom dishes. Cells were cultured for another 48 h in the presence of fatty acid and serum starved (0.5% FBS) for the final 16-18 h.

Following serum starvation, cells were washed once with PBS and scratched using a sterile P-200 pipette tip. Cells were then washed twice with PBS and incubated with serum-free media supplemented with 25 ng/mL EGF. Cells were then imaged with a 10X Plan Fluor phase objective on a Nikon TiE inverted microscope equipped with perfect focus system to maintain focus over time and an incubation chamber at 33°C with 5% CO_2. Images were taken with a Photometrics CoolSNAP HQ^2, 14 Bit, 20 MHz, monochrome cooled CCD camera. The software used in image acquisition and analysis was NIS Elements AR. Images were taken every 15 min for 24 h to observe wound healing. Wound healing was quantified by counting the number of cells that infiltrated the wounded area at 12 and 24 h following the wounding event.

4.2.5 Migration assay

Cell migration was assessed using the QCM 24-well colorimetric cell migration assay (Millipore). YAMC cells were seeded into T-75 flasks and untreated or treated with fatty acids (LA, DHA, EPA) for 72 h. For the final 16-18 h of treatment, cells were serum-starved (0.5% FBS). Cells were then trypsinized and seeded into inserts at a density of 0.5 x 10^6 cells/mL in serum free media. The inserts are composed of membranes with 8 μm pores through which the cells can migrate. The inserts were set into wells containing media supplemented with 25 ng/mL EGF, and the membrane of the insert was placed into contact with the media. The cells were incubated for 12 h at 33°C and 5% CO_2 and allowed to migrate through the membrane. Following incubation, the cells on the top side of the insert were thoroughly removed, and the migration insert was stained using the kit provided cell stain. Subsequently, the stain was eluted using the

provided extraction buffer, and 100 μL of the dye mixture was added to a 96-well plate. The optical density was measured at 560 nm on a SpectraMax 190 Microplate Reader (Molecular Devices).

4.2.6 Animals

Male C57BL/6 wild-type mice aged 12-15 weeks were purchased from Jackson Laboratories. All procedures followed guidelines approved by the U.S. Public Health Service and the Institutional Animal Care and Use Committee at Texas A&M University. This study and all animal protocols and procedures were approved by the Institutional Animal Care and Use Committee at Texas A&M University. Mice were maintained under barrier conditions and initially consumed a Teklad commercial mouse non-purified diet (Harlan, Indianapolis, IN) ad libitum. Mice were maintained for 15-21 days on a semi-purified defined diet that was adequate in all nutrients, containing 440 (g/kg diet) sucrose, 200 casein, 220 corn starch, 3 DL-methionine, 35 AIN 76 salt mix, 10 AIN 76 mineral mix, 2 choline chloride, 60 cellulose (Bio-Serv, Frenchtown, NJ), 30 corn oil (CO) (Dyets, Bethlehem, PA) or 10 DHA (Incromega DHA700E SR; Bioriginal Food & Science Corp, Saskatchewan, Canada) plus 20 CO or 10 EPA (SLA Pharma, Watford, UK). The DHA utilized is highly purified (>70%) DHA ethyl ester, and the EPA is highly purified (>95%) EPA free fatty acid. The mice received the diet for 10 days prior to treatment with 2.5% DSS in the drinking water for 5 days. Following DSS treatment, mice were allowed to recover for 0, 3, or 6 days. Mice were terminated using CO_2 asphyxiation. The colon was then removed and cut into a longitudinal half. One half of the colon was rolled into a Swiss roll, fixed in paraformaldehyde, embedded in

paraffin, and sectioned. The sections were then analyzed in a blinded manner by a board certified pathologist. From the other half of the colon, colonic mucosa was isolated by scraping and combining with lysis buffer from the Rac1 activation assay buffer. Lysates were sheared by passage through a 27G needle, incubated on ice for 30 min, and then centrifuged at 16,000 x *g* for 20 min. The supernatant was collected. Protein concentration was determined using Coomassie Protein Plus assay (Pierce).

4.2.7 Statistics

The effect of independent variables (treatment effects) was assessed using the one-way analysis of variance test (ANOVA), and differences among means were evaluated using Tukey's post-hoc test of contrast. *P* values <0.05 were considered to be statistically significant.

4.3 Results

4.3.1 EGFR transactivation by wounding.

We have previously shown that EGFR phosphorylation in response to direct stimulation with ligand is increased by DHA (Fig. 4). However, other long chain polyunsaturated fatty acids, including LA, AA, and EPA do not exert the same effect (Figs. 4 and 6). Therefore, we wanted to expand upon these observations by determining if fatty acids can alter EGFR transactivation in response to injury. Since in response to wounding, EGFR becomes transactivated (Egan et al., 2003), we wounded a monolayer of colonic epithelial cells by scratching the monolayer extensively. We found that phosphorylation of EGFR was strongly induced in untreated control cells and LA treated

cells (Fig. 22). Treatment of cells with DHA or EPA, however, reduced the injury-induced transactivation of EGFR.

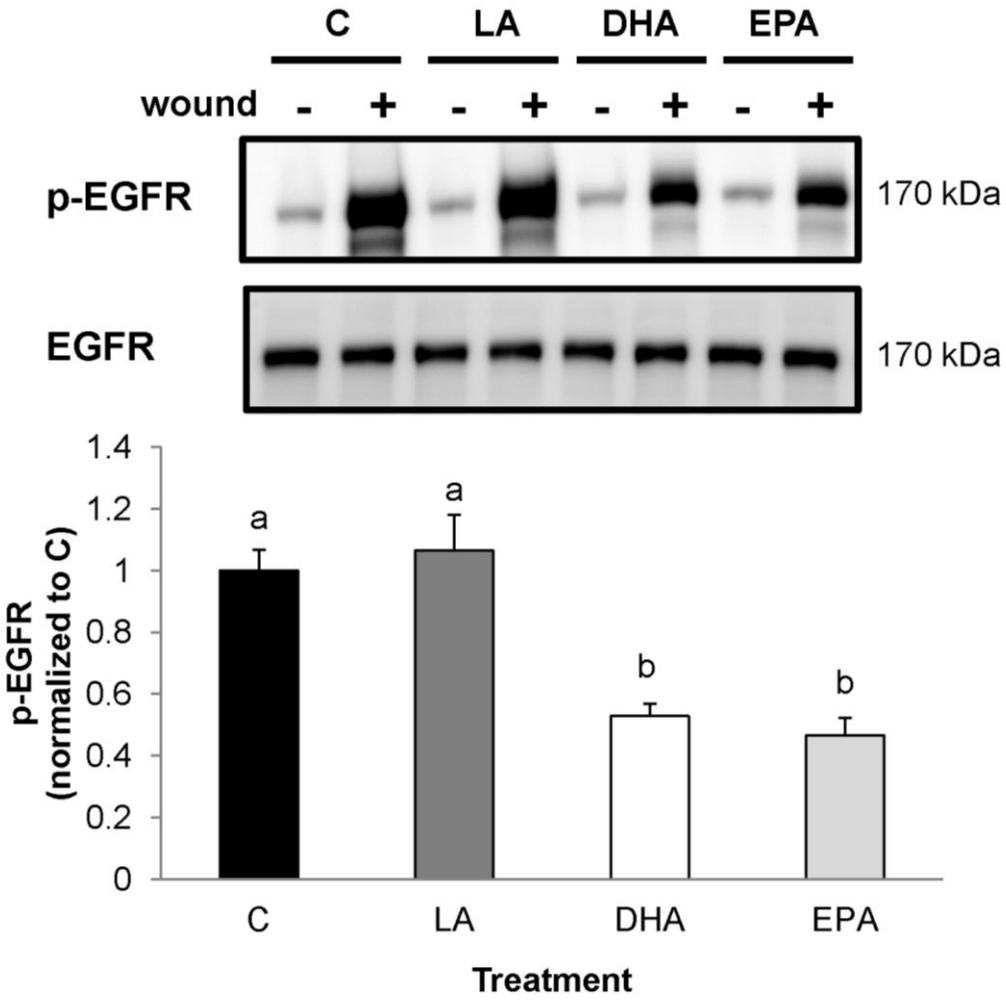

Figure 22. DHA and EPA reduce wound-induced EGFR phosphorylation. YAMC cells were either untreated (control) or treated with 50 μM fatty acid (LA, DHA, or EPA) for 72 h. For the final 16-18 h, cells were serum starved (0.5% FBS) followed by extensive wounding. Following wounding, cells were incubated for 2 min. Cells were then harvested and the cell lysates were collected. Total cell lysates were analyzed by western blotting for phosphorylated and total EGFR. Two independent experiments were conducted. Band volumes were quantified using QuantityOne software. Representative immunoblot and data are presented; mean ± SEM (n=4). Statistical difference as indicated by different numbers ($P<0.05$) was measured using one-way ANOVA and Tukey's test of contrast. C, control; DHA, docosahexaenoic acid; EPA, eicosapentaenoic acid; LA, linoleic acid.

4.3.2 Activation of Rho-GTPases in response to EGF or injury

EGFR activates many important mediators in order to stimulate cellular events that are required for wound healing. For example, EGFR-mediated activation of PLC-γ1, Rac1, and Cdc42 has been shown to be integral in wound healing (Dise et al., 2008; El-Sibai et al., 2007; Li et al., 2009). Therefore, we assessed activation of each of these signaling mediators in response to direct stimulation with an EGFR specific ligand, EGF, or in response to injury. We assessed activation of Rac1 and Cdc42 with an assay that specifically recognizes the activated, GTP-bound forms of these molecules. We found that EGF stimulated activation of Rac1 to a similar extent in control, LA, and EPA treated cells (Fig. 23 A). Treatment with DHA significantly reduced EGF-stimulated activation of Rac1. Furthermore, whereas Cdc42 activation was equally induced in control, LA, and EPA treated cells, DHA significantly reduced activation of Cdc42 in response to EGF (Fig. 24 A). We additionally assessed activation of Rac1 and Cdc42 in response to injury. The same degree of Rac1 activation upon injury was observed in control and LA treated cells (Fig. 23 A). DHA and EPA, however, significantly reduced activation of Rac1 by injury. Similarly, compared to control treated cells, DHA and EPA decreased injury-mediated activation of Cdc42 (Fig. 24 B). Additionally, DHA suppressed Cdc42 activation to a greater extent than EPA.

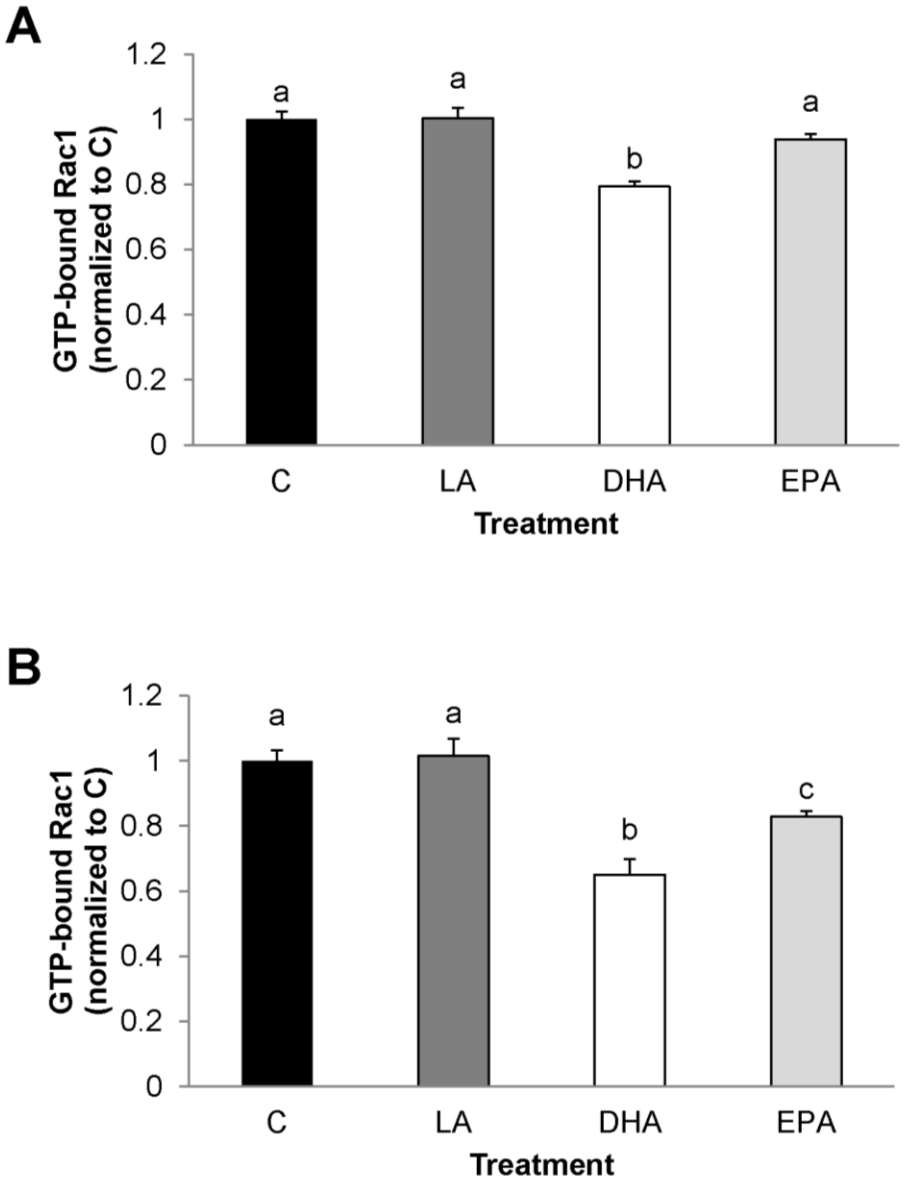

Figure 23. DHA and EPA alter EGFR-mediated Rac1 activation. YAMC cells were either untreated (control) or treated with 50 μM fatty acid (LA, DHA, or EPA) for 72 h. For the final 16-18 h, cells were serum starved (0.5% FBS). Cells were then stimulated either with (A) 25 ng/mL EGF or (B) by extensive wounding. Following stimulation, cells were incubated for 2 min, harvested, and the cell lysates were collected. Total cell lysates were analyzed by G-LISA for active, GTP-bound Rac1. Two independent assays were conducted. Representative data are presented as mean ± SEM (n=6). Statistical difference as indicated by different numbers *(P*<0.05) and was measured using one-way ANOVA and Tukey's test of contrast. C, control; DHA, docosahexaenoic acid; EPA, eicosapentaenoic acid; LA, linoleic acid.

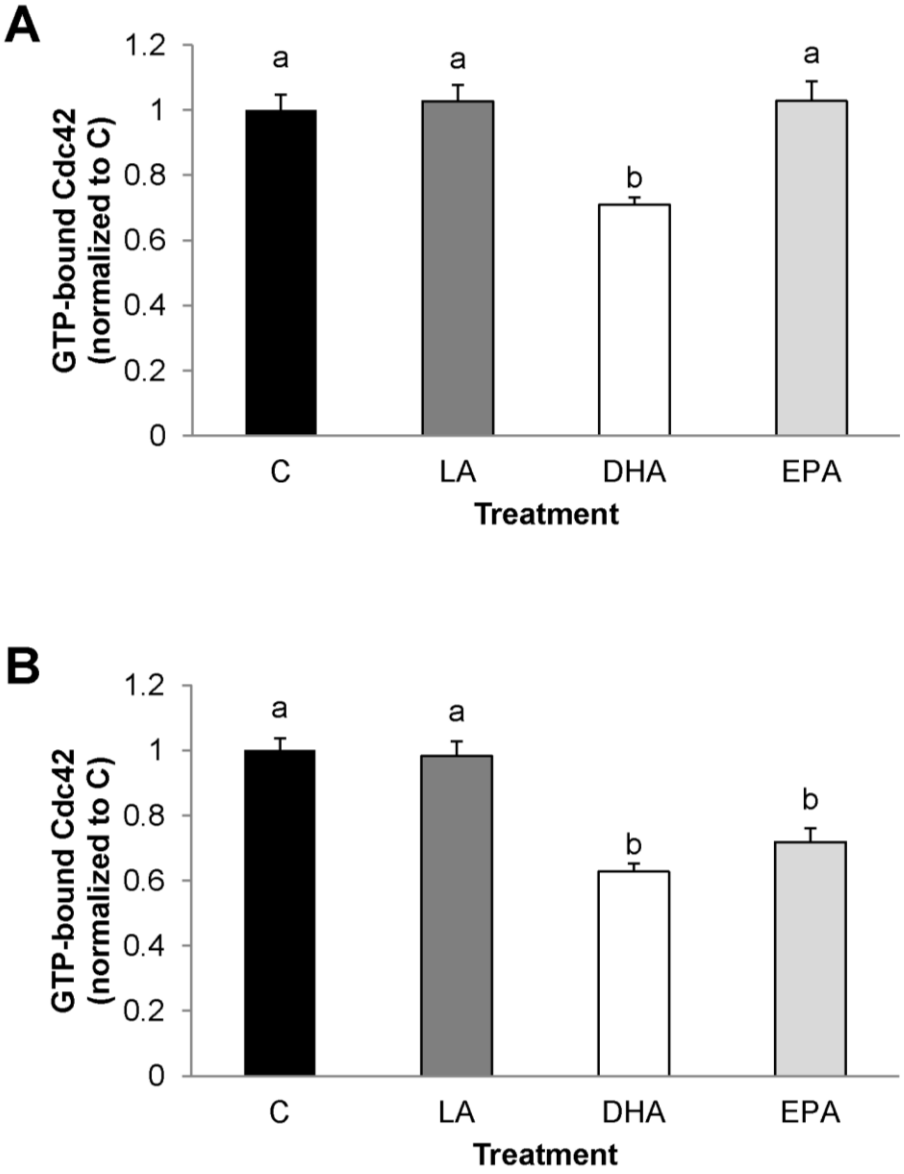

Figure 24. DHA and EPA alter EGFR-mediated activation of Cdc42. YAMC cells were either untreated (control) or treated with 50 μM fatty acid (LA, DHA, or EPA) for 72 h. For the final 16-18 h, cells were serum starved (0.5% FBS). Cells were then stimulated either with (A) 25 ng/mL EGF or (B) by extensive wounding. Following stimulation, cells were incubated for 2 min, harvested, and the cell lysates were collected. Total cell lysates were analyzed by G-LISA for active, GTP-bound Cdc42. Two independent assays were conducted. Representative data are presented as mean ± SEM (n=6). Statistical difference as indicated by different numbers ($P<0.05$) was measured using one-way ANOVA and Tukey's test of contrast. C, control; DHA, docosahexaenoic acid; EPA, eicosapentaenoic acid; LA, linoleic acid.

4.3.3 Effect of EGF or injury on PLC-γ1 signaling

We additionally assessed activation of PLC-γ1 by EGF stimulation or wounding by western blotting for phosphorylated and total PLC-γ1. We probed for Tyr783 phosphorylated PLC-γ1 because phosphorylation at this residue is directly mediated by its binding to EGFR (Kim et al., 1990). EGF stimulated phosphorylation of PLC-γ1 in all treatment groups, but stimulation in DHA treated cells was significantly lower than all other treatment groups (Fig. 25 A). Similar to Rac1 and Cdc42, treatment with either EPA or DHA inhibited injury-induced activation of PLC-γ1 (Fig. 25 B).

4.3.4 Scratch and migration assays

Based on our initial observation that DHA impedes important processes required for wound healing, we next wanted to perform a functional assay to observe wound healing. Cells were scrape-wounded and treated with or without EGF. The wound was imaged every 15 min for 24 h. Wound healing was measured by counting the number of cells that had infiltrated the wounded area at 12 and 24 h after the wounding event. Unstimulated cells exhibited slow and ineffective wound healing (Fig. 26). In contrast, EGF strongly stimulated wound healing in control and LA treated cells. However, EGF-mediated wound healing of both DHA and EPA treated cells was significantly delayed (Fig. 26).

Cell migration was assessed using a transwell migration assay. We utilized EGF to stimulate cell migration through a membrane with 8 μm pores and allowed the cells to

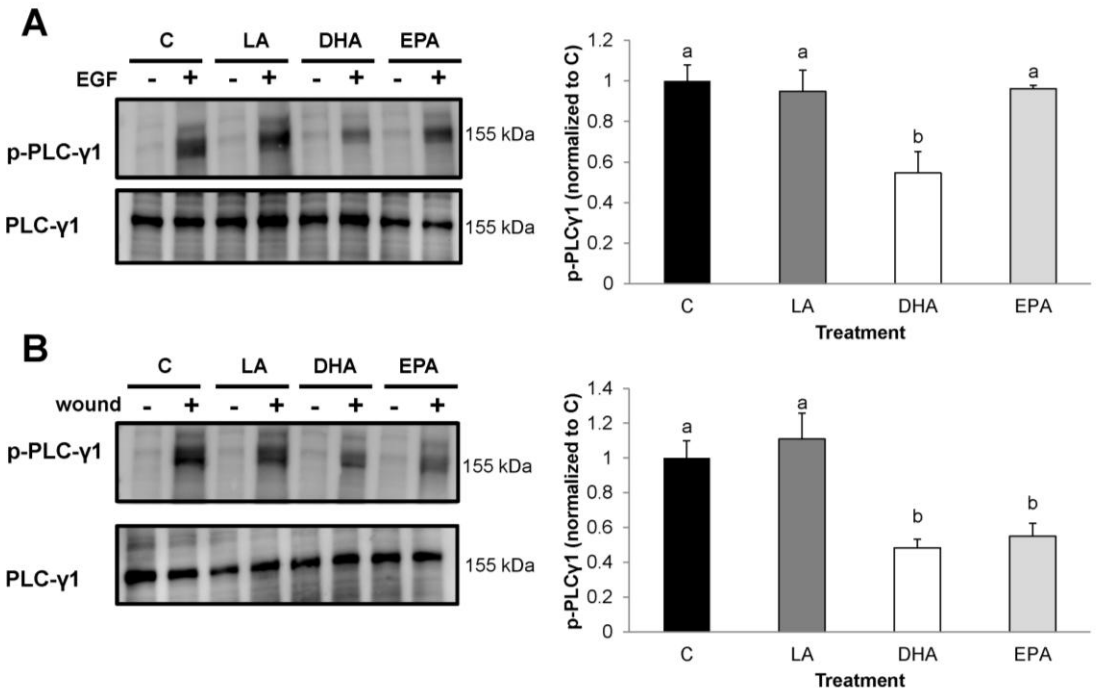

Figure 25. DHA and EPA alter EGFR-mediated activation of PLC-γ1. YAMC cells were either untreated (control) or treated with 50 μM fatty acid (LA, DHA, or EPA) for 72 h. For the final 16-18 h, cells were serum starved (0.5% FBS). Cells were then stimulated with (A) 25 ng/mL EGF or (B) by extensive wounding. Following stimulation, cells were incubated for 2 min, harvested, and the cell lysates were collected. Total cell lysates were analyzed by western blotting for phosphorylated and total PLC-γ1. Band volume was quantified using QuantityOne software. Two independent experiments were conducted. Representative immunoblots and data are presented; mean ± SEM (n=4). Statistical difference as indicated by different numbers ($P<0.05$) was measured using one-way ANOVA and Tukey's test of contrast. C, control; DHA, docosahexaenoic acid; EPA, eicosapentaenoic acid; LA, linoleic acid.

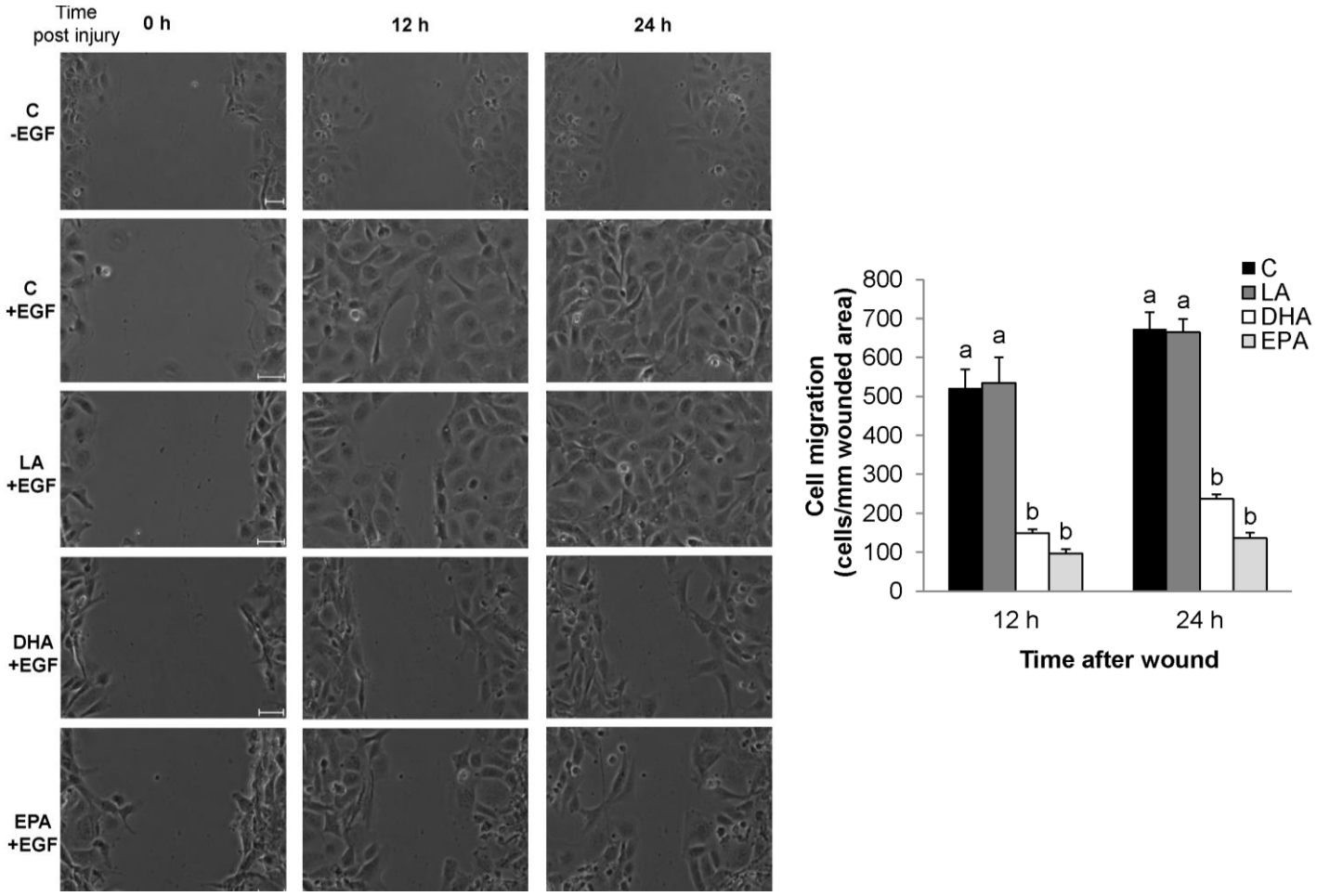

Figure 26. DHA and EPA impede EGF-stimulated wound healing. YAMC cells were either untreated (control) or treated with 50 μM fatty acid (LA, DHA, or EPA) for 72 h. For the final 16-18 h, cells were serum starved (0.5% FBS). Cells were then scratched with a p-200 pipette tip and stimulated with 25 ng/mL EGF. Cell migration into the wounded area was imaged every 15 min on a Nikon TiE inverted microscope for 24 h. Cell migration was quantified by counting the number of cells that had migrated into the wounded area at 12 and 24 h after the initial wound. Four independent experiments were conducted. Representative images and data are presented; mean ± SEM (n=10). Statistical difference as indicated by different numbers ($P<0.05$) was measured using one-way ANOVA and Tukey's test of contrast. C, control; DHA, docosahexaenoic acid; EPA, eicosapentaenoic acid; LA, linoleic acid. Bar=50 um.

migrate for 12 h. Cells migrated to a similar extent in control and LA treated cells (Fig. 27). However, treatment with either DHA or EPA significantly reduced cell migration.

4.3.6 Survival rates in vivo

Based on these observations, we wanted to determine whether consuming dietary lipids can alter acute wound healing in an animal model. Therefore, we fed mice a diet enriched in either corn oil (CO), purified EPA, or purified DHA for 10 days. Next, the animals were exposed for 5 days to 2.5% DSS in the drinking water. DSS is a wounding agent that is often utilized to induce a form of mouse colitis that presents similar clinical and histological features of human inflammatory bowel diseases (Yan et al., 2009). DSS causes colonic wounding by interfering with intestinal barrier function and stimulating local inflammation (Laroui et al., 2012). In this study following DSS treatment, mice received either no recovery period or were allowed to recover for a period of 3 or 6 days. The mice were maintained on the diets throughout the entire study period. We assessed changes in body weight over the entire period. Interestingly, mice fed a DHA-enriched or EPA-enriched diet lost significantly more weight than mice on the CO-enriched diet (Fig. 28). Furthermore, mice on the DHA diet began to gain back weight between 3 and 6 days of recovery, whereas mice on the other diets did not. We additionally analyzed survival in mice allowed to recover for 6 days. We found that survival of mice fed the EPA diet was reduced compared to the CO diet (Fig. 29). The DHA diet, however, did not reduce overall survival compared to the CO diet. We are additionally currently assessing inflammation and injury, as well as colonocytes proliferation and apoptosis, in these mice.

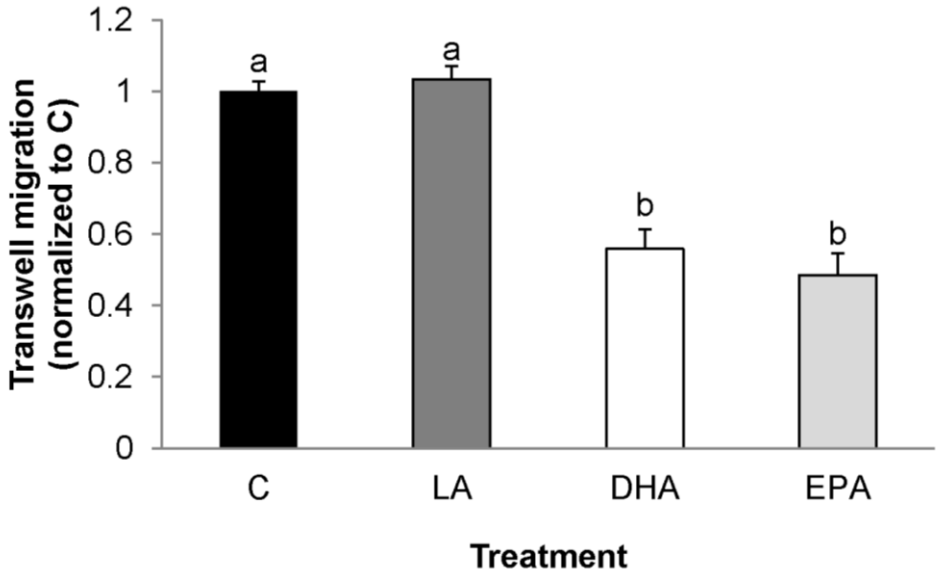

Figure 27. DHA and EPA hinder EGF-stimulated cell migration. YAMC cells were either untreated (control) or treated with 50 μM fatty acid (LA, DHA, or EPA) for 72 h. For the final 16-18 h, cells were serum starved (0.5% FBS). Following serum starvation, cells were trypsinized, counted, and an equal number of cells were seeded into the top chamber of a 2-chamber well in serum free media. The bottom chamber was filled with media supplemented with 25 ng/mL EGF. Cells were incubated for 12 h and allowed to migrate through the membrane between the chambers. Cells were then stained, and the cells remaining in the top chamber were removed. The dye was then eluted from the stained cells that had migrated through the membrane. The optical density of the dye/elution mixture was then measured on a spectrophotometer. Two independent experiments were conducted. Data are presented as mean ± SEM (n=6). Statistical difference as indicated by different numbers *(P*<0.05) was measured using a one-way ANOVA and Tukey's test of contrast. C, control; DHA, docosahexaenoic acid; EPA, eicosapentaenoic acid; LA, linoleic acid.

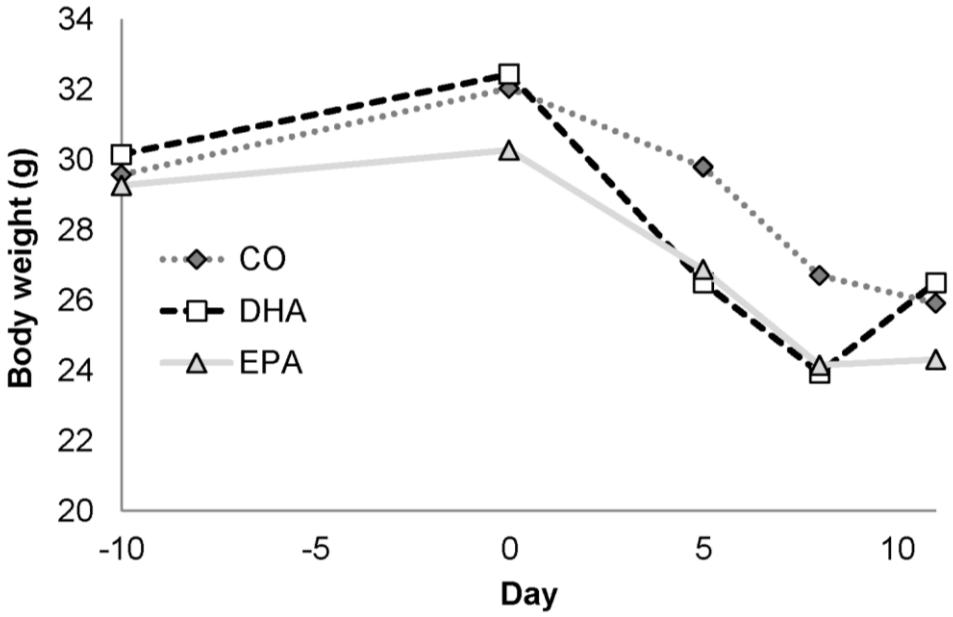

Figure 28. Diets enriched in different fatty acids have varying effects on mouse weights. Mice were fed a diet with CO as the sole lipid source or a diet enriched with purified DHA or EPA for 10 days. Mice were then continued on the diet and exposed to 2.5% DSS for 5 days. Mice were then allowed to recover from DSS for 0, 3 or 6 days. The body weights of mice were measured before beginning diet (day -10), at the beginning of DSS treatment (day 0), at the end of DSS treatment (day 5), and following recovery (days 8 and 11). The average body weight was calculated and graphed over time for each diet group (n=25-75).

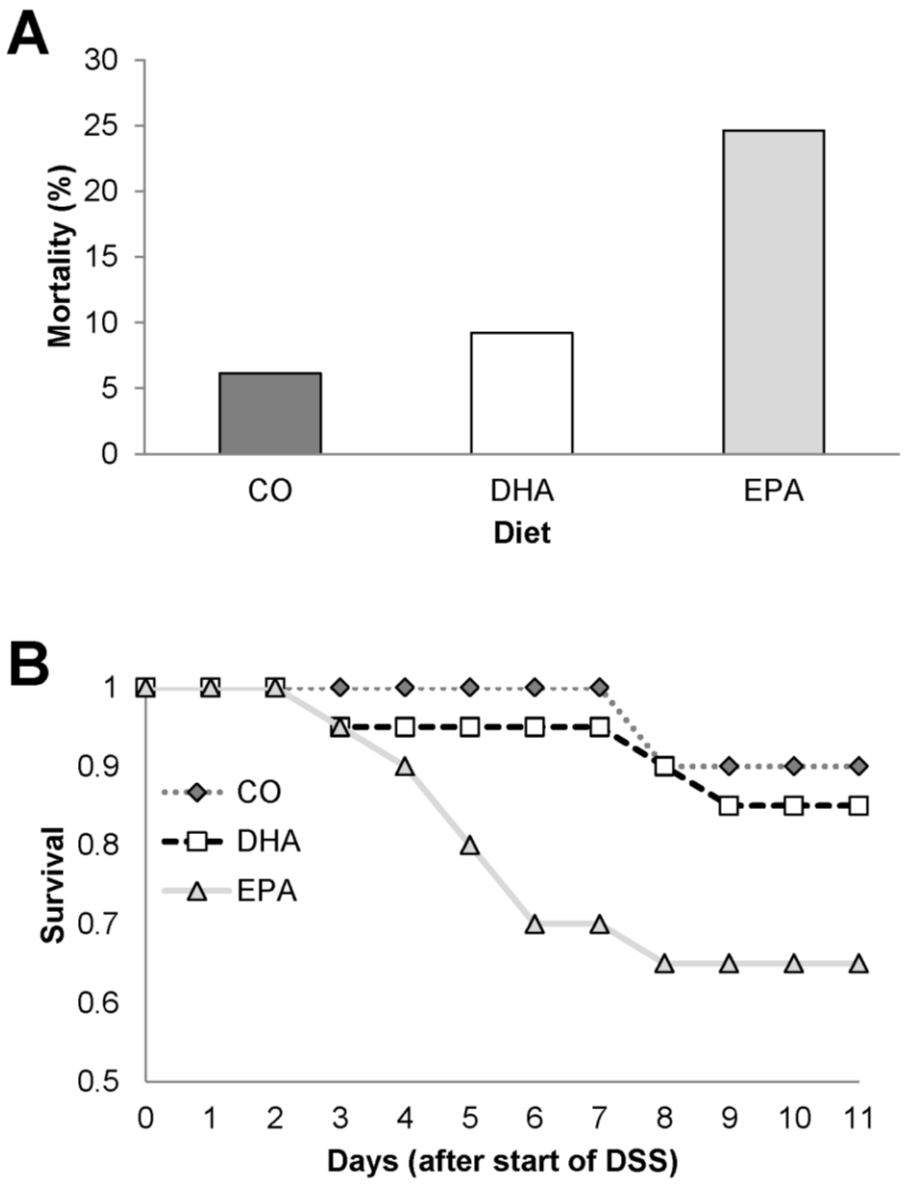

Figure 29. EPA reduces survival of mice treated with DSS. Mice were fed a diet with CO as the sole lipid source or a diet enriched with purified DHA or EPA for 10 days. Mice were then continued on the diet and exposed to 2.5% DSS for 5 days. Mice were then allowed to recover from DSS for 0, 3 or 6 days. (A) Overall mortality of mice at all time points was quantified (n=65-75 mice per diet). (B) The survival of animals that were allowed to recover for 6 days was assessed using a Kaplan-Meier Survival Curve (n=20 mice per diet).

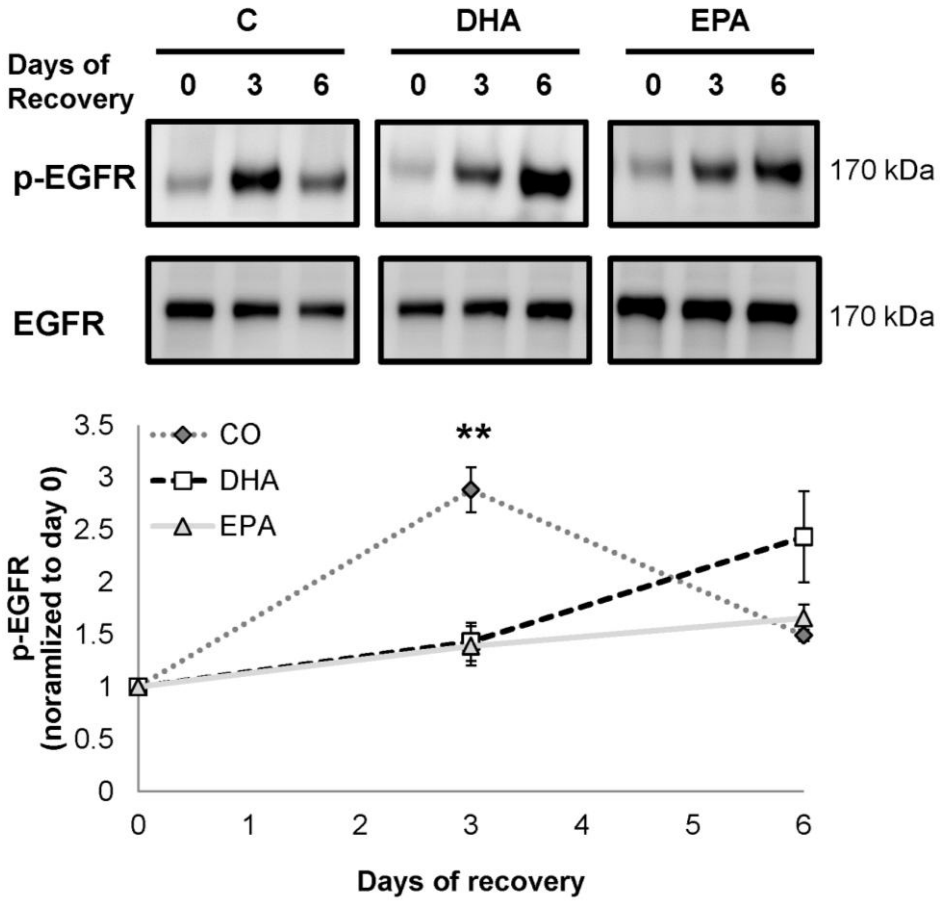

Figure 30. The pattern of EGFR phosphorylation differs in mice fed different lipids. Mice were fed a diet with CO as the sole lipid source or a diet enriched with purified DHA or EPA for 10 days. Mice were then continued on the diet and exposed to 2.5% DSS for 5 days. Mice were then allowed to recover from DSS for 0, 3 or 6 days. Whole cell lysates were isolated from scraped colonic mucosa and probed by western blotting for total and phosphorylated EGFR. Quantification of band volume was performed, and data are presented as mean ± SEM normalized to 0 day recovery (n=4). Statistical significance between diets was determined using a one-way ANOVA and Tukey's test of contrast. At day 3, CO fed animals had significantly higher levels of p-EGFR than DHA or EPA fed animals (**P≤0.001). CO, corn oil; DHA, docosahexaenoic acid; EPA, eicosapentaenoic acid.

4.3.6 EGFR activation in mice

Next, we wanted to assess EGFR activation status over the recovery period. EGFR phosphorylation was determined in the scraped colonic mucosa of the mice to observe changes in EGFR activation. We compared EGFR phosphorylation after 0, 3, or 6 days of recovery from DSS. EGFR phosphorylation peaked at day 3 of recovery in mice fed the CO diet and then decreased by day 6 (Fig. 30). In the DHA and EPA treated animals, we found that peak EGFR phosphorylation did not occur until day 6 of recovery, with EGFR phosphorylation constantly increasing from day 0 to day 6 (Fig. 30).

4.3.7 Mucosa cytoskeletal-remodeling signaling in mice

After observing diet-induced differences in EGFR phosphorylation, we next wanted to compare downstream activation of Rac1 and Cdc42. Consistent with EGFR phosphorylation, Cdc42 activation peaked at day 3 of recovery in CO fed mice, and activation then decreased by day 6 of recovery (Fig. 31). In contrast, Cdc42 activation continued to increase in DHA or EPA fed mice throughout the entire observed recovery period. Activation of Cdc42 in CO fed mice was significantly higher than in DHA or EPA fed mice at day 3 of recovery but significantly lower at day 6. A similar overall pattern was additionally observed in activation of Rac1 (Fig. 32). Rac1 activation in CO fed mice at day 3 of recovery was significantly higher than DHA or EPA fed mice, but no significant difference was observed at day 6 of recovery.

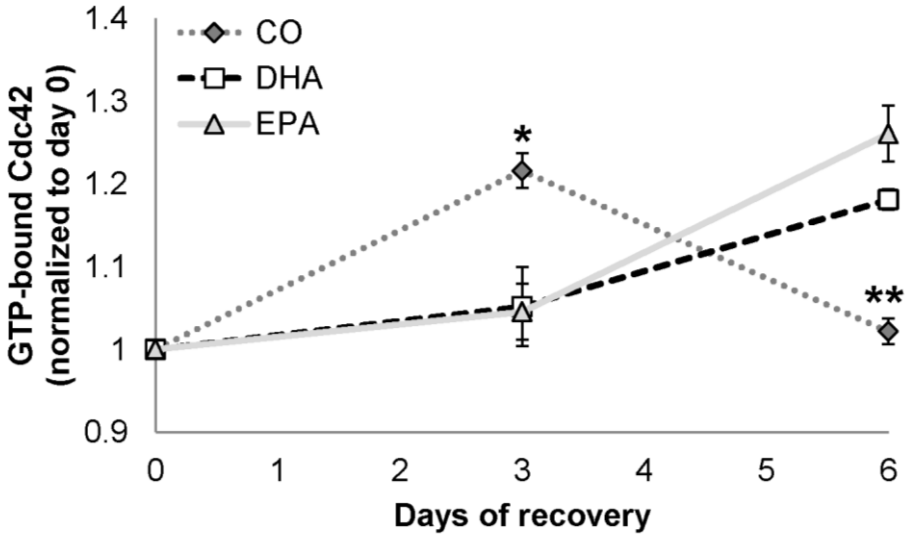

Figure 31. **The pattern of Cdc42 activation differs in mice fed different lipids.** Mice were fed a diet with CO as the sole lipid source or a diet enriched with purified DHA or EPA for 10 days. Mice were then continued on the diet and exposed to 2.5% DSS for 5 days. Mice were then allowed to recover from DSS for 0, 3 or 6 days. Whole cell lysates were isolated from scraped colonic mucosa and probed by G-LISA for GTP-bound Cdc42. Two independent assays were conducted. Data are presented as mean ± SEM (n=6-8). Statistical significance between groups was quantified using a one-way ANOVA and Tukey's test of contrast. At day 3, CO fed mice had significantly higher levels of GTP-bound Cdc42 than DHA or EPA fed mice (*$P \leq 0.05$). At day 6, CO fed mice had significantly lower levels of GTP-bound Cdc42 than DHA or EPA fed mice (**$P \leq 0.001$).

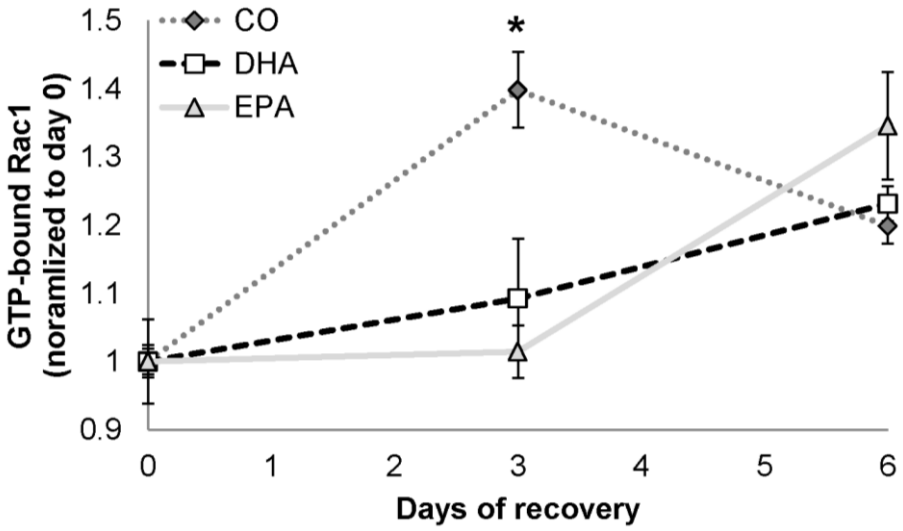

Figure 32. The pattern of Rac1 activation differs in mice fed different lipids. Mice were fed a diet with CO as the sole lipid source or a diet enriched with purified DHA or EPA for 10 days. Mice were then continued on the diet and exposed to 2.5% DSS for 5 days. Mice were then allowed to recover from DSS for 0, 3 or 6 days. Whole cell lysates were isolated from scraped colonic mucosa and probed by G-LISA for GTP-bound Rac1. Two independent assays were conducted. Data are presented as mean ± SEM (n=6-8). Statistical significance between groups was quantified using a one-way ANOVA and Tukey's test of contrast. At day 3, CO fed mice had significantly higher levels of GTP-bound Rac1 than DHA or EPA fed mice (*P≤0.05). At day 6, CO fed mice had significantly lower levels of GTP-bound Rac1 than DHA or EPA fed mice (**P≤0.001).

4.4 Discussion

To our knowledge, this is the first time that the differential effects of DHA and EPA on EGFR signaling in the context of wound healing have been assessed. There is an abundance of interest in this field, especially since many Americans currently take fish oil supplements due to their well-established health benefits (Wu et al., 2011). Interestingly, our data indicate that n-3 PUFA may not always promote optimal health, which may help clarify some of the inconsistencies in the literature.

We found that both DHA and EPA reduce wound-induced transactivation of EGFR. Multiple signaling pathways have been found to be involved in the transactivation of EGFR. Interestingly, prostaglandin E_2 (PGE_2) mediates activation of MMPs, which cleave EGFR-ligands from the plasma membrane (Al-Salihi et al., 2007; Oshima et al., 2011; Pai et al., 2002). It is well-established that DHA and EPA reduce production of PGE_2 (Calder, 2005; Trebble et al., 2003), which could in turn prevent transactivation of EGFR. Additionally, Src has been shown to mediate activation of MMPs to induce EGFR activation (Pai et al., 2002; Xu et al., 2006). Interestingly, Src signaling has been shown to be facilitated by lipid rafts (Holzer et al., 2011), and n-3 PUFA have profound effects on lipid rafts and signaling events that emanate from these heterogeneous domains (Chapkin et al., 2008b; Siddiqui et al., 2007). The observed effect of DHA and EPA on activation of EGFR could be caused by inhibition of one of these mechanisms, but further work is required to pinpoint the mechanism by which n-3 PUFA inhibit transactivation of EGFR in response to injury.

We next observed that in response to ligand, DHA, but not EPA, inhibited EGFR signaling through PLC-γ1, Rac1, and Cdc42. This is consistent with our previous observations that DHA suppresses EGFR signal transduction (Fig. 8). In response to wounding, both EPA and DHA reduced activation of PLC-γ1, Rac1 and Cdc42, which is consistent with the data indicating that EPA and DHA inhibit transactivation of EGFR (Fig. 22). In addition to these mediators, we have previously shown that DHA inhibits EGFR-mediated activation of ERK1/2 and STAT3 (Fig. 8). All of these factors are integral in mediating wound healing, which further suggests that n-3 PUFA could be unfavorable for recovery from injury.

With respect to the analysis of wound healing and cell migration *in vitro*, EGF enhanced wound healing in control and LA treated cells (Fig. 26). However, wound healing was strongly impeded by treatment with DHA or EPA. Similar results were observed for cell migration. It is intriguing that although EPA did not impair ligand-induced EGFR signaling, it did impair EGF-induced biological responses. This suggests that the effects of EPA in regard to wound healing and migration may be independent of EGFR. This hypothesis could be tested by utilizing an EGFR-null cell line. Additionally, EGF-induced cytoskeleton remodeling has been shown to be mediated by the products of 5-lipoxygenase and cyclooxygenase (Peppelenbosch et al., 1993). DHA and EPA compete with arachidonic acid as substrates for these enzymes, which could affect cytoskeleton remodeling and cell migration in a manner independent of activation of the EGFR signaling mediators we analyzed.

The *in vivo* results further demonstrate that DHA and EPA alter wound healing in part by modifying EGFR-mediated signaling events. DHA and EPA fed animals exhibited greater losses in body weight in response to DSS treatment. Additionally, consistent with the *in vitro* effect of EPA on wound healing, EPA fed animals displayed the lowest survival levels. These data together suggest that early wound healing events are being inhibited by DHA and EPA. Upon assessment of downstream signaling, we found that peak activation of EGFR and downstream signaling mediators are delayed in animals fed EPA or DHA. This suggests that the CO fed mice are recovering more quickly than the n-3 PUFA fed mice. Although we cannot specify that the changes in downstream signaling are only due to changes in EGFR regulation and not other parallel pathways, the data clearly demonstrate differential regulation of important wound healing signaling events in n-3 PUFA fed mice compared to CO fed mice. It is important to keep in mind the multitude of pathways that can be altered by dietary components. Here, we focused specifically on signaling through EGFR, but future studies will assess diet effects on the regulation of other essential regulators of wound healing.

Although it still remains unclear how DHA and EPA alter EGFR activation in colonic wound healing, it is patently obvious that these bioactive lipids present a barrier to wound healing due to altered cell signaling. However, the process of wound healing is complex and complicated, and this study only focused on the EGFR-mediated signaling events that contribute to wound healing. DHA and EPA are known to have many beneficial effects, and research on both DHA and EPA clearly detail a role for

these fatty acids in reducing inflammation (Calder, 2005). Although early immune-mediated events are required for wound healing, prolonged inflammation can be detrimental to this process. DHA and EPA can be metabolized into a number of different lipid mediators, including resolvins, protectins, and maresins, which facilitate resolution of inflammation (Bannenberg, 2010). These lipid mediators have varying biological activities, which contributes to differential effects of EPA and DHA. In this study, we observed that DHA fed animals started gaining weight between days 3 and 6 of recovery, whereas other diet groups did not. This suggests that DHA could be facilitating events that expedite later stages of wound healing, perhaps by resolving inflammation.

This work is particularly important for people who experience colonic wounding, e.g., IBD. IBD patients undergo multiple sequences of active disease and recovery. These individuals have low expression of EGFR ligands (Oikonomou et al., 2010), and current work suggests that supplementation with EGF elicits a positive response in IBD patients (Sinha et al., 2003). Some data suggest a beneficial role for n-3 PUFA in IBD (Gravaghi et al., 2011; Hudert et al., 2006), but other data indicate no effect or even a detrimental role (Hawthorne et al., 1992; Hou et al., 2011; Lorenz et al., 1989). A systematic review and meta-analysis of human studies indicated no clear beneficial role for n-3 PUFA in IBD patients (Turner et al., 2011). The data presented here suggests that the inhibition of EGFR signaling by n-3 PUFA could delay wound healing in these individuals. However, the anti-inflammatory effects of n-3 PUFA could be beneficial during some disease stages, e.g., resolution of chronic inflammation. Future work

should focus on determining optimal timing and dosing of n-3 PUFA to elicit the beneficial effects of these dietary lipids while avoiding the detrimental effects.

Overall, the focus of this study was to determine whether the effects of n-3 PUFA on EGFR signaling affects colonic wound healing. This study for the first time demonstrates a potential mechanism to explain why n-3 PUFA do not facilitate recovery and remission of IBD patients. This research illustrates that the inhibitory effects of DHA and EPA on injury-induced transactivation of EGFR likely contribute to delayed wound healing.

5. SUMMARY AND CONCLUSIONS*

5.1 Summary

DHA, an n-3 PUFA highly enriched in fish oil, was found to uniquely disrupt canonical functioning of EGFR, a transmembrane receptor tyrosine kinase. DHA altered the plasma membrane localization of EGFR, which resulted in increased receptor dimerization and phosphorylation. DHA also enhanced receptor internalization and degradation. The modified localization and endocytosis of the receptor contributed to a suppression of downstream signal transduction, which ultimately impeded biological processes, e.g., cell proliferation and wound healing. Additionally, we found that both DHA and another n-3 PUFA, EPA, prevented transactivation of EGFR in response to injury. These observations have been summarized in Fig. 33 to detail the effect of n-3 PUFA on cellular functions that directly impact mucosal physiology.

5.2 Conclusions

Because of the broad-acting effects of n-3 PUFA on mammalian physiology, it has been postulated that these dietary fatty acids act at a fundamental level common to all cells, i.e., by altering the physical properties of biological membranes (Chapkin et al., 2008a; Shaikh et al., 2009b; Wassall et al., 2004; Wassall and Stillwell, 2008). A wealth of published literature supports the hypothesis that n-3 PUFA play an important role in mediating lipid raft composition.

---

*Part of this chapter is reprinted with permission from "Membrane lipid raft organization is uniquely modified by n-3 polyunsaturated fatty acids" by Harmony F. Turk and Robert S. Chapkin, 2012. *Prostaglandins Leukotrienes and Essential Fatty Acids*, doi: 10.1016/j.plefa.2012.03.008, Copyright 2012 by Elsevier Ltd.

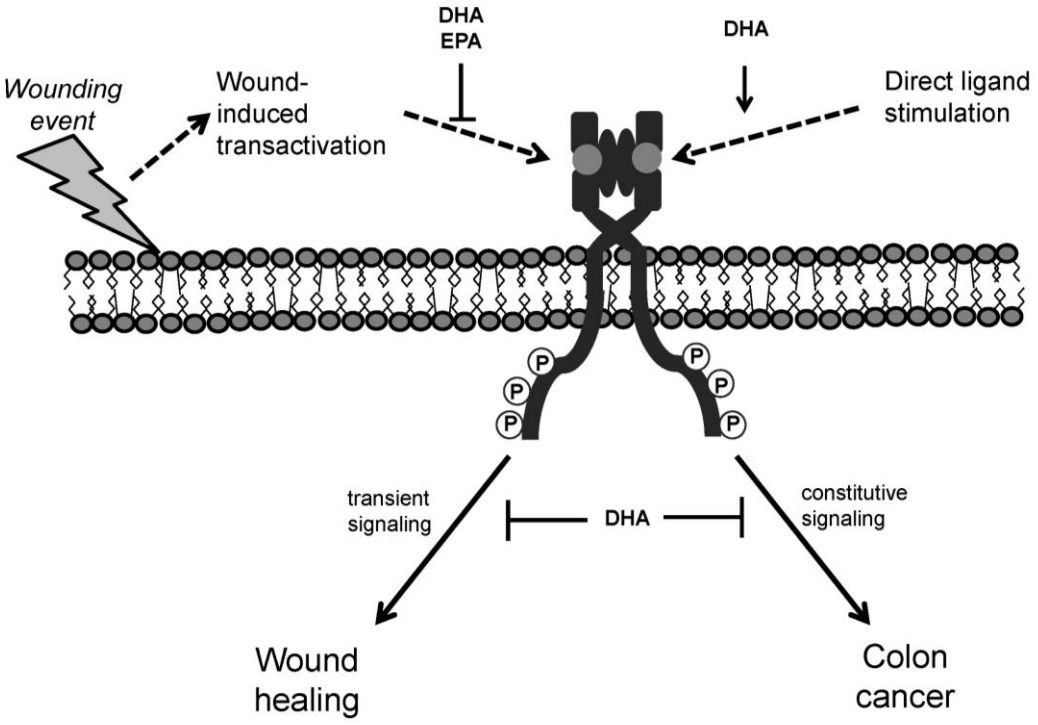

Figure 33. Proposed model for the differential effects of DHA and EPA on EGFR signaling. Transient EGFR signaling is important for cellular functions that promote wound healing. However, constitutive activation of EGFR signaling can facilitate malignant transformation of the colon. We have demonstrated that n-3 PUFA suppress EGFR signaling, but DHA and EPA function through different mechanisms. DHA, but not EPA, increases ligand-induced activation of EGFR but inhibits signal transduction. Additionally, both DHA and EPA impede transactivation of EGFR stimulated by injury. The disease state dictates the overall effect of n-3 PUFA on health.

Previous data from our lab (Chapkin et al., 2008c; Kim et al., 2008), along with the data presented herein, clearly demonstrate that n-3 PUFA modify lipid raft organization and composition, leading to altered cell signaling and function. EGFR, a lipid raft resident and important signaling mediator, is significantly affected by DHA. DHA shifts the lateral distribution of EGFR from lipid rafts into the bulk domain, which directly impacts EGFR function. EGFR phosphorylation is increased, but signal transduction is impaired. These observations are important because they are contrary to the traditional dogma of receptor tyrosine kinase signaling. DHA alters EGFR trafficking, as evidenced by altered EGFR localization within the plasma membrane, reduction in the receptor at the plasma membrane, and increased receptor endocytosis and degradation following activation. Our lab has previously documented effects of DHA on trafficking of other lipid-raft localized proteins, including H- and N-Ras (Seo et al., 2006). Therefore, the effect of DHA on protein trafficking is likely pervasive.

The role for n-3 PUFA in prevention and treatment of colon cancer is well documented, but the efficacy of n-3 PUFA is still a source of contention. Many current prevention and treatment options are aimed at suppression of aberrant cell growth. We have demonstrated a role for DHA in the regulation of this process by modifying the organization of lipid rafts and reducing oncogenic signaling that radiates from these domains. Lipid rafts play a central role in multiple cellular processes involved in colonic tumorigenesis. A number of studies have indicated that cholesterol, a major component of lipid rafts, accumulates in various tumors, and it has been proposed that progressive increases in membrane cholesterol contribute to the expansion of lipid rafts to potentiate

oncogenic cell signaling pathways (Freeman and Solomon, 2004; Li et al., 2006). Additionally, studies have clearly illustrated that lipid rafts play a functional role during tumorigenesis of multiple types of cancer (Staubach and Hanisch, 2011). Therefore, the disruption of rafts by n-3 PUFA indicates a potentially protective and therapeutic role for these dietary lipids in cancer. This mechanism of action could also impact other complex disease states that rely on lipid raft-mediated processes for potentiation of the disease pathology, including Alzheimer's disease, Parkinson's disease, cardiovascular diseases, HIV, and many others (Michel and Bakovic, 2007). Overall, the basic knowledge obtained from our studies provides a solid mechanistic underpinning for the role of n-3 PUFA in colon cancer prevention.

One should always be conscious of the physiological relevance of the dose of n-3 PUFA utilized in studies. Typically, our fish oil-enriched diets contain ~1% energy as DHA, and diets using purified DHA contain ~2% energy as DHA. In contrast, corn oil control diets contain only trace amounts of EPA and DHA. The amount of these lipids consumed by human populations varies greatly. The Japanese typically consume 1–2% of energy in the diet from DHA (Nagata et al., 2002), whereas those in most European countries and the United States consume 0.1–0.2% of energy as total n-3 PUFA (Gibney, 1997). Therefore, our experimental diets contain quantities of n-3 PUFA that are within the range that can be consumed in the human diet. In cell culture experiments, we typically utilize low, physiologically relevant doses of DHA (50 μM), which replicates our *in vivo* results without inducing apoptosis (Turk et al., 2011). Duration of treatment is another important issue. Typically, we treat cell cultures with n-3 PUFA for at least 3

days, and feed animals diets enriched in n-3 PUFA for a minimum of 2 weeks. Since upon supplementation, DHA is very rapidly incorporated into the phospholipids of the plasma membrane of many tissues (Arterburn et al., 2006), relatively little time is required in order to observe an effect of n-3 PUFA exposure. Additionally, removal of n-3 PUFA supplementation has been shown to result in a rapid release of n-3 PUFA from the plasma membrane and reversal of induced effects (Seo et al., 2006). This demonstrates the need for constant consumption of n-3 PUFA in order to maintain some of the effects.

A significant proportion of the literature describing the effects of n-3 PUFA on cellular functions utilizes either fish oil, purified DHA, or a combination of EPA and DHA (Chapkin et al., 2008c; Fan et al., 2004; Schley et al., 2007). This can likely be a source of some of the inconsistencies in the literature. Specifically, although many commercially available fish oils contain approximately a 2:1 ratio of EPA to DHA, fish oils from different sources contain variable mixtures of EPA and DHA. This can make it difficult or impossible to compare results from different studies. Furthermore, whether the effects of n-3 PUFA supplementation are due to EPA, DHA, or both is often undetermined and unappreciated. EPA is both shorter and less unsaturated than DHA, and the structural differences between these two fatty acids are enough to result in functional differences (Corsetto et al., 2012). A recent biophysical study in model membranes demonstrated differential efficacies of DHA and EPA to modify lipid raft composition and organization (Williams et al., 2012). The data presented herein indicate that DHA and EPA have some distinct biological functions but also share some common

effects. It is important for nutritional researchers to appreciate differences in related classes of dietary molecules and to not overlook differential effects.

This research is integral because it clearly elucidates a mechanism by which DHA inhibits colon carcinogenesis. This knowledge is required to know how to best administer DHA to patients, as well as determining which patients are most likely to respond to DHA therapy. This research indicates that patients with cancer that is dependent on overexpression or hyperactivation of EGFR might be more responsive to DHA therapy than patients who have mutations in other oncogenic pathways. Additionally, the work on both DHA and EPA suggests a role for these fatty acids in preventing transactivation of EGFR. Therefore, it is likely that each of these fatty acids could benefit some cancer patients whereas others may not respond. Many of the human clinical trials on the role of n-3 PUFA in colon cancer prevention and treatment have not observed beneficial effects. However, this work suggests that patients who are more likely to respond to n-3 PUFA therapy could be targeted based on their genetic backgrounds, which might make it possible to clearly demonstrate a beneficial effect. Comparable to the therapeutic drugs utilized in cancer treatment, dietary interventions should be tailored based on individual diseases.

It is important to appreciate what these data mean for human health. It is noteworthy that DHA can be either beneficial or detrimental for colon health, depending on the disease state and severity. We detailed the effects of DHA on EGFR signaling in the context of two diseases, with contrasting health outcomes. DHA prevented efficient wound healing in an acute wounding model by inhibiting EGFR signaling, but reduced

carcinogen and inflammation induced colon cancer in part through the same mechanism. Therefore, it is imperative that we further elucidate the complexity of the diet-environment interaction. The future for the field of nutrition, and medicine in general, is in personalization for optimal health.

Overall, this body of work demonstrates a mechanism by which DHA alters the regulation and signaling of an important oncogenic protein, EGFR. We detailed a mechanism that contributes to the effect of DHA on EGFR. We observed this effect in different disease states, which helps to clarify some of the conflicting literature on the role of n-3 PUFA in these diseases. This work is important for overall human health, and it will likely assist future researchers in understanding the role that dietary n-3 PUFA play in optimal nutrition.

5.3 Future directions

The research presented herein set the groundwork for a number of futures studies that could further delve into the effects of DHA on receptor signaling and function.

5.3.1 EGFR localization

One question remaining is how DHA is altering the localization of EGFR. EGFR has been shown to be localized to lipid rafts due to a cysteine-rich juxtamembrane region and N-glycosylation (Cummings et al., 1985; Yamabhai and Anderson, 2002). Additionally, targeting of proteins to lipid rafts has been shown to be facilitated by lipid shells (Anderson and Jacobson, 2002). Therefore, future studies should focus on

determining how DHA alters EGFR localization to lipid rafts. This type of study would then facilitate determining how other receptors might be similarly affected by DHA.

5.3.2 EGFR ligand binding

We have clearly demonstrated that DHA alters EGFR dimerization and activation, but we did not assess the effect of DHA on ligand binding to the receptor. This is obviously a critical step in receptor activation. Evidence suggests that EGFR within lipid rafts is under restraint that confines some receptors from binding to ligand (Matveev and Smart, 2002; Ringerike et al., 2002). Additionally, EGFR within rafts is localized in close proximity of other receptors (Saffarian et al., 2007). Evidence suggests that ligand binding to EGFR dimers follows a model of negative-cooperativity (Macdonald and Pike, 2008). This model indicates that receptor dimerization following binding of ligand to one monomer reduces the affinity of the unoccupied monomer in the dimer for the ligand. The reduced clustering of EGFR upon treatment with DHA could then directly affect ligand binding. Future studies on binding affinity of EGFR in the presence of DHA could further our understanding of the role of DHA in increasing receptor dimerization and phosphorylation. In addition to ligand binding studies, it would be interesting to measure the amount of EGFR ligands upon treatment with EPA or DHA, both free and tethered to the membrane. Our transactivation studies indicate that both EPA and DHA prevent transactivation of EGFR, perhaps by reducing the amount of EGFR ligands that are being cleaved from the plasma membrane. Therefore, measuring the amount of ligand present upon treatment with DHA or EPA could clarify

the mechanism of action of these dietary lipids. Additional studies should further study the mechanism by which n-3 PUFA reduce ectodomain cleavage of EGFR ligands.

5.3.3 Suppression of signal transduction

In this study, we found two potential contributing mechanisms whereby DHA suppresses EGFR signal transduction. These included reduced colocalization of signaling partners within the plasma membrane and increased receptor endocytosis and degradation. However, the contribution of each of these mechanisms to signal perturbation remains undetermined. Future studies should focus on teasing apart the impact of these mechanisms on signaling. One potential way to study this would be to inhibit receptor endocytosis and assess EGFR signaling. Dynamin plays a fundamental role in EGFR endocytosis, and inhibition of dynamin significantly impairs receptor endocytosis and degradation (Sousa et al., 2012). Therefore, future studies could utilize dynamin inhibition to analyze the effects of DHA on EGFR signaling under endocytosis-competent and endocytosis-impaired conditions. This would provide further understanding of the mechanisms of action of DHA.

5.3.4 Mode of receptor endocytosis

It is also important to probe more fully into the observed effect of DHA on EGFR endocytosis. Multiple modes of receptor endocytosis, including clathrin-dependent and lipid-raft dependent endocytosis, have been shown to be involved in EGFR internalization, and the mode of internalization often dictates the fate of the receptor (Goh et al., 2010; Orth et al., 2006; Puri et al., 2005; Roepstorff et al., 2009; Sigismund et al., 2008; Sorkin and Goh, 2009). Therefore, future studies should focus

on elucidating which of these endocytosis mechanism(s) DHA is altering to increase EGFR endocytosis.

5.3.5 EGFR trafficking

Additionally, following EGFR endocytosis, EGFR is trafficked through multiple endosomes, which can ultimately lead to translocation of the receptor to distinct destinations. EGFR can be trafficked to lysosomes for degradation, returned to the plasma membrane to signal, or targeted for key organelles including the nucleus and the mitochondria (Demory et al., 2009; Sorkin and Goh, 2009; Wang et al., 2010). The evidence provided herein that EGFR localization, internalization, and degradation are being affected by DHA strongly indicates that this fatty acid can affect EGFR trafficking. Due to the importance of EGFR localization in cancer (Lo, 2010), it is imperative for future studies to analyze intracellular receptor trafficking.

5.3.6 Ras activation

Another obvious future direction is to determine the localization of Ras activation. Ras has been shown to be activated largely at the plasma membrane but also in endosomes (Prior and Hancock, 2011; Wiley and Burke, 2001). We hypothesize that activation of Ras is inhibited at both sites by treatment with DHA. Based on current evidence, we predict that activation at the plasma membrane would be suppressed due to the altered localization of EGFR and Ras, specifically H-Ras. Additionally, rapid ubiquitination and degradation of the receptor would reduce the amount of Ras being activated in endosomes. Additionally, the altered PM localization of EGFR could modify the amount of EGFR and Ras that would be localized within an endosome and

thereby diminish the capacity of EGFR to activate Ras in endosomes. We currently have probes that bind specifically to activated Ras. These could be utilized to determine where Ras is being activated in order to assess how DHA is altering its activation. Due to the role of Ras activation in colon cancer, further understanding of the role of DHA in regulating Ras activation could be beneficial.

5.3.7 Human study

We have performed both cell culture and animal studies to observe the effect of DHA on EGFR function. A logical extension of this research is to move into a human model. We predict that long term exposure to DHA could prevent colon carcinogenesis by impeding early transformation events that are mediated by EGFR. Furthermore, we hypothesize that humans with overexpression and/or hyperactivation of EGFR are more likely to respond to treatment with DHA. A human study with careful attention to the genetics of patients who respond to this therapy could fully elucidate the mechanism of action of DHA. Studies on the efficacy of anti-EGFR therapies have shown that only approximately 10% of patients are responsive (Fiske et al., 2009), and patients with activating mutations of K-Ras are not responsive to this therapy (De Roock et al., 2008). It is likely that DHA will be effective in patients with a similar genetic background. Furthermore, it would be interesting to extend our EPA versus DHA comparisons in a human model. We predict that, by reducing transactivation of EGFR, EPA could be effective in preventing EGFR-mediated colon cancer. Due to the complexities of cancer and the multiple mechanisms of action of n-3 PUFA, well designed and thorough human studies are imperative.

5.3.8 Activation of other ErbB family receptors

EGFR does not function alone. There are three other members of the ErbB family in addition to EGFR, including ErbB2, ErbB3, and ErbB4. Compared to EGFR, the other ErbB family members are not as well researched, especially in the context of the colon. ErbB2 is very sparsely expressed in normal colonic tissue, but it is highly expressed in colon cancers (Kapitanovic et al., 1997). Additionally, targeted deletion of ErbB3 in the mouse intestine was found to prevent colon tumor formation (Lee et al., 2009). Little is known about the role of ErbB4 in colon cancer, but it has been found to promote cell survival of colon epithelial cells (Frey et al., 2010). Each of the ErbB family members has been indicated to be important during different stages of colon cancer (Lee et al., 2002). Evidence has been presented for localization of ErbB2 and ErbB4 to lipid rafts (Chinni et al., 2008; Ma et al., 2003; Nagy et al., 2002), suggesting that DHA could affect activation of these receptors in a similar manner to EGFR. Moreover, EGFR can function in a heterodimer with each of the other family members, and each of the heterodimers serves to stimulate different cellular functions (Fiske et al., 2009; Olayioye et al., 2000). Research focused on the effect of DHA on activation, dimerization, heterodimerization, and signaling of the entire family of ErbB receptors may reveal additional aspects of the role of DHA in colon cancer prevention.

5.3.9 Lipid raft receptors

This research suggests that the effect of DHA on lipid rafts could potentially affect other lipid raft localized receptors. Many receptors have been found to be localized to lipid rafts and caveolae, and there is substantial evidence that lipid rafts

mediate numerous signal transduction events. Other receptor tyrosine kinases that have been shown to be localized to lipid microdomains or signal from rafts in the plasma membrane include platelet-derived growth factor receptor (localized to caveolae), insulin receptor (localized to caveolae), and fibroblast growth factor receptor (signals from rafts) (Pike, 2005). Although it is unclear whether DHA equally affects caveolae and lipid rafts, it would be interesting to evaluate the effect of DHA on signaling through these receptors.

5.3.10 Lipid rafts

Cogent evidence has been presented to show that different classes of lipid rafts exist (Asanov et al., 2010; Hofman et al., 2008; Lingwood et al., 2009; Patra, 2008). Current work on the effects of DHA on lipid rafts has largely grouped all lipid rafts, along with caveolae where applicable, into one category. With significant strides being made in the field of microscopy, future work should focus on differentiating between rafts and determining the unique effects of DHA on each class of raft. This type of work could substantially impact the field of membrane research, which directly ties into innumerable aspects of human health.

REFERENCES

Adachi, S., T. Nagao, H.I. Ingolfsson, F.R. Maxfield, O.S. Andersen, L. Kopelovich, and I.B. Weinstein. 2007. The inhibitory effect of (-)-epigallocatechin gallate on activation of the epidermal growth factor receptor is associated with altered lipid order in HT29 colon cancer cells. *Cancer Res*. 67:6493-6501.

Al-Salihi, M.A., S.C. Ulmer, T. Doan, C.D. Nelson, T. Crotty, S.M. Prescott, D.M. Stafforini, and M.K. Topham. 2007. Cyclooxygenase-2 transactivates the epidermal growth factor receptor through specific E-prostanoid receptors and tumor necrosis factor-alpha converting enzyme. *Cell Signal*. 19:1956-1963.

Algeciras-Schimnich, A., L. Shen, B.C. Barnhart, A.E. Murmann, J.K. Burkhardt, and M.E. Peter. 2002. Molecular ordering of the initial signaling events of CD95. *Mol Cell Biol*. 22:207-220.

Alonso, M.A., and J. Millan. 2001. The role of lipid rafts in signalling and membrane trafficking in T lymphocytes. *J Cell Sci*. 114:3957-3965.

Anderson, D., C.A. Koch, L. Grey, C. Ellis, M.F. Moran, and T. Pawson. 1990. Binding of SH2 domains of phospholipase C gamma 1, GAP, and Src to activated growth factor receptors. *Science*. 250:979-982.

Anderson, R.E., and L. Sperling. 1971. Lipids of ocular tissues. VII. Positional distribution of the fatty acids in the phospholipids of bovine retina rod outer segments. *Arch Biochem Biophys*. 144:673-677.

Anderson, R.G. 1998. The caveolae membrane system. *Annu Rev Biochem*. 67:199-225.

Anderson, R.G., and K. Jacobson. 2002. A role for lipid shells in targeting proteins to caveolae, rafts, and other lipid domains. *Science*. 296:1821-1825.

Angeles Puertollano, M., I. Algarra, E. Ortega, M.A. de Pablo, and G. Alvarez de Cienfuegos. 2001. Loss of natural killer cell activity after murine tumor transplantation appears as a consequence of dietary lipid administration. *Anticancer Res*. 21:2697-2702.

Anti, M., F. Armelao, G. Marra, A. Percesepe, G.M. Bartoli, P. Palozza, P. Parrella, C. Canetta, N. Gentiloni, I. De Vitis, and et al. 1994. Effects of different doses of fish oil on rectal cell proliferation in patients with sporadic colonic adenomas. *Gastroenterology*. 107:1709-1718.

Anti, M., G. Marra, F. Armelao, G.M. Bartoli, R. Ficarelli, A. Percesepe, I. De Vitis, G. Maria, L. Sofo, G.L. Rapaccini, and et al. 1992. Effect of omega-3 fatty acids on rectal mucosal cell proliferation in subjects at risk for colon cancer. *Gastroenterology*. 103:883-891.

Apolloni, A., I.A. Prior, M. Lindsay, R.G. Parton, and J.F. Hancock. 2000. H-ras but not K-ras traffics to the plasma membrane through the exocytic pathway. *Mol Cell Biol*. 20:2475-2487.

Arita, M., F. Bianchini, J. Aliberti, A. Sher, N. Chiang, S. Hong, R. Yang, N.A. Petasis, and C.N. Serhan. 2005. Stereochemical assignment, antiinflammatory properties, and receptor for the omega-3 lipid mediator resolvin E1. *J Exp Med*. 201:713-722.

Arita, M., T. Ohira, Y.P. Sun, S. Elangovan, N. Chiang, and C.N. Serhan. 2007. Resolvin E1 selectively interacts with leukotriene B4 receptor BLT1 and ChemR23 to regulate inflammation. *J Immunol*. 178:3912-3917.

Arteaga, C.L. 2001. The epidermal growth factor receptor: from mutant oncogene in nonhuman cancers to therapeutic target in human neoplasia. *J Clin Oncol*. 19:32S-40S.

Arterburn, L.M., E.B. Hall, and H. Oken. 2006. Distribution, interconversion, and dose response of n-3 fatty acids in humans. *Am J Clin Nutr*. 83:1467S-1476S.

Asanov, A., A. Zepeda, and L. Vaca. 2010. A novel form of Total Internal Reflection Fluorescence Microscopy (LG-TIRFM) reveals different and independent lipid raft domains in living cells. *Biochim Biophys Acta*. 1801:147-155.

Augsten, M., R. Pusch, C. Biskup, K. Rennert, U. Wittig, K. Beyer, A. Blume, R. Wetzker, K. Friedrich, and I. Rubio. 2006. Live-cell imaging of endogenous Ras-GTP illustrates predominant Ras activation at the plasma membrane. *EMBO Rep*. 7:46-51.

Avraham, R., and Y. Yarden. 2011. Feedback regulation of EGFR signalling: decision making by early and delayed loops. *Nature Rev Mol Cell Biol*. 12:104-117.

Bacso, Z., L. Bene, L. Damjanovich, and S. Damjanovich. 2002. INF-gamma rearranges membrane topography of MHC-I and ICAM-1 in colon carcinoma cells. *Biochem Biophys Rev Commun*. 290:635-640.

Bajaj, M., M.D. Waterfield, J. Schlessinger, W.R. Taylor, and T. Blundell. 1987. On the tertiary structure of the extracellular domains of the epidermal growth factor and insulin receptors. *Biochim Biophys Acta*. 916:220-226.

Bang, B., R. Gniadecki, and B. Gajkowska. 2005. Disruption of lipid rafts causes apoptotic cell death in HaCaT keratinocytes. *Exp Dermatol*. 14:266-272.

Bannenberg, G., M. Arita, and C.N. Serhan. 2007. Endogenous receptor agonists: resolving inflammation. *ScientificWorldJournal*. 7:1440-1462.

Bannenberg, G.L. 2010. Therapeutic applicability of anti-inflammatory and proresolving polyunsaturated fatty acid-derived lipid mediators. *ScientificWorldJournal*. 10:676-712.

Barber, T.D., K. McManus, K.W. Yuen, M. Reis, G. Parmigiani, D. Shen, I. Barrett, Y. Nouhi, F. Spencer, S. Markowitz, V.E. Velculescu, K.W. Kinzler, B. Vogelstein, C. Lengauer, and P. Hieter. 2008. Chromatid cohesion defects may underlie chromosome instability in human colorectal cancers. *Proc Natl Acad Sci U S A*. 105:3443-3448.

Barber, T.D., B. Vogelstein, K.W. Kinzler, and V.E. Velculescu. 2004. Somatic mutations of EGFR in colorectal cancers and glioblastomas. *N Engl J Med*. 351:2883.

Bartram, H.P., A. Gostner, W. Scheppach, B.S. Reddy, C.V. Rao, G. Dusel, F. Richter, A. Richter, and H. Kasper. 1993. Effects of fish oil on rectal cell proliferation, mucosal fatty acids, and prostaglandin E2 release in healthy subjects. *Gastroenterology*. 105:1317-1322.

Batzer, A.G., D. Rotin, J.M. Urena, E.Y. Skolnik, and J. Schlessinger. 1994. Hierarchy of binding sites for Grb2 and Shc on the epidermal growth factor receptor. *Mol Cell Biol*. 14:5192-5201.

Bell, M.V., J.R. Dick, and C. Buda. 1997. Molecular speciation of fish sperm phospholipids: large amounts of dipolyunsaturated phosphatidylserine. *Lipids*. 32:1085-1091.

Ben-Neriah, Y., and M. Karin. 2011. Inflammation meets cancer, with NF-kappaB as the matchmaker. *Nature Immunol*. 12:715-723.

Benais-Pont, G., Y.M. Dupertuis, M.P. Kossovsky, P. Nouet, A.S. Allal, F. Buchegger, and C. Pichard. 2006. Omega-3 polyunsaturated fatty acids and ionizing radiation: combined cytotoxicity on human colorectal adenocarcinoma cells. *Nutrition*. 22:931-939.

Biscardi, J.S., M.C. Maa, D.A. Tice, M.E. Cox, T.H. Leu, and S.J. Parsons. 1999. c-Src-mediated phosphorylation of the epidermal growth factor receptor on Tyr845 and Tyr1101 is associated with modulation of receptor function. *J Biol Chem*. 274:8335-8343.

Bleeker, W.A., V.M. Hayes, A. Karrenbeld, R.M. Hofstra, J. Hermans, C.C. Buys, and J.T. Plukker. 2000. Impact of KRAS and TP53 mutations on survival in patients with left- and right-sided Dukes' C colon cancer. *Am J Gastroenterol*. 95:2953-2957.

Boerner, J.L., M.L. Demory, C. Silva, and S.J. Parsons. 2004. Phosphorylation of Y845 on the epidermal growth factor receptor mediates binding to the mitochondrial protein cytochrome c oxidase subunit II. *Mol Cell Biol*. 24:7059-7071.

Bos, J.L., E.R. Fearon, S.R. Hamilton, M. Verlaan-de Vries, J.H. van Boom, A.J. van der Eb, and B. Vogelstein. 1987. Prevalence of ras gene mutations in human colorectal cancers. *Nature*. 327:293-297.

Breckenridge, W.C., G. Gombos, and I.G. Morgan. 1972. The lipid composition of adult rat brain synaptosomal plasma membranes. *Biochim Biophys Acta*. 266:695-707.

Brown, D.A., and E. London. 2000. Structure and function of sphingolipid- and cholesterol-rich membrane rafts. *J Biol Chem*. 275:17221-17224.

Buday, L., and J. Downward. 1993. Epidermal growth factor regulates p21ras through the formation of a complex of receptor, Grb2 adapter protein, and Sos nucleotide exchange factor. *Cell*. 73:611-620.

Burke, P., K. Schooler, and H.S. Wiley. 2001. Regulation of epidermal growth factor receptor signaling by endocytosis and intracellular trafficking. *Mol Biol Cell*. 12:1897-1910.

Calder, P.C. 2005. Polyunsaturated fatty acids and inflammation. *Biochem Soc Trans*. 33:423-427.

Calviello, G., F. Di Nicuolo, S. Gragnoli, E. Piccioni, S. Serini, N. Maggiano, G. Tringali, P. Navarra, F.O. Ranelletti, and P. Palozza. 2004. n-3 PUFAs reduce VEGF expression in human colon cancer cells modulating the COX-2/PGE2 induced ERK-1 and -2 and HIF-1alpha induction pathway. *Carcinogenesis*. 25:2303-2310.

Cancer Genome Atlas, N. 2012. Comprehensive molecular characterization of human colon and rectal cancer. *Nature*. 487:330-337.

Cao, X., H. Zhu, F. Ali-Osman, and H.W. Lo. 2011. EGFR and EGFRvIII undergo stress- and EGFR kinase inhibitor-induced mitochondrial translocalization: a potential mechanism of EGFR-driven antagonism of apoptosis. *Mol Cancer*. 10:26.

Cargnello, M., and P.P. Roux. 2011. Activation and function of the MAPKs and their substrates, the MAPK-activated protein kinases. *Microbiol Mol Biol R.* 75:50-83.

Carpenter, G., L. King, Jr., and S. Cohen. 1978. Epidermal growth factor stimulates phosphorylation in membrane preparations in vitro. *Nature*. 276:409-410.

Carpenter, G., K.J. Lembach, M.M. Morrison, and S. Cohen. 1975. Characterization of the binding of 125-I-labeled epidermal growth factor to human fibroblasts. *J Biol Chem*. 250:4297-4304.

Carpenter, G., and H.J. Liao. 2009. Trafficking of receptor tyrosine kinases to the nucleus. *Exp Cell Res*. 315:1556-1566.

Caygill, C.P., A. Charlett, and M.J. Hill. 1996. Fat, fish, fish oil and cancer. *Br J Cancer*. 74:159-164.

Chambers, A.F., A.C. Groom, and I.C. MacDonald. 2002. Dissemination and growth of cancer cells in metastatic sites. *Nature Rev Cancer*. 2:563-572.

Chang, W.L., R.S. Chapkin, and J.R. Lupton. 1998. Fish oil blocks azoxymethane-induced rat colon tumorigenesis by increasing cell differentiation and apoptosis rather than decreasing cell proliferation. *J Nutr*. 128:491-497.

Chapkin, R.S., D.N. McMurray, L.A. Davidson, B.S. Patil, Y.Y. Fan, and J.R. Lupton. 2008a. Bioactive dietary long-chain fatty acids: emerging mechanisms of action. *Br J Nutr*. 100:1152-1157.

Chapkin, R.S., J. Seo, D.N. McMurray, and J.R. Lupton. 2008b. Mechanisms by which docosahexaenoic acid and related fatty acids reduce colon cancer risk and inflammatory disorders of the intestine. *Chem Phys Lipids*. 153:14-23.

Chapkin, R.S., N. Wang, Y.Y. Fan, J.R. Lupton, and I.A. Prior. 2008c. Docosahexaenoic acid alters the size and distribution of cell surface microdomains. *Biochim Biophys Acta*. 1778:466-471.

Chardin, P., J.H. Camonis, N.W. Gale, L. van Aelst, J. Schlessinger, M.H. Wigler, and D. Bar-Sagi. 1993. Human Sos1: a guanine nucleotide exchange factor for Ras that binds to GRB2. *Science*. 260:1338-1343.

Chen, X., and M.D. Resh. 2002. Cholesterol depletion from the plasma membrane triggers ligand-independent activation of the epidermal growth factor receptor. *J Biol Chem*. 277:49631-49637.

Chen, Z.Y., and N.W. Istfan. 2000. Docosahexaenoic acid is a potent inducer of apoptosis in HT-29 colon cancer cells. *Prostaglandins Leukot Essent Fatty Acids*. 63:301-308.

Chinni, S.R., H. Yamamoto, Z. Dong, A. Sabbota, R.D. Bonfil, and M.L. Cher. 2008. CXCL12/CXCR4 transactivates HER2 in lipid rafts of prostate cancer cells and promotes growth of metastatic deposits in bone. *Mol Cancer Res*. 6:446-457.

Clapper, M.L., H.S. Cooper, and W.C. Chang. 2007. Dextran sulfate sodium-induced colitis-associated neoplasia: a promising model for the development of chemopreventive interventions. *Acta Pharmacol Sin*. 28:1450-1459.

Clayton, A.H., F. Walker, S.G. Orchard, C. Henderson, D. Fuchs, J. Rothacker, E.C. Nice, and A.W. Burgess. 2005. Ligand-induced dimer-tetramer transition during the activation of the cell surface epidermal growth factor receptor-A multidimensional microscopy analysis. *J Biol Chem*. 280:30392-30399.

Coffey, R.J., Jr., R. Graves-Deal, P.J. Dempsey, R.H. Whitehead, and M.R. Pittelkow. 1992. Differential regulation of transforming growth factor alpha autoinduction in a nontransformed and transformed epithelial cell. *Cell Growth Differ*. 3:347-354.

Cohen, G., R. Mustafi, A. Chumsangsri, N. Little, J. Nathanson, S. Cerda, S. Jagadeeswaran, U. Dougherty, L. Joseph, J. Hart, L. Yerian, M. Tretiakova, W. Yuan, P. Obara, S. Khare, F.A. Sinicrope, A. Fichera, G.R. Boss, R. Carroll, and M. Bissonnette. 2006. Epidermal growth factor receptor signaling is up-regulated in human colonic aberrant crypt foci. *Cancer Res*. 66:5656-5664.

Cohen, S. 1962. Isolation of a mouse submaxillary gland protein accelerating incisor eruption and eyelid opening in the new-born animal. *J Biol Chem*. 237:1555-1562.

Cohen, S. 1965. The stimulation of epidermal proliferation by a specific protein (EGF). *Dev Biol*. 12:394-407.

Coker, K.J., J.V. Staros, and C.A. Guyer. 1994. A kinase-negative epidermal growth factor receptor that retains the capacity to stimulate DNA synthesis. *Proc Natl Acad Sci U S A*. 91:6967-6971.

Collett, E.D., L.A. Davidson, Y.Y. Fan, J.R. Lupton, and R.S. Chapkin. 2001. n-6 and n-3 polyunsaturated fatty acids differentially modulate oncogenic Ras activation in colonocytes. *Am J Physiol Cell Physiol*. 280:C1066-1075.

Conquer, J.A., and B.J. Holub. 1998. Effect of supplementation with different doses of DHA on the levels of circulating DHA as non-esterified fatty acid in subjects of Asian Indian background. *J Lipid Res*. 39:286-292.

Corcoran, R.B., G. Contino, V. Deshpande, A. Tzatsos, C. Conrad, C.H. Benes, D.E. Levy, J. Settleman, J.A. Engelman, and N. Bardeesy. 2011. STAT3 plays a critical role in KRAS-induced pancreatic tumorigenesis. *Cancer Res*. 71:5020-5029.

Corpet, D.E., and S. Tache. 2002. Most effective colon cancer chemopreventive agents in rats: a systematic review of aberrant crypt foci and tumor data, ranked by potency. *Nutr Cancer*. 43:1-21.

Corsetto, P.A., A. Cremona, G. Montorfano, I.E. Jovenitti, F. Orsini, P. Arosio, and A.M. Rizzo. 2012. Chemical-Physical Changes in Cell Membrane Microdomains of Breast Cancer Cells After Omega-3 PUFA Incorporation. *Cell Biochem Biophys*.

Coskun, U., M. Grzybek, D. Drechsel, and K. Simons. 2011. Regulation of human EGF receptor by lipids. *Proc Natl Acad Sci U S A*. 108:9044-9048.

Coskun, U., and K. Simons. 2010. Membrane rafting: from apical sorting to phase segregation. *FEBS Lett*. 584:1685-1693.

Courtney, E.D., S. Matthews, C. Finlayson, D. Di Pierro, A. Belluzzi, E. Roda, J.Y. Kang, and R.J. Leicester. 2007. Eicosapentaenoic acid (EPA) reduces crypt cell proliferation and increases apoptosis in normal colonic mucosa in subjects with a history of colorectal adenomas. *Int J Colorectal Dis*. 22:765-776.

Crnkovic, S., M. Riederer, M. Lechleitner, S. Hallstrom, R. Malli, W.F. Graier, J. Lindenmann, H. Popper, H. Olschewski, A. Olschewski, and S. Frank. 2012. Docosahexaenoic acid-induced unfolded protein response, cell cycle arrest, and apoptosis in vascular smooth muscle cells are triggered by Ca(2)(+)-dependent induction of oxidative stress. *Free Radic Biol Med*. 52:1786-1795.

Cummings, R.D., A.M. Soderquist, and G. Carpenter. 1985. The oligosaccharide moieties of the epidermal growth factor receptor in A-431 cells. Presence of complex-type N-linked chains that contain terminal N-acetylgalactosamine residues. *J Biol Chem*. 260:11944-11952.

D'Ambola, J.B., E.E. Aeberhard, N. Trang, S. Gaffar, C.T. Barrett, and M.P. Sherman. 1991. Effect of dietary (n-3) and (n-6) fatty acids on in vivo pulmonary bacterial clearance by neonatal rabbits. *J Nutr*. 121:1262-1269.

Davidson, L.A., J.R. Lupton, Y.H. Jiang, and R.S. Chapkin. 1999. Carcinogen and dietary lipid regulate ras expression and localization in rat colon without affecting farnesylation kinetics. *Carcinogenesis*. 20:785-791.

Davies, H., G.R. Bignell, C. Cox, P. Stephens, S. Edkins, S. Clegg, J. Teague, H. Woffendin, M.J. Garnett, W. Bottomley, N. Davis, E. Dicks, R. Ewing, Y. Floyd, K. Gray, S. Hall, R. Hawes, J. Hughes, V. Kosmidou, A. Menzies, C. Mould, A. Parker, C. Stevens, S. Watt, S. Hooper, R. Wilson, H. Jayatilake, B.A. Gusterson, C. Cooper, J. Shipley, D. Hargrave, K. Pritchard-Jones, N. Maitland, G. Chenevix-Trench, G.J. Riggins, D.D. Bigner, G. Palmieri, A. Cossu, A. Flanagan, A. Nicholson, J.W. Ho, S.Y. Leung, S.T. Yuen, B.L. Weber, H.F. Seigler, T.L. Darrow, H. Paterson, R. Marais, C.J. Marshall, R. Wooster, M.R. Stratton, and P.A. Futreal. 2002. Mutations of the BRAF gene in human cancer. *Nature*. 417:949-954.

De Roock, W., H. Piessevaux, J. De Schutter, M. Janssens, G. De Hertogh, N. Personeni, B. Biesmans, J.L. Van Laethem, M. Peeters, Y. Humblet, E. Van Cutsem, and S. Tejpar. 2008. KRAS wild-type state predicts survival and is associated to early radiological response in metastatic colorectal cancer treated with cetuximab. *Ann Oncol*. 19:508-515.

Deans, J.P., S.M. Robbins, M.J. Polyak, and J.A. Savage. 1998. Rapid redistribution of CD20 to a low density detergent-insoluble membrane compartment. *J Biol Chem*. 273:344-348.

Deb, T.B., L. Su, L. Wong, E. Bonvini, A. Wells, M. David, and G.R. Johnson. 2001. Epidermal growth factor (EGF) receptor kinase-independent signaling by EGF. *J Biol Chem*. 276:15554-15560.

Demory, M.L., J.L. Boerner, R. Davidson, W. Faust, T. Miyake, I. Lee, M. Huttemann, R. Douglas, G. Haddad, and S.J. Parsons. 2009. Epidermal growth factor receptor translocation to the mitochondria: regulation and effect. *J Biol Chem*. 284:36592-36604.

Di Fiore, F., R. Sesboue, P. Michel, J.C. Sabourin, and T. Frebourg. 2010. Molecular determinants of anti-EGFR sensitivity and resistance in metastatic colorectal cancer. *Br J Cancer*. 103:1765-1772.

Dignass, A.U., and D.K. Podolsky. 1993. Cytokine modulation of intestinal epithelial cell restitution: central role of transforming growth factor beta. *Gastroenterology*. 105:1323-1332.

Dise, R.S., M.R. Frey, R.H. Whitehead, and D.B. Polk. 2008. Epidermal growth factor stimulates Rac activation through Src and phosphatidylinositol 3-kinase to promote colonic epithelial cell migration. *Am J Physiol Gastrointest Liver Physiol*. 294:G276-285.

Drbal, K., M. Moertelmaier, C. Holzhauser, A. Muhammad, E. Fuertbauer, S. Howorka, M. Hinterberger, H. Stockinger, and G.J. Schutz. 2007. Single-molecule microscopy reveals heterogeneous dynamics of lipid raft components upon TCR engagement. *Int Immunol*. 19:675-684.

Dupertuis, Y.M., M.M. Meguid, and C. Pichard. 2007. Colon cancer therapy: new perspectives of nutritional manipulations using polyunsaturated fatty acids. *Curr Opin Clin Nutr Metab Care*. 10:427-432.

Duraisamy, Y., D. Lambert, C.A. O'Neill, and P.J. Padfield. 2007. Differential incorporation of docosahexaenoic acid into distinct cholesterol-rich membrane raft domains. *Biochem Biophys Res Commun*. 360:885-890.

Eden, E.R., F. Huang, A. Sorkin, and C.E. Futter. 2011. The role of EGF receptor ubiquitination in regulating its intracellular traffic. *Traffic*.

Eden, S., R. Rohatgi, A.V. Podtelejnikov, M. Mann, and M.W. Kirschner. 2002. Mechanism of regulation of WAVE1-induced actin nucleation by Rac1 and Nck. *Nature*. 418:790-793.

Egan, L.J., A. de Lecea, E.D. Lehrman, G.M. Myhre, L. Eckmann, and M.F. Kagnoff. 2003. Nuclear factor-kappa B activation promotes restitution of wounded intestinal epithelial monolayers. *Am J Physiol Cell Physiol*. 285:C1028-1035.

Eisenberg, S., and Y.I. Henis. 2008. Interactions of Ras proteins with the plasma membrane and their roles in signaling. *Cell Signal*. 20:31-39.

Eisenberg, S., D.E. Shvartsman, M. Ehrlich, and Y.I. Henis. 2006. Clustering of raft-associated proteins in the external membrane leaflet modulates internal leaflet H-ras diffusion and signaling. *Mol Cell Biol*. 26:7190-7200.

El-Assal, O.N., and G.E. Besner. 2005. HB-EGF enhances restitution after intestinal ischemia/reperfusion via PI3K/Akt and MEK/ERK1/2 activation. *Gastroenterology*. 129:609-625.

El-Sibai, M., P. Nalbant, H. Pang, R.J. Flinn, C. Sarmiento, F. Macaluso, M. Cammer, J.S. Condeelis, K.M. Hahn, and J.M. Backer. 2007. Cdc42 is required for EGF-stimulated protrusion and motility in MTLn3 carcinoma cells. *J Cell Sci*. 120:3465-3474.

Emmons, K.M., C.M. McBride, E. Puleo, K.I. Pollak, E. Clipp, K. Kuntz, B.H. Marcus, M. Napolitano, J. Onken, F. Farraye, and R. Fletcher. 2005. Project PREVENT: a randomized trial to reduce multiple behavioral risk factors for colon cancer. *Cancer Epidemiol Biomarkers Prev*. 14:1453-1459.

Engel, R.H., and A.M. Evens. 2006. Oxidative stress and apoptosis: a new treatment paradigm in cancer. *Front Biosci*. 11:300-312.

Eppert, K., S.W. Scherer, H. Ozcelik, R. Pirone, P. Hoodless, H. Kim, L.C. Tsui, B. Bapat, S. Gallinger, I.L. Andrulis, G.H. Thomsen, J.L. Wrana, and L. Attisano. 1996. MADR2 maps to 18q21 and encodes a TGFbeta-regulated MAD-related protein that is functionally mutated in colorectal carcinoma. *Cell*. 86:543-552.

Ewald, J.A., J.C. Wilkinson, C.A. Guyer, and J.V. Staros. 2003. Ligand- and kinase activity-independent cell survival mediated by the epidermal growth factor receptor expressed in 32D cells. *Exp Cell Res*. 282:121-131.

Fan, Y.Y., L.H. Ly, R. Barhoumi, D.N. McMurray, and R.S. Chapkin. 2004. Dietary docosahexaenoic acid suppresses T cell protein kinase C theta lipid raft recruitment and IL-2 production. *J Immunol*. 173:6151-6160.

Fan, Y.Y., D.N. McMurray, L.H. Ly, and R.S. Chapkin. 2003a. Dietary (n-3) polyunsaturated fatty acids remodel mouse T-cell lipid rafts. *J Nutr*. 133:1913-1920.

Fan, Y.Y., T.E. Spencer, N. Wang, M.P. Moyer, and R.S. Chapkin. 2003b. Chemopreventive n-3 fatty acids activate RXRalpha in colonocytes. *Carcinogenesis*. 24:1541-1548.

Fedida-Metula, S., B. Feldman, V. Koshelev, U. Levin-Gromiko, E. Voronov, and D. Fishman. 2012. Lipid rafts couple store-operated Ca2+ entry to constitutive activation of PKB/Akt in a Ca2+/calmodulin-, Src- and PP2A-mediated pathway and promote melanoma tumor growth. *Carcinogenesis*. 33:740-750.

Ferguson, K.M., M.B. Berger, J.M. Mendrola, H.S. Cho, D.J. Leahy, and M.A. Lemmon. 2003. EGF activates its receptor by removing interactions that autoinhibit ectodomain dimerization. *Mol Cell*. 11:507-517.

Fernandez, E., S. Gallus, C. La Vecchia, R. Talamini, E. Negri, and S. Franceschi. 2004. Family history and environmental risk factors for colon cancer. *Cancer Epidemiol Biomarkers Prev*. 13:658-661.

Fichera, A., N. Little, S. Jagadeeswaran, U. Dougherty, A. Sehdev, R. Mustafi, S. Cerda, W. Yuan, S. Khare, M. Tretiakova, C. Gong, M. Tallerico, G. Cohen, L. Joseph, J. Hart, J.R. Turner, and M. Bissonnette. 2007. Epidermal growth factor receptor signaling is required for microadenoma formation in the mouse azoxymethane model of colonic carcinogenesis. *Cancer Res*. 67:827-835.

Fiedler, K., T. Kobayashi, T.V. Kurzchalia, and K. Simons. 1993. Glycosphingolipid-enriched, detergent-insoluble complexes in protein sorting in epithelial cells. *Biochemistry*. 32:6365-6373.

Field, K.A., D. Holowka, and B. Baird. 1997. Compartmentalized activation of the high affinity immunoglobulin E receptor within membrane domains. *J Biol Chem*. 272:4276-4280.

Fiske, W.H., D. Threadgill, and R.J. Coffey. 2009. ERBBs in the gastrointestinal tract: recent progress and new perspectives. *Exp Cell Res*. 315:583-601.

Freeman, M.R., and K.R. Solomon. 2004. Cholesterol and prostate cancer. *J Cell Biochem*. 91:54-69.

Frey, M.R., V.C. Hilliard, M.T. Mullane, and D.B. Polk. 2010. ErbB4 promotes cyclooxygenase-2 expression and cell survival in colon epithelial cells. *Lab Invest*. 90:1415-1424.

Gadella, T.W., Jr., and T.M. Jovin. 1995. Oligomerization of epidermal growth factor receptors on A431 cells studied by time-resolved fluorescence imaging microscopy. A stereochemical model for tyrosine kinase receptor activation. *J Cell Biol*. 129:1543-1558.

Galizia, G., E. Lieto, F. Ferraraccio, F. De Vita, P. Castellano, M. Orditura, V. Imperatore, A. La Mura, G. La Manna, M. Pinto, G. Catalano, C. Pignatelli, and F. Ciardiello. 2006. Prognostic significance of epidermal growth factor receptor expression in colon cancer patients undergoing curative surgery. *Ann Surg Oncol*. 13:823-835.

Gan, Y., C. Shi, L. Inge, M. Hibner, J. Balducci, and Y. Huang. 2010. Differential roles of ERK and Akt pathways in regulation of EGFR-mediated signaling and motility in prostate cancer cells. *Oncogene*. 29:4947-4958.

Gatza, C.E., A. Holtzhausen, K.C. Kirkbride, A. Morton, M.L. Gatza, M.B. Datto, and G.C. Blobe. 2011. Type III TGF-beta receptor enhances colon cancer cell migration and anchorage-independent growth. *Neoplasia*. 13:758-770.

Geelen, A., J.M. Schouten, C. Kamphuis, B.E. Stam, J. Burema, J.M. Renkema, E.J. Bakker, P. van't Veer, and E. Kampman. 2007. Fish consumption, n-3 fatty acids, and colorectal cancer: a meta-analysis of prospective cohort studies. *Am J Epidemiol*. 166:1116-1125.

George, K.S., and S. Wu. 2012. Lipid raft: A floating island of death or survival. *Toxicol Appl Pharmacol*. 259:311-319.

Georgiades, I.B., L.J. Curtis, R.M. Morris, C.C. Bird, and A.H. Wyllie. 1999. Heterogeneity studies identify a subset of sporadic colorectal cancers without evidence for chromosomal or microsatellite instability. *Oncogene*. 18:7933-7940.

Gibney, M.J. 1997. Incorporation of n-3 polyunsaturated fatty acids into processed foods. *Br J Nutr*. 78:193-195.

Goh, L.K., F. Huang, W. Kim, S. Gygi, and A. Sorkin. 2010. Multiple mechanisms collectively regulate clathrin-mediated endocytosis of the epidermal growth factor receptor. *J Cell Biol*. 189:871-883.

Goke, M., M. Kanai, K. Lynch-Devaney, and D.K. Podolsky. 1998. Rapid mitogen-activated protein kinase activation by transforming growth factor alpha in wounded rat intestinal epithelial cells. *Gastroenterology*. 114:697-705.

Goss, K.H., and J. Groden. 2000. Biology of the adenomatous polyposis coli tumor suppressor. *J Clin Oncol*. 18:1967-1979.

Grady, W.M., L.L. Myeroff, S.E. Swinler, A. Rajput, S. Thiagalingam, J.D. Lutterbaugh, A. Neumann, M.G. Brattain, J. Chang, S.J. Kim, K.W. Kinzler, B. Vogelstein, J.K. Willson, and S. Markowitz. 1999. Mutational inactivation of transforming growth factor beta receptor type II in microsatellite stable colon cancers. *Cancer Res*. 59:320-324.

Grady, W.M., A. Rajput, L. Myeroff, D.F. Liu, K. Kwon, J. Willis, and S. Markowitz. 1998. Mutation of the type II transforming growth factor-beta receptor is coincident with the transformation of human colon adenomas to malignant carcinomas. *Cancer Res*. 58:3101-3104.

Gravaghi, C., K.M. La Perle, P. Ogrodwski, J.X. Kang, F. Quimby, M. Lipkin, and S.A. Lamprecht. 2011. Cox-2 expression, PGE(2) and cytokines production are inhibited by endogenously synthesized n-3 PUFAs in inflamed colon of fat-1 mice. *J Nutr Biochem*. 22:360-365.

Guo, L., C.J. Kozlosky, L.H. Ericsson, T.O. Daniel, D.P. Cerretti, and R.S. Johnson. 2003. Studies of ligand-induced site-specific phosphorylation of epidermal growth factor receptor. *J Am Soc Mass Spectrom*. 14:1022-1031.

Habbel, P., K.H. Weylandt, K. Lichopoj, J. Nowak, M. Purschke, J.D. Wang, C.W. He, D.C. Baumgart, and J.X. Kang. 2009. Docosahexaenoic acid suppresses arachidonic acid-induced proliferation of LS-174T human colon carcinoma cells. *World J Gastroenterol*. 15:1079-1084.

Hall, A. 1998. Rho GTPases and the actin cytoskeleton. *Science*. 279:509-514.

Hall, M.N., J.E. Chavarro, I.M. Lee, W.C. Willett, and J. Ma. 2008. A 22-year prospective study of fish, n-3 fatty acid intake, and colorectal cancer risk in men. *Cancer Epidemiol Biomarkers Prev*. 17:1136-1143.

Han, W., and H.W. Lo. 2012. Landscape of EGFR signaling network in human cancers: biology and therapeutic response in relation to receptor subcellular locations. *Cancer Lett*. 318:124-134.

Hanada, N., H.W. Lo, C.P. Day, Y. Pan, Y. Nakajima, and M.C. Hung. 2006. Co-regulation of B-Myb expression by E2F1 and EGF receptor. *Mol Carcinog*. 45:10-17.

Hawkins, N., M. Norrie, K. Cheong, E. Mokany, S.L. Ku, A. Meagher, T. O'Connor, and R. Ward. 2002. CpG island methylation in sporadic colorectal cancers and its relationship to microsatellite instability. *Gastroenterology*. 122:1376-1387.

Hawthorne, A.B., T.K. Daneshmend, C.J. Hawkey, A. Belluzzi, S.J. Everitt, G.K. Holmes, C. Malkinson, M.Z. Shaheen, and J.E. Willars. 1992. Treatment of ulcerative colitis with fish oil supplementation: a prospective 12 month randomised controlled trial. *Gut*. 33:922-928.

Hazarika, P., M.F. McCarty, V.G. Prieto, S. George, D. Babu, D. Koul, M. Bar-Eli, and M. Duvic. 2004. Up-regulation of Flotillin-2 is associated with melanoma progression and modulates expression of the thrombin receptor protease activated receptor 1. *Cancer Res*. 64:7361-7369.

Hess, J., P. Angel, and M. Schorpp-Kistner. 2004. AP-1 subunits: quarrel and harmony among siblings. *J Cell Sci*. 117:5965-5973.

Higashiyama, S., and D. Nanba. 2005. ADAM-mediated ectodomain shedding of HB-EGF in receptor cross-talk. *Biochim Biophys Acta*. 1751:110-117.

Hofman, E.G., M.O. Ruonala, A.N. Bader, D. van den Heuvel, J. Voortman, R.C. Roovers, A.J. Verkleij, H.C. Gerritsen, and P.M. van Bergen En Henegouwen. 2008. EGF induces coalescence of different lipid rafts. *J Cell Sci*. 121:2519-2528.

Holt, K.H., S.B. Waters, S. Okada, K. Yamauchi, S.J. Decker, A.R. Saltiel, D.G. Motto, G.A. Koretzky, and J.E. Pessin. 1996. Epidermal growth factor receptor targeting prevents uncoupling of the Grb2-SOS complex. *J Biol Chem*. 271:8300-8306.

Holzer, R.G., E.J. Park, N. Li, H. Tran, M. Chen, C. Choi, G. Solinas, and M. Karin. 2011. Saturated fatty acids induce c-Src clustering within membrane subdomains, leading to JNK activation. *Cell*. 147:173-184.

Hopkins, A.M., A.A. Pineda, L.M. Winfree, G.T. Brown, M.G. Laukoetter, and A. Nusrat. 2007. Organized migration of epithelial cells requires control of adhesion and protrusion through Rho kinase effectors. *Am J Physiol Gastrointest Liver Physiol*. 292:G806-817.

Hou, J.K., B. Abraham, and H. El-Serag. 2011. Dietary intake and risk of developing inflammatory bowel disease: a systematic review of the literature. *Am J Gastroenterol*. 106:563-573.

Hou, T.Y., J.M. Monk, Y.Y. Fan, R. Barhoumi, Y.Q. Chen, G.M. Rivera, D.N. McMurray, and R.S. Chapkin. 2012. n-3 polyunsaturated fatty acids suppress phosphatidylinositol 4,5-bisphosphate-dependent actin remodelling during CD4+ T-cell activation. *Biochem J*. 443:27-37.

Hudert, C.A., K.H. Weylandt, Y. Lu, J. Wang, S. Hong, A. Dignass, C.N. Serhan, and J.X. Kang. 2006. Transgenic mice rich in endogenous omega-3 fatty acids are protected from colitis. *Proc Natl Acad Sci U S A*. 103:11276-11281.

Hung, L.Y., J.T. Tseng, Y.C. Lee, W. Xia, Y.N. Wang, M.L. Wu, Y.H. Chuang, C.H. Lai, and W.C. Chang. 2008. Nuclear epidermal growth factor receptor (EGFR) interacts with signal transducer and activator of transcription 5 (STAT5) in activating Aurora-A gene expression. *Nucleic Acids Res*. 36:4337-4351.

Iacopetta, B. 2002. Are there two sides to colorectal cancer? *Int J Cancer*. 101:403-408.

Ianoul, A., and L.J. Johnston. 2007. Near-field scanning optical microscopy to identify membrane microdomains. *Methods Mol Biol*. 400:469-480.

Ibrahim, A., K. Mbodji, A. Hassan, M. Aziz, N. Boukhettala, M. Coeffier, G. Savoye, P. Dechelotte, and R. Marion-Letellier. 2011. Anti-inflammatory and anti-angiogenic effect of long chain n-3 polyunsaturated fatty acids in intestinal microvascular endothelium. *Clin Nutr*. 30:678-687.

Iizuka, M., and S. Konno. 2011. Wound healing of intestinal epithelial cells. *World J Gastroenterol*. 17:2161-2171.

Ilangumaran, S., and D.C. Hoessli. 1998. Effects of cholesterol depletion by cyclodextrin on the sphingolipid microdomains of the plasma membrane. *Biochem J*. 335 (Pt 2):433-440.

Im, D.S. 2012. Omega-3 fatty acids in anti-inflammation (pro-resolution) and GPCRs. *Prog Lipid Res*. 51:232-237.

Irwin, M.E., K.L. Mueller, N. Bohin, Y. Ge, and J.L. Boerner. 2010. Lipid raft localization of EGFR alters the response of cancer cells to the EGFR tyrosine kinase inhibitor gefitinib. *J Cell Physiol*.

Jacobson, K., O.G. Mouritsen, and R.G. Anderson. 2007. Lipid rafts: at a crossroad between cell biology and physics. *Nature Cell Biol*. 9:7-14.

Jaganathan, S., P. Yue, D.C. Paladino, J. Bogdanovic, Q. Huo, and J. Turkson. 2011. A functional nuclear epidermal growth factor receptor, SRC and Stat3 heteromeric complex in pancreatic cancer cells. *PLoS One*. 6:e19605.

Jemal, A., F. Bray, M.M. Center, J. Ferlay, E. Ward, and D. Forman. 2011. Global cancer statistics. *CA Cancer J Clin*. 61:69-90.

Jemal, A., R. Siegel, J. Xu, and E. Ward. 2010. Cancer statistics, 2010. *CA Cancer J Clin*. 60:277-300.

Jia, Q., J.R. Lupton, R. Smith, B.R. Weeks, E. Callaway, L.A. Davidson, W. Kim, Y.Y. Fan, P. Yang, R.A. Newman, J.X. Kang, D.N. McMurray, and R.S. Chapkin. 2008. Reduced colitis-associated colon cancer in Fat-1 (n-3 fatty acid desaturase) transgenic mice. *Cancer Res*. 68:3985-3991.

Jiang, X., F. Huang, A. Marusyk, and A. Sorkin. 2003. Grb2 regulates internalization of EGF receptors through clathrin-coated pits. *Mol Biol Cell*. 14:858-870.

Jorissen, R.N., F. Walker, N. Pouliot, T.P. Garrett, C.W. Ward, and A.W. Burgess. 2003. Epidermal growth factor receptor: mechanisms of activation and signalling. *Exp Cell Res*. 284:31-53.

Jura, N., N.F. Endres, K. Engel, S. Deindl, R. Das, M.H. Lamers, D.E. Wemmer, X. Zhang, and J. Kuriyan. 2009. Mechanism for activation of the EGF receptor catalytic domain by the juxtamembrane segment. *Cell*. 137:1293-1307.

Kamat, A., and G. Carpenter. 1997. Phospholipase C-gamma1: regulation of enzyme function and role in growth factor-dependent signal transduction. *Cytokine Growth Factor Rev*. 8:109-117.

Kang, J.X., J. Wang, L. Wu, and Z.B. Kang. 2004. Transgenic mice: fat-1 mice convert n-6 to n-3 fatty acids. *Nature*. 427:504.

Kapitanovic, S., S. Radosevic, M. Kapitanovic, S. Andelinovic, Z. Ferencic, M. Tavassoli, D. Primorac, Z. Sonicki, S. Spaventi, K. Pavelic, and R. Spaventi. 1997. The expression of p185(HER-2/neu) correlates with the stage of disease and survival in colorectal cancer. *Gastroenterology*. 112:1103-1113.

Kim, J.W., S.S. Sim, U.H. Kim, S. Nishibe, M.I. Wahl, G. Carpenter, and S.G. Rhee. 1990. Tyrosine residues in bovine phospholipase C-gamma phosphorylated by the epidermal growth factor receptor in vitro. *J Biol Chem*. 265:3940-3943.

Kim, S., D.P. Sandler, J. Galanko, C. Martin, and R.S. Sandler. 2010a. Intake of polyunsaturated fatty acids and distal large bowel cancer risk in whites and African Americans. *Am J Epidemiol*. 171:969-979.

Kim, W., Y.Y. Fan, R. Barhoumi, R. Smith, D.N. McMurray, and R.S. Chapkin. 2008. n-3 polyunsaturated fatty acids suppress the localization and activation of signaling proteins at the immunological synapse in murine CD4+ T cells by affecting lipid raft formation. *J Immunol*. 181:6236-6243.

Kim, W., D.N. McMurray, and R.S. Chapkin. 2010b. n-3 polyunsaturated fatty acids--physiological relevance of dose. *Prostaglandins Leukot Essent Fatty Acids*. 82:155-158.

Kinzler, K.W., and B. Vogelstein. 2002. Colorectal tumors. In The Genetic Basis of Human Cancer. K.W. Kinzler, editor. McGraw Hill, New York. 583-612.

Klampfer, L. 2008. The role of signal transducers and activators of transcription in colon cancer. *Front Biosci*. 13:2888-2899.

Klemm, R.W., C.S. Ejsing, M.A. Surma, H.J. Kaiser, M.J. Gerl, J.L. Sampaio, Q. de Robillard, C. Ferguson, T.J. Proszynski, A. Shevchenko, and K. Simons. 2009. Segregation of sphingolipids and sterols during formation of secretory vesicles at the trans-Golgi network. *J Cell Biol*. 185:601-612.

Knapp, H.R., F. Hullin, and N. Salem, Jr. 1994. Asymmetric incorporation of dietary n-3 fatty acids into membrane aminophospholipids of human erythrocytes. *J Lipid Res*. 35:1283-1291.

Kolar, S.S., R. Barhoumi, J.R. Lupton, and R.S. Chapkin. 2007. Docosahexaenoic acid and butyrate synergistically induce colonocyte apoptosis by enhancing mitochondrial Ca2+ accumulation. *Cancer Res*. 67:5561-5568.

Kondo, Y., and J.P. Issa. 2004. Epigenetic changes in colorectal cancer. *Cancer Metastasis Rev*. 23:29-39.

Kono, H., T. Suzuki, K. Yamamoto, M. Okada, T. Yamamoto, and Z. Honda. 2002. Spatial raft coalescence represents an initial step in Fc gamma R signaling. *J Immunol*. 169:193-203.

Koretz, K., P. Schlag, and P. Moller. 1990. Expression of epidermal growth factor receptor in normal colorectal mucosa, adenoma, and carcinoma. *Virchows Arch A Pathol Anat Histopathol*. 416:343-349.

Kris-Etherton, P.M., D.S. Taylor, S. Yu-Poth, P. Huth, K. Moriarty, V. Fishell, R.L. Hargrove, G. Zhao, and T.D. Etherton. 2000. Polyunsaturated fatty acids in the food chain in the United States. *Am J Clin Nutr*. 71:179S-188S.

Krishnamoorthy, S., A. Recchiuti, N. Chiang, S. Yacoubian, C.H. Lee, R. Yang, N.A. Petasis, and C.N. Serhan. 2010. Resolvin D1 binds human phagocytes with evidence for proresolving receptors. *Proc Natl Acad Sci U S A*. 107:1660-1665.

Kusumi, A., K.G. Suzuki, R.S. Kasai, K. Ritchie, and T.K. Fujiwara. 2011. Hierarchical mesoscale domain organization of the plasma membrane. *Trends Biochem Sci*. 36:604-615.

Lacour, S., A. Hammann, S. Grazide, D. Lagadic-Gossmann, A. Athias, O. Sergent, G. Laurent, P. Gambert, E. Solary, and M.T. Dimanche-Boitrel. 2004. Cisplatin-induced CD95 redistribution into membrane lipid rafts of HT29 human colon cancer cells. *Cancer Res*. 64:3593-3598.

Lambert, S., D. Vind-Kezunovic, S. Karvinen, and R. Gniadecki. 2006. Ligand-independent activation of the EGFR by lipid raft disruption. *J Invest Dermatol*. 126:954-962.

Lao, V.V., and W.M. Grady. 2011. Epigenetics and colorectal cancer. *Nature Rev Gastroenterol Hepatol*. 8:686-700.

Laplante, M., and D.M. Sabatini. 2012. mTOR signaling in growth control and disease. *Cell*. 149:274-293.

Laroui, H., S.A. Ingersoll, H.C. Liu, M.T. Baker, S. Ayyadurai, M.A. Charania, F. Laroui, Y. Yan, S.V. Sitaraman, and D. Merlin. 2012. Dextran sodium sulfate (DSS) induces colitis in mice by forming nano-lipocomplexes with medium-chain-length fatty acids in the colon. *PLoS One*. 7:e32084.

Lasserre, R., X.J. Guo, F. Conchonaud, Y. Hamon, O. Hawchar, A.M. Bernard, S.M. Soudja, P.F. Lenne, H. Rigneault, D. Olive, G. Bismuth, J.A. Nunes, B. Payrastre, D. Marguet, and H.T. He. 2008. Raft nanodomains contribute to Akt/PKB plasma membrane recruitment and activation. *Nature Chem Biol*. 4:538-547.

Lee, D., M. Yu, E. Lee, H. Kim, Y. Yang, K. Kim, C. Pannicia, J.M. Kurie, and D.W. Threadgill. 2009. Tumor-specific apoptosis caused by deletion of the ERBB3 pseudo-kinase in mouse intestinal epithelium. *J Clin Invest*. 119:2702-2713.

Lee, J.C., S.T. Wang, N.H. Chow, and H.B. Yang. 2002. Investigation of the prognostic value of coexpressed erbB family members for the survival of colorectal cancer patients after curative surgery. *Eur J Cancer*. 38:1065-1071.

Leitenberg, D., F. Balamuth, and K. Bottomly. 2001. Changes in the T cell receptor macromolecular signaling complex and membrane microdomains during T cell development and activation. *Semin Immunol*. 13:129-138.

Lengauer, C., K.W. Kinzler, and B. Vogelstein. 1997. Genetic instability in colorectal cancers. *Nature*. 386:623-627.

Levental, I., M. Grzybek, and K. Simons. 2010. Greasing their way: lipid modifications determine protein association with membrane rafts. *Biochemistry*. 49:6305-6316.

Li, Q., M. Wang, L. Tan, C. Wang, J. Ma, N. Li, Y. Li, G. Xu, and J. Li. 2005. Docosahexaenoic acid changes lipid composition and interleukin-2 receptor signaling in membrane rafts. *J Lipid Res*. 46:1904-1913.

Li, S., Q. Wang, Y. Wang, X. Chen, and Z. Wang. 2009. PLC-gamma1 and Rac1 coregulate EGF-induced cytoskeleton remodeling and cell migration. *Mol Endocrinol*. 23:901-913.

Li, Y.C., M.J. Park, S.K. Ye, C.W. Kim, and Y.N. Kim. 2006. Elevated levels of cholesterol-rich lipid rafts in cancer cells are correlated with apoptosis sensitivity induced by cholesterol-depleting agents. *Am J Pathol*. 168:1107-1118; quiz 1404-1105.

Liao, H.J., and G. Carpenter. 2007. Role of the Sec61 translocon in EGF receptor trafficking to the nucleus and gene expression. *Mol Biol Cell*. 18:1064-1072.

Lieberman, D.A., S. Prindiville, D.G. Weiss, and W. Willett. 2003. Risk factors for advanced colonic neoplasia and hyperplastic polyps in asymptomatic individuals. *JAMA*. 290:2959-2967.

Lievre, A., H. Blons, and P. Laurent-Puig. 2010. Oncogenic mutations as predictive factors in colorectal cancer. *Oncogene*. 29:3033-3043.

Lin, S.Y., K. Makino, W. Xia, A. Matin, Y. Wen, K.Y. Kwong, L. Bourguignon, and M.C. Hung. 2001. Nuclear localization of EGF receptor and its potential new role as a transcription factor. *Nature Cell Biol*. 3:802-808.

Lindblom, A. 2001. Different mechanisms in the tumorigenesis of proximal and distal colon cancers. *Curr Opin Oncol*. 13:63-69.

Lingwood, D., H.J. Kaiser, I. Levental, and K. Simons. 2009. Lipid rafts as functional heterogeneity in cell membranes. *Biochem Soc Trans*. 37:955-960.

Lingwood, D., and K. Simons. 2010. Lipid rafts as a membrane-organizing principle. *Science*. 327:46-50.

Liu, G., D.M. Bibus, A.M. Bode, W.Y. Ma, R.T. Holman, and Z. Dong. 2001. Omega 3 but not omega 6 fatty acids inhibit AP-1 activity and cell transformation in JB6 cells. *Proc Natl Acad Sci U S A*. 98:7510-7515.

Lo, H.W. 2010. Nuclear mode of the EGFR signaling network: biology, prognostic value, and therapeutic implications. *Discov Med*. 10:44-51.

Lo, H.W., X. Cao, H. Zhu, and F. Ali-Osman. 2010. Cyclooxygenase-2 is a novel transcriptional target of the nuclear EGFR-STAT3 and EGFRvIII-STAT3 signaling axes. *Mol Cancer Res*. 8:232-245.

Lo, H.W., S.C. Hsu, M. Ali-Seyed, M. Gunduz, W. Xia, Y. Wei, G. Bartholomeusz, J.Y. Shih, and M.C. Hung. 2005. Nuclear interaction of EGFR and STAT3 in the activation of the iNOS/NO pathway. *Cancer Cell*. 7:575-589.

Lorenz, R., P.C. Weber, P. Szimnau, W. Heldwein, T. Strasser, and K. Loeschke. 1989. Supplementation with n-3 fatty acids from fish oil in chronic inflammatory bowel disease--a randomized, placebo-controlled, double-blind cross-over trial. *J Intern Med Suppl*. 731:225-232.

Loura, L.M., and M. Prieto. 2007. Fluorescence resonance energy transfer to characterize cholesterol-induced domains. *Methods Mol Biol*. 400:489-501.

Lowenstein, E.J., R.J. Daly, A.G. Batzer, W. Li, B. Margolis, R. Lammers, A. Ullrich, E.Y. Skolnik, D. Bar-Sagi, and J. Schlessinger. 1992. The SH2 and SH3 domain-containing protein GRB2 links receptor tyrosine kinases to ras signaling. *Cell*. 70:431-442.

Luetteke, N.C., H.K. Phillips, T.H. Qiu, N.G. Copeland, H.S. Earp, N.A. Jenkins, and D.C. Lee. 1994. The mouse waved-2 phenotype results from a point mutation in the EGF receptor tyrosine kinase. *Genes Dev*. 8:399-413.

Ma, D.W., J. Seo, L.A. Davidson, E.S. Callaway, Y.Y. Fan, J.R. Lupton, and R.S. Chapkin. 2004. n-3 PUFA alter caveolae lipid composition and resident protein localization in mouse colon. *FASEB J*. 18:1040-1042.

Ma, L., Y.Z. Huang, G.M. Pitcher, J.G. Valtschanoff, Y.H. Ma, L.Y. Feng, B. Lu, W.C. Xiong, M.W. Salter, R.J. Weinberg, and L. Mei. 2003. Ligand-dependent recruitment of the ErbB4 signaling complex into neuronal lipid rafts. *J Neurosci*. 23:3164-3175.

Macdonald, J.L., and L.J. Pike. 2008. Heterogeneity in EGF-binding affinities arises from negative cooperativity in an aggregating system. *Proc Natl Acad Sci U S A*. 105:112-117.

Marais, R., Y. Light, H.F. Paterson, and C.J. Marshall. 1995. Ras recruits Raf-1 to the plasma membrane for activation by tyrosine phosphorylation. *EMBO J*. 14:3136-3145.

Marais, R., Y. Light, H.F. Paterson, C.S. Mason, and C.J. Marshall. 1997. Differential regulation of Raf-1, A-Raf, and B-Raf by oncogenic ras and tyrosine kinases. *J Biol Chem*. 272:4378-4383.

Markowitz, S., J. Wang, L. Myeroff, R. Parsons, L. Sun, J. Lutterbaugh, R.S. Fan, E. Zborowska, K.W. Kinzler, B. Vogelstein, and et al. 1995. Inactivation of the type II TGF-beta receptor in colon cancer cells with microsatellite instability. *Science*. 268:1336-1338.

Markowitz, S.D., and M.M. Bertagnolli. 2009. Molecular origins of cancer: Molecular basis of colorectal cancer. *N Engl J Med*. 361:2449-2460.

Marmor, M.D., and Y. Yarden. 2004. Role of protein ubiquitylation in regulating endocytosis of receptor tyrosine kinases. *Oncogene*. 23:2057-2070.

Marquer, C., S. Leveque-Fort, and M.C. Potier. 2012. Determination of lipid raft partitioning of fluorescently-tagged probes in living cells by Fluorescence Correlation Spectroscopy (FCS). *J Vis Exp*:e3513.

Martin-Fernandez, M., D.T. Clarke, M.J. Tobin, S.V. Jones, and G.R. Jones. 2002. Preformed oligomeric epidermal growth factor receptors undergo an ectodomain structure change during signaling. *Biophys J*. 82:2415-2427.

Martínez, M.E., and E.T. Jacobs. 2004. Diet and Environment, Role in Colon Cancer. In Encyclopedia of Gastroenterology. J. Leonard, editor. Elsevier, New York. 593-597.

Mason, C.S., C.J. Springer, R.G. Cooper, G. Superti-Furga, C.J. Marshall, and R. Marais. 1999. Serine and tyrosine phosphorylations cooperate in Raf-1, but not B-Raf activation. *EMBO J*. 18:2137-2148.

Matallanas, D., I. Arozarena, M.T. Berciano, D.S. Aaronson, A. Pellicer, M. Lafarga, and P. Crespo. 2003. Differences on the inhibitory specificities of H-Ras, K-Ras, and N-Ras (N17) dominant negative mutants are related to their membrane microlocalization. *J Biol Chem*. 278:4572-4581.

Matveev, S.V., and E.J. Smart. 2002. Heterologous desensitization of EGF receptors and PDGF receptors by sequestration in caveolae. *Am J Physiol Cell Physiol*. 282:C935-946.

Mayer, A., M. Takimoto, E. Fritz, G. Schellander, K. Kofler, and H. Ludwig. 1993. The prognostic significance of proliferating cell nuclear antigen, epidermal growth factor receptor, and mdr gene expression in colorectal cancer. *Cancer*. 71:2454-2460.

McDaniel, J.C., M. Belury, K. Ahijevych, and W. Blakely. 2008. Omega-3 fatty acids effect on wound healing. *Wound Rep Regen*. 16:337-345.

McKay, J.A., L.J. Murray, S. Curran, V.G. Ross, C. Clark, G.I. Murray, J. Cassidy, and H.L. McLeod. 2002. Evaluation of the epidermal growth factor receptor (EGFR) in colorectal tumours and lymph node metastases. *Eur J Cancer*. 38:2258-2264.

Meisenhelder, J., P.G. Suh, S.G. Rhee, and T. Hunter. 1989. Phospholipase C-gamma is a substrate for the PDGF and EGF receptor protein-tyrosine kinases in vivo and in vitro. *Cell*. 57:1109-1122.

Meza, R., J. Jeon, A.G. Renehan, and E.G. Luebeck. 2010. Colorectal cancer incidence trends in the United States and United kingdom: evidence of right- to left-sided biological gradients with implications for screening. *Cancer Res*. 70:5419-5429.

Michel, V., and M. Bakovic. 2007. Lipid rafts in health and disease. *Biol Cell*. 99:129-140.

Miettinen, P.J., J.E. Berger, J. Meneses, Y. Phung, R.A. Pedersen, Z. Werb, and R. Derynck. 1995. Epithelial immaturity and multiorgan failure in mice lacking epidermal growth factor receptor. *Nature*. 376:337-341.

Mineo, C., G.L. James, E.J. Smart, and R.G. Anderson. 1996. Localization of epidermal growth factor-stimulated Ras/Raf-1 interaction to caveolae membrane. *J Biol Chem*. 271:11930-11935.

Moyer, R.A., M.K. Wendt, P.A. Johanesen, J.R. Turner, and M.B. Dwinell. 2007. Rho activation regulates CXCL12 chemokine stimulated actin rearrangement and restitution in model intestinal epithelia. *Lab Invest*. 87:807-817.

Murai, T. 2012. The role of lipid rafts in cancer cell adhesion and migration. *Int J Cell Biol*. 2012:763283.

Murff, H.J., M.J. Shrubsole, Q. Cai, W.E. Smalley, Q. Dai, G.L. Milne, R.M. Ness, and W. Zheng. 2012. Dietary intake of PUFAs and colorectal polyp risk. *Am J Clin Nutr*. 95:703-712.

Nagahara, H., K. Mimori, M. Ohta, T. Utsunomiya, H. Inoue, G.F. Barnard, M. Ohira, K. Hirakawa, and M. Mori. 2005. Somatic mutations of epidermal growth factor receptor in colorectal carcinoma. *Clin Cancer Res*. 11:1368-1371.

Nagata, C., N. Takatsuka, and H. Shimizu. 2002. Soy and fish oil intake and mortality in a Japanese community. *Am J Epidemiol*. 156:824-831.

Nagy, P., G. Vereb, Z. Sebestyen, G. Horvath, S.J. Lockett, S. Damjanovich, J.W. Park, T.M. Jovin, and J. Szollosi. 2002. Lipid rafts and the local density of ErbB proteins influence the biological role of homo- and heteroassociations of ErbB2. *J Cell Sci*. 115:4251-4262.

Neill, A.R., and C.J. Masters. 1973. Metabolism of fatty acids by ovine spermatozoa. *J Reprod Fertil*. 34:279-287.

Ng, Y., R. Barhoumi, R.B. Tjalkens, Y.Y. Fan, S. Kolar, N. Wang, J.R. Lupton, and R.S. Chapkin. 2005. The role of docosahexaenoic acid in mediating mitochondrial membrane lipid oxidation and apoptosis in colonocytes. *Carcinogenesis*. 26:1914-1921.

Nicholson, K.M., and N.G. Anderson. 2002. The protein kinase B/Akt signalling pathway in human malignancy. *Cell Signal*. 14:381-395.

Nicolau, D.V., Jr., K. Burrage, R.G. Parton, and J.F. Hancock. 2006. Identifying optimal lipid raft characteristics required to promote nanoscale protein-protein interactions on the plasma membrane. *Mol Cell Biol*. 26:313-323.

Nobes, C.D., and A. Hall. 1995a. Rho, rac and cdc42 GTPases: regulators of actin structures, cell adhesion and motility. *Biochem Soc Trans*. 23:456-459.

Nobes, C.D., and A. Hall. 1995b. Rho, rac, and cdc42 GTPases regulate the assembly of multimolecular focal complexes associated with actin stress fibers, lamellipodia, and filopodia. *Cell*. 81:53-62.

Noffsinger, A.E. 2009. Serrated polyps and colorectal cancer: new pathway to malignancy. *Annu Rev Pathol*. 4:343-364.

Nomura, K., H. Imai, T. Koumura, M. Arai, and Y. Nakagawa. 1999. Mitochondrial phospholipid hydroperoxide glutathione peroxidase suppresses apoptosis mediated by a mitochondrial death pathway. *J Biol Chem*. 274:29294-29302.

Normanno, N., A. De Luca, C. Bianco, L. Strizzi, M. Mancino, M.R. Maiello, A. Carotenuto, G. De Feo, F. Caponigro, and D.S. Salomon. 2006. Epidermal growth factor receptor (EGFR) signaling in cancer. *Gene*. 366:2-16.

Ogino, S., J.A. Meyerhardt, M. Cantor, M. Brahmandam, J.W. Clark, C. Namgyal, T. Kawasaki, K. Kinsella, A.L. Michelini, P.C. Enzinger, M.H. Kulke, D.P. Ryan, M. Loda, and C.S. Fuchs. 2005. Molecular alterations in tumors and response to combination chemotherapy with gefitinib for advanced colorectal cancer. *Clin Cancer Res*. 11:6650-6656.

Oh, D.Y., S. Talukdar, E.J. Bae, T. Imamura, H. Morinaga, W. Fan, P. Li, W.J. Lu, S.M. Watkins, and J.M. Olefsky. 2010. GPR120 is an omega-3 fatty acid receptor mediating potent anti-inflammatory and insulin-sensitizing effects. *Cell*. 142:687-698.

Oikonomou, K.A., A.N. Kapsoritakis, A.I. Kapsoritaki, A.C. Manolakis, F.D. Tsiopoulos, A.E. Germenis, and S.P. Potamianos. 2010. Downregulation of serum epidermal growth factor in patients with inflammatory bowel disease. Is there a link with mucosal damage? *Growth Factors*. 28:461-466.

Olayioye, M.A., R.M. Neve, H.A. Lane, and N.E. Hynes. 2000. The ErbB signaling network: receptor heterodimerization in development and cancer. *EMBO J*. 19:3159-3167.

Orth, J.D., E.W. Krueger, S.G. Weller, and M.A. McNiven. 2006. A novel endocytic mechanism of epidermal growth factor receptor sequestration and internalization. *Cancer Res*. 66:3603-3610.

Oshima, H., B.K. Popivanova, K. Oguma, D. Kong, T.O. Ishikawa, and M. Oshima. 2011. Activation of epidermal growth factor receptor signaling by the prostaglandin E(2) receptor EP4 pathway during gastric tumorigenesis. *Cancer Sci*. 102:713-719.

Pai, R., B. Soreghan, I.L. Szabo, M. Pavelka, D. Baatar, and A.S. Tarnawski. 2002. Prostaglandin E2 transactivates EGF receptor: a novel mechanism for promoting colon cancer growth and gastrointestinal hypertrophy. *Nature Med*. 8:289-293.

Papagiorgis, P.C., A.E. Zizi, S. Tseleni, I.N. Oikonomakis, and N.I. Nikiteas. 2012. The pattern of epidermal growth factor receptor variation with disease progression and aggressiveness in colorectal cancer depends on tumor location. *Oncology Lett*. 3:1129-1135.

Parton, R.G. 1996. Caveolae and caveolins. *Curr Opin Cell Biol*. 8:542-548.

Patel, H.H., F. Murray, and P.A. Insel. 2008. G-protein-coupled receptor-signaling components in membrane raft and caveolae microdomains. *Handb Exp Pharmacol*:167-184.

Patra, S.K. 2008. Dissecting lipid raft facilitated cell signaling pathways in cancer. *Biochim Biophys Acta*. 1785:182-206.

Peppelenbosch, M.P., L.G. Tertoolen, W.J. Hage, and S.W. de Laat. 1993. Epidermal growth factor-induced actin remodeling is regulated by 5-lipoxygenase and cyclooxygenase products. *Cell*. 74:565-575.

Pike, L.J. 2003. Lipid rafts: bringing order to chaos. *J Lipid Res*. 44:655-667.

Pike, L.J. 2004. Lipid rafts: heterogeneity on the high seas. *Biochem J*. 378:281-292.

Pike, L.J. 2005. Growth factor receptors, lipid rafts and caveolae: an evolving story. *Biochim Biophys Acta*. 1746:260-273.

Pike, L.J. 2006. Rafts defined: a report on the Keystone Symposium on Lipid Rafts and Cell Function. *J Lipid Res*. 47:1597-1598.

Pike, L.J., and L. Casey. 1996. Localization and turnover of phosphatidylinositol 4,5-bisphosphate in caveolin-enriched membrane domains. *J Biol Chem*. 271:26453-26456.

Pike, L.J., and L. Casey. 2002. Cholesterol levels modulate EGF receptor-mediated signaling by altering receptor function and trafficking. *Biochemistry*. 41:10315-10322.

Pike, L.J., and J.M. Miller. 1998. Cholesterol depletion delocalizes phosphatidylinositol bisphosphate and inhibits hormone-stimulated phosphatidylinositol turnover. *J Biol Chem*. 273:22298-22304.

Plaza-Menacho, I., T. van der Sluis, H. Hollema, O. Gimm, C.H. Buys, A.I. Magee, C.M. Isacke, R.M. Hofstra, and B.J. Eggen. 2007. Ras/ERK1/2-mediated STAT3 Ser727 phosphorylation by familial medullary thyroid carcinoma-associated RET mutants induces full activation of STAT3 and is required for c-fos promoter activation, cell mitogenicity, and transformation. *J Biol Chem*. 282:6415-6424.

Plesec, T.P., and J.L. Hunt. 2009. KRAS mutation testing in colorectal cancer. *Adv Anat Pathol*. 16:196-203.

Plowman, S.J., C. Muncke, R.G. Parton, and J.F. Hancock. 2005. H-ras, K-ras, and inner plasma membrane raft proteins operate in nanoclusters with differential dependence on the actin cytoskeleton. *Proc Natl Acad Sci U S A*. 102:15500-15505.

Polk, D.B. 1998. Epidermal growth factor receptor-stimulated intestinal epithelial cell migration requires phospholipase C activity. *Gastroenterology*. 114:493-502.

Polo, S., and P.P. Di Fiore. 2006. Endocytosis conducts the cell signaling orchestra. *Cell*. 124:897-900.

Pot, G.K., A. Geelen, E.M. van Heijningen, C.L. Siezen, H.J. van Kranen, and E. Kampman. 2008. Opposing associations of serum n-3 and n-6 polyunsaturated fatty acids with colorectal adenoma risk: an endoscopy-based case-control study. *Int J Cancer*. 123:1974-1977.

Prior, I.A., and J.F. Hancock. 2011. Ras trafficking, localization and compartmentalized signalling. *Semin Cell Dev Biol*. doi:10.1016/j.semcdb.2011.09.002.

Prior, I.A., A. Harding, J. Yan, J. Sluimer, R.G. Parton, and J.F. Hancock. 2001. GTP-dependent segregation of H-ras from lipid rafts is required for biological activity. *Nature Cell Biol*. 3:368-375.

Prior, I.A., C. Muncke, R.G. Parton, and J.F. Hancock. 2003. Direct visualization of Ras proteins in spatially distinct cell surface microdomains. *J Cell Biol*. 160:165-170.

Puri, C., D. Tosoni, R. Comai, A. Rabellino, D. Segat, F. Caneva, P. Luzzi, P.P. Di Fiore, and C. Tacchetti. 2005. Relationships between EGFR signaling-competent and endocytosis-competent membrane microdomains. *Mol Biol Cell*. 16:2704-2718.

Quesnelle, K.M., A.L. Boehm, and J.R. Grandis. 2007. STAT-mediated EGFR signaling in cancer. *J Cell Biochem*. 102:311-319.

Radinsky, R. 1995. Modulation of tumor cell gene expression and phenotype by the organ-specific metastatic environment. *Cancer Metastasis Rev*. 14:323-338.

Rao, C.V., Y. Hirose, C. Indranie, and B.S. Reddy. 2001. Modulation of experimental colon tumorigenesis by types and amounts of dietary fatty acids. *Cancer Res*. 61:1927-1933.

Ravacci, G.R., M.M. Brentani, T. Tortelli, Jr., R.S. Torrinhas, T. Saldanha, E.A. Torres, and D.L. Waitzberg. 2012. Lipid raft disruption by docosahexaenoic acid induces apoptosis in transformed human mammary luminal epithelial cells harboring HER-2 overexpression. *J Nutr Biochem*. doi:10.1016/j.jnutbio.2012.02.001.

Rebillard, A., X. Tekpli, O. Meurette, O. Sergent, G. LeMoigne-Muller, L. Vernhet, M. Gorria, M. Chevanne, M. Christmann, B. Kaina, L. Counillon, E. Gulbins, D. Lagadic-Gossmann, and M.T. Dimanche-Boitrel. 2007. Cisplatin-induced apoptosis involves membrane fluidification via inhibition of NHE1 in human colon cancer cells. *Cancer Res*. 67:7865-7874.

Ringerike, T., F.D. Blystad, F.O. Levy, I.H. Madshus, and E. Stang. 2002. Cholesterol is important in control of EGF receptor kinase activity but EGF receptors are not concentrated in caveolae. *J Cell Sci*. 115:1331-1340.

Robinson, D.R., L.L. Xu, C.T. Knoell, S. Tateno, and W. Olesiak. 1993. Modification of spleen phospholipid fatty acid composition by dietary fish oil and by n-3 fatty acid ethyl esters. *J Lipid Res*. 34:1423-1434.

Rockett, B.D., H. Teague, M. Harris, M. Melton, J. Williams, S.R. Wassall, and S.R. Shaikh. 2012. Fish oil increases raft size and membrane order of B cells accompanied by differential effects on function. *J Lipid Res*. 53:674-685.

Roepstorff, K., M.V. Grandal, L. Henriksen, S.L. Knudsen, M. Lerdrup, L. Grovdal, B.M. Willumsen, and B. van Deurs. 2009. Differential effects of EGFR ligands on endocytic sorting of the receptor. *Traffic*. 10:1115-1127.

Roepstorff, K., P. Thomsen, K. Sandvig, and B. van Deurs. 2002. Sequestration of epidermal growth factor receptors in non-caveolar lipid rafts inhibits ligand binding. *J Biol Chem*. 277:18954-18960.

Rogers, K.R., K.D. Kikawa, M. Mouradian, K. Hernandez, K.M. McKinnon, S.M. Ahwah, and R.S. Pardini. 2010. Docosahexaenoic acid alters epidermal growth factor receptor-related signaling by disrupting its lipid raft association. *Carcinogenesis*. 31:1523-1530.

Rohatgi, R., L. Ma, H. Miki, M. Lopez, T. Kirchhausen, T. Takenawa, and M.W. Kirschner. 1999. The interaction between N-WASP and the Arp2/3 complex links Cdc42-dependent signals to actin assembly. *Cell*. 97:221-231.

Rosetti, C., and C. Pastorino. 2011. Polyunsaturated and saturated phospholipids in mixed bilayers: a study from the molecular scale to the lateral lipid organization. *J Phys Chem B*. 115:1002-1013.

Roskoski, R., Jr. 2012. MEK1/2 dual-specificity protein kinases: structure and regulation. *Biochem Biophys Res Commun*. 417:5-10.

Rotblat, B., I.A. Prior, C. Muncke, R.G. Parton, Y. Kloog, Y.I. Henis, and J.F. Hancock. 2004. Three separable domains regulate GTP-dependent association of H-ras with the plasma membrane. *Mol Cell Biol*. 24:6799-6810.

Roy, S., R. Luetterforst, A. Harding, A. Apolloni, M. Etheridge, E. Stang, B. Rolls, J.F. Hancock, and R.G. Parton. 1999. Dominant-negative caveolin inhibits H-Ras function by disrupting cholesterol-rich plasma membrane domains. *Nature Cell Biol*. 1:98-105.

Roy, U.K., N.S. Rial, K.L. Kachel, and E.W. Gerner. 2008. Activated K-RAS increases polyamine uptake in human colon cancer cells through modulation of caveolar endocytosis. *Mol Carcinog*. 47:538-553.

Rudolph, R.E., J.A. Dominitz, J.W. Lampe, L. Levy, P. Qu, S.S. Li, P.D. Lampe, M.P. Bronner, and J.D. Potter. 2005. Risk factors for colorectal cancer in relation to number and size of aberrant crypt foci in humans. *Cancer Epidemiol Biomarkers Prev*. 14:605-608.

Sadowski, L., I. Pilecka, and M. Miaczynska. 2009. Signaling from endosomes: location makes a difference. *Exp Cell Res*. 315:1601-1609.

Saffarian, S., Y. Li, E.L. Elson, and L.J. Pike. 2007. Oligomerization of the EGF receptor investigated by live cell fluorescence intensity distribution analysis. *Biophys J*. 93:1021-1031.

Sahin, U., G. Weskamp, K. Kelly, H.M. Zhou, S. Higashiyama, J. Peschon, D. Hartmann, P. Saftig, and C.P. Blobel. 2004. Distinct roles for ADAM10 and ADAM17 in ectodomain shedding of six EGFR ligands. *J Cell Biol*. 164:769-779.

Saif, M.W., and E. Chu. 2010. Biology of colorectal cancer. *Cancer J*. 16:196-201.

Samowitz, W.S., K. Curtin, D. Schaffer, M. Robertson, M. Leppert, and M.L. Slattery. 2000. Relationship of Ki-ras mutations in colon cancers to tumor location, stage, and survival: a population-based study. *Cancer Epidemiol Biomarkers Prev*. 9:1193-1197.

Samuels, Y., Z. Wang, A. Bardelli, N. Silliman, J. Ptak, S. Szabo, H. Yan, A. Gazdar, S.M. Powell, G.J. Riggins, J.K. Willson, S. Markowitz, K.W. Kinzler, B. Vogelstein, and V.E. Velculescu. 2004. High frequency of mutations of the PIK3CA gene in human cancers. *Science*. 304:554.

Salem Jr., N., H.Y. Kim, and J.A. Yergey. 1986. Docosahexaenoic acid: membrane function and metabolism. In Health Effects of Polyunsaturated Fatty Acids in Seafoods. A.P. Simopolous, R.R. Kifer, and R.E. Martin, editors. Academic Press, New York. 319-351.

Sasazuki, S., M. Inoue, M. Iwasaki, N. Sawada, T. Shimazu, T. Yamaji, R. Takachi, and S. Tsugane. 2011. Intake of n-3 and n-6 polyunsaturated fatty acids and development of colorectal cancer by subsite: Japan Public Health Center-based prospective study. *Int J Cancer*. 129:1718-1729.

Schley, P.D., D.N. Brindley, and C.J. Field. 2007. (n-3) PUFA alter raft lipid composition and decrease epidermal growth factor receptor levels in lipid rafts of human breast cancer cells. *J Nutr*. 137:548-553.

Sehgal, P.B., G.G. Guo, M. Shah, V. Kumar, and K. Patel. 2002. Cytokine signaling: STATS in plasma membrane rafts. *J Biol Chem*. 277:12067-12074.

Seo, J., R. Barhoumi, A.E. Johnson, J.R. Lupton, and R.S. Chapkin. 2006. Docosahexaenoic acid selectively inhibits plasma membrane targeting of lipidated proteins. *FASEB J*. 20:770-772.

Serhan, C.N., S. Krishnamoorthy, A. Recchiuti, and N. Chiang. 2011. Novel anti-inflammatory--pro-resolving mediators and their receptors. *Curr Top Med Chem*. 11:629-647.

Shaikh, S.R., D.S. Locascio, S.P. Soni, S.R. Wassall, and W. Stillwell. 2009a. Oleic- and docosahexaenoic acid-containing phosphatidylethanolamines differentially phase separate from sphingomyelin. *Biochim Biophys Acta*. 1788:2421-2426.

Shaikh, S.R., B.D. Rockett, M. Salameh, and K. Carraway. 2009b. Docosahexaenoic acid modifies the clustering and size of lipid rafts and the lateral organization and surface expression of MHC class I of EL4 cells. *J Nutr*. 139:1632-1639.

Shia, J., D.S. Klimstra, A.R. Li, J. Qin, L. Saltz, J. Teruya-Feldstein, M. Akram, K.Y. Chung, D. Yao, P.B. Paty, W. Gerald, and B. Chen. 2005. Epidermal growth factor receptor expression and gene amplification in colorectal carcinoma: an immunohistochemical and chromogenic in situ hybridization study. *Mod Pathol*. 18:1350-1356.

Siddiqui, R.A., K.A. Harvey, G.P. Zaloga, and W. Stillwell. 2007. Modulation of lipid rafts by Omega-3 fatty acids in inflammation and cancer: implications for use of lipids during nutrition support. *Nutr Clin Pract*. 22:74-88.

Siegel, R., D. Naishadham, and A. Jemal. 2012. Cancer statistics, 2012. *CA Cancer J Clin*. 62:10-29.

Sigismund, S., E. Argenzio, D. Tosoni, E. Cavallaro, S. Polo, and P.P. Di Fiore. 2008. Clathrin-mediated internalization is essential for sustained EGFR signaling but dispensable for degradation. *Dev Cell*. 15:209-219.

Simons, K., and J.L. Sampaio. 2011. Membrane organization and lipid rafts. *Cold Spring Harb Perspect Biol*. 3:a004697.

Simons, K., and D. Toomre. 2000. Lipid rafts and signal transduction. *Nature Rev Mol Cell Biol*. 1:31-39.

Simons, K., and G. van Meer. 1988. Lipid sorting in epithelial cells. *Biochemistry*. 27:6197-6202.

Sinha, A., J. Nightingale, K.P. West, J. Berlanga-Acosta, and R.J. Playford. 2003. Epidermal growth factor enemas with oral mesalamine for mild-to-moderate left-sided ulcerative colitis or proctitis. *N Engl J Med*. 349:350-357.

Smart, E.J., G.A. Graf, M.A. McNiven, W.C. Sessa, J.A. Engelman, P.E. Scherer, T. Okamoto, and M.P. Lisanti. 1999a. Caveolins, liquid-ordered domains, and signal transduction. *Mol Cell Biol*. 19:7289-7304.

Smart, E.J., G.A. Graf, M.A. McNiven, W.C. Sessa, J.A. Engelman, P.E. Scherer, T. Okamoto, and M.P. Lisanti. 1999b. Caveolins, liquid-ordered domains, and signal transduction. *Mol Cell Biol*. 19:7289-7304.

Smart, E.J., Y.S. Ying, C. Mineo, and R.G. Anderson. 1995. A detergent-free method for purifying caveolae membrane from tissue culture cells. *Proc Natl Acad Sci U S A*. 92:10104-10108.

Soni, S.P., D.S. LoCascio, Y. Liu, J.A. Williams, R. Bittman, W. Stillwell, and S.R. Wassall. 2008. Docosahexaenoic acid enhances segregation of lipids between : 2H-NMR study. *Biophys J*. 95:203-214.

Sorkin, A., and L.K. Goh. 2009. Endocytosis and intracellular trafficking of ErbBs. *Exp Cell Res*. 315:683-696.

Sorkin, A., M. McClure, F. Huang, and R. Carter. 2000. Interaction of EGF receptor and grb2 in living cells visualized by fluorescence resonance energy transfer (FRET) microscopy. *Curr Biol*. 10:1395-1398.

Sousa, L.P., I. Lax, H. Shen, S.M. Ferguson, P. De Camilli, and J. Schlessinger. 2012. Suppression of EGFR endocytosis by dynamin depletion reveals that EGFR signaling occurs primarily at the plasma membrane. *Proc Natl Acad Sci U S A*. 109:4419-4424.

Staubach, S., and F.G. Hanisch. 2011. Lipid rafts: signaling and sorting platforms of cells and their roles in cancer. *Expert Rev Proteomics*. 8:263-277.

Stillwell, W., L.J. Jenski, F.T. Crump, and W. Ehringer. 1997. Effect of docosahexaenoic acid on mouse mitochondrial membrane properties. *Lipids*. 32:497-506.

Stillwell, W., and S.R. Wassall. 2003. Docosahexaenoic acid: membrane properties of a unique fatty acid. *Chem Phys Lipids*. 126:1-27.

Stubbs, C.D., and A.D. Smith. 1984. The modification of mammalian membrane polyunsaturated fatty acid composition in relation to membrane fluidity and function. *Biochim Biophys Acta*. 779:89-137.

Sturm, A., and A.U. Dignass. 2008. Epithelial restitution and wound healing in inflammatory bowel disease. *World J Gastroenterol*. 14:348-353.

Sugai, T., W. Habano, Y.F. Jiao, M. Tsukahara, Y. Takeda, K. Otsuka, and S. Nakamura. 2006. Analysis of molecular alterations in left- and right-sided colorectal carcinomas reveals distinct pathways of carcinogenesis: proposal for new molecular profile of colorectal carcinomas. *J Mol Diagn*. 8:193-201.

Sun, H., Z. Chen, H. Poppleton, K. Scholich, J. Mullenix, G.J. Weipz, D.L. Fulgham, P.J. Bertics, and T.B. Patel. 1997. The juxtamembrane, cytosolic region of the epidermal growth factor receptor is involved in association with alpha-subunit of Gs. *J Biol Chem*. 272:5413-5420.

Swamy, M.V., I. Cooma, J.M. Patlolla, B. Simi, B.S. Reddy, and C.V. Rao. 2004. Modulation of cyclooxygenase-2 activities by the combined action of celecoxib and decosahexaenoic acid: novel strategies for colon cancer prevention and treatment. *Mol Cancer Ther*. 3:215-221.

Tahin, Q.S., M. Blum, and E. Carafoli. 1981. The fatty acid composition of subcellular membranes of rat liver, heart, and brain: diet-induced modifications. *Eur J Biochem*. 121:5-13.

Takayama, T., S. Katsuki, Y. Takahashi, M. Ohi, S. Nojiri, S. Sakamaki, J. Kato, K. Kogawa, H. Miyake, and Y. Niitsu. 1998. Aberrant crypt foci of the colon as precursors of adenoma and cancer. *N Engl J Med*. 339:1277-1284.

Toyota, M., N. Ahuja, M. Ohe-Toyota, J.G. Herman, S.B. Baylin, and J.P. Issa. 1999. CpG island methylator phenotype in colorectal cancer. *Proc Natl Acad Sci U S A*. 96:8681-8686.

Trebble, T.M., S.A. Wootton, E.A. Miles, M. Mullee, N.K. Arden, A.B. Ballinger, M.A. Stroud, G.C. Burdge, and P.C. Calder. 2003. Prostaglandin E2 production and T cell function after fish-oil supplementation: response to antioxidant cosupplementation. *Am J Clin Nutr*. 78:376-382.

Turk, H.F., S.S. Kolar, Y.Y. Fan, C.A. Cozby, J.R. Lupton, and R.S. Chapkin. 2011. Linoleic acid and butyrate synergize to increase Bcl-2 levels in colonocytes. *Int J Cancer*. 128:63-71.

Turner, D., P.S. Shah, A.H. Steinhart, S. Zlotkin, and A.M. Griffiths. 2011. Maintenance of remission in inflammatory bowel disease using omega-3 fatty acids (fish oil): a systematic review and meta-analyses. *Inflamm Bowel Dis*. 17:336-345.

Ullman, T.A., and S.H. Itzkowitz. 2011. Intestinal inflammation and cancer. *Gastroenterology*. 140:1807-1816.

Ullrich, A., L. Coussens, J.S. Hayflick, T.J. Dull, A. Gray, A.W. Tam, J. Lee, Y. Yarden, T.A. Libermann, J. Schlessinger, and et al. 1984. Human epidermal growth factor receptor cDNA sequence and aberrant expression of the amplified gene in A431 epidermoid carcinoma cells. *Nature*. 309:418-425.

Umebayashi, K., H. Stenmark, and T. Yoshimori. 2008. Ubc4/5 and c-Cbl continue to ubiquitinate EGF receptor after internalization to facilitate polyubiquitination and degradation. *Mol Biol Cell*. 19:3454-3462.

van Zanten, T.S., A. Cambi, M. Koopman, B. Joosten, C.G. Figdor, and M.F. Garcia-Parajo. 2009. Hotspots of GPI-anchored proteins and integrin nanoclusters function as nucleation sites for cell adhesion. *Proc Natl Acad Sci U S A*. 106:18557-18562.

VanMeter, A.R., W.D. Ehringer, W. Stillwell, E.J. Blumenthal, and L.J. Jenski. 1994. Aged lymphocyte proliferation following incorporation and retention of dietary omega-3 fatty acids. *Mech Ageing Dev*. 75:95-114.

Vazquez, A., E.E. Bond, A.J. Levine, and G.L. Bond. 2008. The genetics of the p53 pathway, apoptosis and cancer therapy. *Nature Rev Drug Discov*. 7:979-987.

Vogelstein, B., E.R. Fearon, S.R. Hamilton, S.E. Kern, A.C. Preisinger, M. Leppert, Y. Nakamura, R. White, A.M. Smits, and J.L. Bos. 1988. Genetic alterations during colorectal-tumor development. *N Engl J Med*. 319:525-532.

Vogelstein, B., E.R. Fearon, S.E. Kern, S.R. Hamilton, A.C. Preisinger, Y. Nakamura, and R. White. 1989. Allelotype of colorectal carcinomas. *Science*. 244:207-211.

Wang, T.G., Y. Gotoh, M.H. Jennings, C.A. Rhoads, and T.Y. Aw. 2000. Lipid hydroperoxide-induced apoptosis in human colonic CaCo-2 cells is associated with an early loss of cellular redox balance. *FASEB J*. 14:1567-1576.

Wang, Y.N., H. Yamaguchi, J.M. Hsu, and M.C. Hung. 2010. Nuclear trafficking of the epidermal growth factor receptor family membrane proteins. *Oncogene*. 29:3997-4006.

Wassall, S.R., M.R. Brzustowicz, S.R. Shaikh, V. Cherezov, M. Caffrey, and W. Stillwell. 2004. Order from disorder, corralling cholesterol with chaotic lipids. The role of polyunsaturated lipids in membrane raft formation. *Chem Phys Lipids*. 132:79-88.

Wassall, S.R., and W. Stillwell. 2008. Docosahexaenoic acid domains: the ultimate non-raft membrane domain. *Chem Phys Lipids*. 153:57-63.

Webb, Y., L. Hermida-Matsumoto, and M.D. Resh. 2000. Inhibition of protein palmitoylation, raft localization, and T cell signaling by 2-bromopalmitate and polyunsaturated fatty acids. *J Biol Chem*. 275:261-270.

Weihua, Z., R. Tsan, W.C. Huang, Q. Wu, C.H. Chiu, I.J. Fidler, and M.C. Hung. 2008. Survival of cancer cells is maintained by EGFR independent of its kinase activity. *Cancer Cell*. 13:385-393.

Wells, A. 1999. EGF receptor. *Int J Biochem Cell Biol*. 31:637-643.

Westover, E.J., D.F. Covey, H.L. Brockman, R.E. Brown, and L.J. Pike. 2003. Cholesterol depletion results in site-specific increases in epidermal growth factor receptor phosphorylation due to membrane level effects. Studies with cholesterol enantiomers. *J Biol Chem*. 278:51125-51133.

Whitehead, R.H., P.E. VanEeden, M.D. Noble, P. Ataliotis, and P.S. Jat. 1993. Establishment of conditionally immortalized epithelial cell lines from both colon and small intestine of adult H-2Kb-tsA58 transgenic mice. *Proc Natl Acad Sci U S A*. 90:587-591.

Wiley, H.S., and P.M. Burke. 2001. Regulation of receptor tyrosine kinase signaling by endocytic trafficking. *Traffic*. 2:12-18.

Williams, J.A., S.E. Batten, M. Harris, B.D. Rockett, S.R. Shaikh, W. Stillwell, and S.R. Wassall. 2012. Docosahexaenoic and Eicosapentaenoic Acids Segregate Differently between Raft and Nonraft Domains. *Biophys J*. 103:228-237.

Wong, S.W., M.J. Kwon, A.M. Choi, H.P. Kim, K. Nakahira, and D.H. Hwang. 2009. Fatty acids modulate Toll-like receptor 4 activation through regulation of receptor dimerization and recruitment into lipid rafts in a reactive oxygen species-dependent manner. *J Biol Chem*. 284:27384-27392.

Wood, E.R., A.T. Truesdale, O.B. McDonald, D. Yuan, A. Hassell, S.H. Dickerson, B. Ellis, C. Pennisi, E. Horne, K. Lackey, K.J. Alligood, D.W. Rusnak, T.M. Gilmer, and L. Shewchuk. 2004. A unique structure for epidermal growth factor receptor bound to GW572016 (Lapatinib): relationships among protein conformation, inhibitor off-rate, and receptor activity in tumor cells. *Cancer Res*. 64:6652-6659.

Wood, L.D., D.W. Parsons, S. Jones, J. Lin, T. Sjoblom, R.J. Leary, D. Shen, S.M. Boca, T. Barber, J. Ptak, N. Silliman, S. Szabo, Z. Dezso, V. Ustyanksky, T. Nikolskaya, Y. Nikolsky, R. Karchin, P.A. Wilson, J.S. Kaminker, Z. Zhang, R. Croshaw, J. Willis, D. Dawson, M. Shipitsin, J.K. Willson, S. Sukumar, K. Polyak, B.H. Park, C.L. Pethiyagoda, P.V. Pant, D.G. Ballinger, A.B. Sparks, J. Hartigan, D.R. Smith, E. Suh, N. Papadopoulos, P. Buckhaults, S.D. Markowitz, G. Parmigiani, K.W. Kinzler, V.E. Velculescu, and B. Vogelstein. 2007. The genomic landscapes of human breast and colorectal cancers. *Science*. 318:1108-1113.

Wu, C.H., C.C. Wang, and J. Kennedy. 2011. Changes in herb and dietary supplement use in the U.S. adult population: a comparison of the 2002 and 2007 National Health Interview Surveys. *Clin Ther*. 33:1749-1758.

Xu, K.P., J. Yin, and F.S. Yu. 2006. SRC-family tyrosine kinases in wound- and ligand-induced epidermal growth factor receptor activation in human corneal epithelial cells. *Invest Ophthalmol Vis Sci*. 47:2832-2839.

Yaffe, M.B. 2002. Phosphotyrosine-binding domains in signal transduction. *Nature Rev Mol Cell Biol*. 3:177-186.

Yamabhai, M., and R.G. Anderson. 2002. Second cysteine-rich region of epidermal growth factor receptor contains targeting information for caveolae/rafts. *J Biol Chem*. 277:24843-24846.

Yamauchi, T., K. Ueki, K. Tobe, H. Tamemoto, N. Sekine, M. Wada, M. Honjo, M. Takahashi, T. Takahashi, H. Hirai, T. Tushima, Y. Akanuma, T. Fujita, I. Komuro, Y. Yazaki, and T. Kadowaki. 1997. Tyrosine phosphorylation of the EGF receptor by the kinase Jak2 is induced by growth hormone. *Nature*. 390:91-96.

Yamazaki, T., K. Zaal, D. Hailey, J. Presley, J. Lippincott-Schwartz, and L.E. Samelson. 2002. Role of Grb2 in EGF-stimulated EGFR internalization. *J Cell Sci*. 115:1791-1802.

Yan, Y., V. Kolachala, G. Dalmasso, H. Nguyen, H. Laroui, S.V. Sitaraman, and D. Merlin. 2009. Temporal and spatial analysis of clinical and molecular parameters in dextran sodium sulfate induced colitis. *PLoS One*. 4:e6073.

Yaqoob, P., E.A. Newsholme, and P.C. Calder. 1994. The effect of dietary lipid manipulation on rat lymphocyte subsets and proliferation. *Immunology*. 82:603-610.

Yarden, Y. 2001. The EGFR family and its ligands in human cancer. signalling mechanisms and therapeutic opportunities. *Eur J Cancer*. 37 Suppl 4:S3-8.

Yasui, W., H. Sumiyoshi, J. Hata, T. Kameda, A. Ochiai, H. Ito, and E. Tahara. 1988. Expression of epidermal growth factor receptor in human gastric and colonic carcinomas. *Cancer Res*. 48:137-141.

Ye, S., L. Tan, J. Ma, Q. Shi, and J. Li. 2010. Polyunsaturated docosahexaenoic acid suppresses oxidative stress induced endothelial cell calcium influx by altering lipid composition in membrane caveolar rafts. *Prostaglandins Leukot Essent Fatty Acids*. 83:37-43.

Yeh, H.H., R. Giri, T.Y. Chang, C.Y. Chou, W.C. Su, and H.S. Liu. 2009. Ha-ras oncogene-induced Stat3 phosphorylation enhances oncogenicity of the cell. *DNA Cell Biol*. 28:131-139.

Yin, J., and F.S. Yu. 2009. ERK1/2 mediate wounding- and G-protein-coupled receptor ligands-induced EGFR activation via regulating ADAM17 and HB-EGF shedding. *Invest Ophthalmol Vis Sci*. 50:132-139.

Young, J., L.A. Simms, K.G. Biden, C. Wynter, V. Whitehall, R. Karamatic, J. George, J. Goldblatt, I. Walpole, S.A. Robin, M.M. Borten, R. Stitz, J. Searle, D. McKeone, L. Fraser, D.R. Purdie, K. Podger, R. Price, R. Buttenshaw, M.D. Walsh, M. Barker, B.A. Leggett, and J.R. Jass. 2001. Features of colorectal cancers with high-level microsatellite instability occurring in familial and sporadic settings: parallel pathways of tumorigenesis. *Am J Pathol*. 159:2107-2116.

Zerouga, M., W. Stillwell, J. Stone, A. Powner, and L.J. Jenski. 1996. Phospholipid class as a determinant in docosahexaenoic acid's effect on tumor cell viability. *Anticancer Res*. 16:2863-2868.

Zhang, W., and L.E. Samelson. 2000. The role of membrane-associated adaptors in T cell receptor signalling. *Semin Immunol*. 12:35-41.

Zhang, X., J. Gureasko, K. Shen, P.A. Cole, and J. Kuriyan. 2006. An allosteric mechanism for activation of the kinase domain of epidermal growth factor receptor. *Cell*. 125:1137-1149.

Zhu, H., X. Cao, F. Ali-Osman, S. Keir, and H.W. Lo. 2010. EGFR and EGFRvIII interact with PUMA to inhibit mitochondrial translocalization of PUMA and PUMA-mediated apoptosis independent of EGFR kinase activity. *Cancer Lett*. 294:101-110.

Zhuang, L., J. Lin, M.L. Lu, K.R. Solomon, and M.R. Freeman. 2002. Cholesterol-rich lipid rafts mediate akt-regulated survival in prostate cancer cells. *Cancer Res*. 62:2227-2231.

APPENDIX A

YAMC CULTURING PROTOCOLS

I. Preparation of Complete RPMI media for YAMC culture

Ref: Fan et al. Am J Physiol. 1999 Aug;277(2 Pt 1):C310-9; Ng et al. Carcinogenesis. 2005 Nov;26(11):1914-21.

Purpose: To prepare complete RPMI media for YAMC cell culture

Materials:

500 mL RPMI without glutamine (Mediatech # 15- 040 CV)
26.6 mL Fetal Bovine Serum (Hyclone AK 12434)
5.3 mL Glutamax (Gibco, 35050-061)
0.532 mL ITS "-" minus (Insulin, Transferrin, Selenious acid without Linoleic acid) (Collaborative Biomed products, # 4351)

Reconstitution of ITS "-": add 5 mL of sterile distilled water into lysophylized powder. 1 mL of ITS is sufficient for 1 L of media (0.1% dilution)

Procedure :

1. Thaw Glutamax and FBS at 4°C overnight (You can just thaw them the day of assay in 37°C for short time)
2. Add Glutamax, FBS and ITS "-" into 1 bottle of RPMI 1640 media.
3. Gently tilt the bottle to mix
4. Label with initials, date, sterile, and complete then store at 4°C.

Final volume: 531.9 mL
Final concentration: 5% FBS, 1 % Glutamax, 0.1% ITS

Insulin	5 µg/ mL
Transferin	5 µg/ mL
Selenious acid	5 ng/ mL

The following reagent is to be added *fresh* into the media before use:

5 units γ-IFN (Gibco BRL, #13284-021) per 1 mL complete RPMI 1640 media.

Add 1mL γ-IFN per 10 mL of complete RPMI 1640 medium just prior to use.

II. Preparation of YAMC Cell Culture

Ref: Fan et al. Am J Physiol. 1999 Aug;277(2 Pt 1):C310-9; Ng et al. Carcinogenesis. 2005 Nov;26(11):1914-21.

Purpose: To start YAMC culture by growing cells in a T-75 flask.

Preparation:
Turn on the UV in the hood for at least 15 min prior to keep it sterile for culture

Procedure:

1. Warm complete RPMI 1640 media to room temperature
2. Aliquot 10 mL media in a 15 mL conical tube (to spin down frozen cells) and make up 20 mL complete media with 2 μL γ-IFN (to resuspend and grow cells)
3. Take a vial of YAMC cells from the liquid nitrogen storage system
4. Thaw it in the water-bath immediately by gently twirling around in the water bath for ~ 30sec. to reduce the condensation
5. Add thawed cells into the media in the conical tube
6. Centrifuge at 200 x g (1096 rpm: tabletop centrifuge) for 5 min
7. Using sterile technique, open a T-75 flask and add 12 mL complete media (with γ-IFN)
8. Following completion of spin, vacuum aspirate the supernatant being careful not to disturb pellet
9. Resuspend the pellet in 5 mL complete RPMI 1640 (with γ-IFN)
10. Add resuspended cells into the T-75 flask with media, label the flask - specify the cell type, passage number, date and initials
11. Gently rotate the flask to distribute the cells evenly
12. Incubate the flask at 33˚C under 5% CO_2 atmospheric pressure

III. Feeding of YAMC Cell Culture
Ref: Fan et al. Am J Physiol. 1999 Aug;277(2 Pt 1):C310-9; Ng et al. Carcinogenesis. 2005 Nov;26(11):1914-21.

Purpose: To feed YAMC culture by growing cells in a T-75 flask.

Preparation:
Turn on the UV in the hood for at least 15 min prior to keep it sterile for culture

Feeding cells:
Check cell confluence every day
Feed cells every 24-48 h (maximum 72 h)

Procedure:

1. Prepare 20 mL RPMI 1640 media with 2.0 μL γ-IFN. Warm to 33^{o}C.
2. Vacuum aspirate old media from the flask of cells using sterile glass pipette.
3. Add the pre-warmed fresh RPMI 1640 media with γ-IFN to the flask.
4. When culture reaches 70-90% confluence, trypsinize the cells and pass them (refer to protocol).

IV. YAMC Cell Culture: Seeding, Passing or Freezing

Purpose: To pass and seed or freeze YAMC cell culture.

Preparation:
Use sterile hood conditions for the procedure
Warm 50 mL complete RPMI 1640 and trypsin-EDTA (Gibco, #25300-054) to room temperature

Procedure:
For any 70% confluent cell culture in a T-75 flask:

1. Add 15 mL complete media in a 50 mL conical (to spin cells) – always use at least 2X as much media as trypsin to spin down cells after trypsinization.
2. Add 25 mL media plus 2.5 μL γ-IFN to a 50 mL conical (to grow cells)
3. Warm both conical of media in water bath (37^{o}C)
4. Aspirate old media from flask
5. Rinse monolayer of cells with ~10mL HBSS (Sigma, H-6648) by adding and aspirating gently without disturbing the cell monolayer
6. Add 5 mL Trypsin-EDTA to the flask and incubate cells at 37˚C for 3 minutes or until > 90% cells are lifted. Gently tap the bottom of the flask to assist in cells lifting.
7. Add the 15 mL complete media (step 1) from the conical tube to the flask of trypsinized cells (add by rapidly dispensing the media and moving the pipette in a back and forth motion across the flask to dislodge any stuck cells). Then, transfer the media and trypsin to the 50 mL conical tube.
8. Use a glass pipette to transfer approximately 10 μl of the cell suspension onto each end of the hemacytometer.

   Count the number of cells: Cell number (per mL) = $\frac{\text{Living cells count x 10,000}}{\text{\# Squares counted}}$

9. Centrifuge cells at 200 x g (1096 rpm, countertop centrifuge for 5 min)
10. Vacuum aspirate supernatant (media with trypsin), taking care not to disturb the pellet

A. Procedure to reseed cells

a) Add 5 mL of complete RPMI 1640 (with γ-IFN) and resuspend the pellet by gently pipetting up and down to make a homogenous suspension.
(you can also gently tap the "almost dry" pellet before resuspend with medium, to help with resuspension)
b) Seed cell according to desired density in complete RPMI 1640 with γ-IFN.

B. Procedure for cell freezing (to store) cells in liquid nitrogen

a) After step 8 in the cell passage protocol, resuspend cells in freezing media (EmbryoMax, # S-002-D) Normally, we want to freeze ~ 1-2 million cells/mL
b) Add 1 – 1.5 mL of cell suspension to cryovials
c) Label the vials with the cell type, passage number, date, and initials
d) Keep vials in Mr. Frosty (Nalgene, #5100-0001) at –80˚C for 24-48 h and then transfer vials into liquid nitrogen for storage
e) Enter the rack, box # and vial position into cell culture log book.

APPENDIX B

GENERAL EGF STIMULATION OF YAMC

Purpose: To stimulate EGFR activation in YAMC

Materials:

EGF (Sigma Sigma #E 1257)

RPMI 1640 (Mediatech # 15040CV) *complete and serum starvation*:

Complete: To a 500 mL bottle, add 532 µL ITS Premix (BD Biosciences #354351), 26.6 mL fetal bovine serum (FBS, Hyclone SH30070.01), and 5.3 mL Glutamax (Gibco 35050). Immediately prior to use, add 1 µL IFNγ (Gibco #13284-021) per 10 mL complete media.

Serum starvation: Immediately prior to use, to plain unsupplemented RPMI 1640 add FBS to a final concentration of 0.5%. Also add 1 µL IFNγ (Gibco #13284-021) per 10 mL complete media.

Procedure:

1. Culture YAMC cells in complete media (plus any treatment) at 33°C and 5% CO_2 until they become ~95% confluent.
2. Aspirate complete media and wash cells 2X with PBS.
3. Add serum starvation (0.5% FBS) media and incubate overnight (16-18 h) at 33°C and 5% CO_2.
4. Add EGF to plain unsupplemented RPMI 1640 to a final concentration of 25 ng/mL (stock EGF is 10 ng/µL).
5. Remove serum starvation media from the cells and replace with EGF-supplemented media. Incubate cells 33°C and 5% CO_2 for the amount of time required by the experiment (typically 2-30 min).
6. Aspirate media from the cells and wash with PBS.
7. Harvest cells according to the experiment.

APPENDIX C

TOTAL CELL LYSATE ISOLATION

Purpose: To isolate cell lysate from YAMC cells in 150 mm dishes

Materials:
Prepare 5 mL of Homegenization buffer (this is the standard HB used in the Chapkin lab, but buffer is subject to change based on the experiment):
500 µl of 500 mM Tris-HCl (Sigma #T1503) – Final concentration = 50 mM
1.25 mL of 1 M sucrose (Sigma #S9278) **–** Final concentration = 250 nM
50 µL of 200 mM EDTA(Sigma #ED4SS) **–** Final concentration = 2 mM
50 µL of 100 mM EGTA (Sigma #34596) – Final concentration = 1 mM
0.625 µL of 0.4 M NaF (Sigma #S6521) – Final concentration = 50 µM
500 µL of 10% Triton-**X** (Sigma #T6878) – Final concentration = 1%
2395.875 µL of double distilled water
50 µL of 10 mM activated sodium orthovanadate (Sigma #S6508) – Final concentration = 100 µM
200 µL of protease inhibitor cocktail (Sigma #P8340)
3.5 µL of 14.2 M β-mercaptoethanol (Bio-Rad #161-0710) – Final concentration = 10 mM
Items in red are to be added on the day of use
Cell scrapers
29-gauge needles

Procedure:
1. Aspirate media from the dishes and wash with 15 mL ice-cold PBS. Gently swirl the plate and suck off the PBS (to thoroughly remove all traces of media). Repeat PBS washes 3X. Make sure to remove all PBS after the final wash to prevent diluting the homogenization buffer.
2. Keep the plates on ice and add 300 µl of HB per dish and scrape cells using a cell scraper.
3. Transfer the lysate into eppy tubes.
4. Pass through 29G needle once into the same set of eppy tubes, flush the suspension very hard to sheer the cells (perform on ice).
5. Incubate the total lysate in ice for 30 min.
6. Centrifuge at 16, 000 x g at 4°C for 20 min.
7. Transfer the supernatant (lysate) to clean eppy-tube and pipette up and down to mix.
8. Prepare 30 µl aliquots and one 10 µL aliquot of each sample, and save aliquots at -80°C for further protein estimation using Coomassie Plus and immunoblotting.

APPENDIX D

COOMASSIE ASSAY

Purpose: To determine the protein concentration of samples

Materials:
Homogenization buffer (whichever was used to collect samples)
EIA/RIA clear polystyrene 96-well plate (Corning #9017)
Coomassie Plus assay reagent (ThermoFisher #23238)
Disposable borosilicate glass tubes (VWR #47729-572)

Procedure:
1. Use this assay with homogenization buffer (HB) used to collect the total cell lysate (TCL).
2. Before beginning, turn on SpectroMax and prepare a template.
3. Prepare samples and standards in glass tubes by mixing the amounts of standard/sample, water, HB, and reagent listed below. Make triplicates of all samples and standards.
4. After adding everything to each tube, vortex tubes for 3 s and transfer 300 µl of standard/sample to the designated well on the 96-well plate.
5. Immediately after adding all standards and samples to the plate, bring to the SpectroMax plate reader and read at 595 nm.

Standards:

Total µg Protein	Water	0.25µg/µl BSA HB	Reagent	1µg/µl BSA Position	2 µg/µl BSA		
0	0 µl A 1-3	--	--	497.5µl	2.5µl	500µl	
0.5	2 µl	--	--	495.5	2.5	500µl	B 1-3
1.0	4 µl	--	--	493.5	2.5	500µl	C 1-3
2.0	--	2 µl	--	495.5	2.5	500µl	D 1-3
4.0	--	4 µl	--	493.5	2.5	500µl	E 1-3
10.0	--	10 µl	--	487.5	2.5	500µl	F 1-3
20.0	--	--	10 µl	487.5	2.5	500µl	G 1-3

Samples:

Amt Sample	Water	Reagent
2.5 µl	497.5 µl	500µl

APPENDIX E

LIPID RAFT ISOLATION

Purpose: To isolate the plasma membrane and use gradient ultracentrifugation to harvest lipid raft/caveolae fraction for analysis.

Reference: Kim W, et al. Methods Mol Biol 2009;579:261-70

Materials:
Sucrose (Sigma #S9378)
Na_4EDTA (Sigma #ED4SS)
Tricine (Sigma #T-5816)
Optiprep (Sigma #D1556)
Percoll (Sigma #P1644)
Slide-a-lyzer dialysis cassettes (Pierce #66205 and 66203)
Protease inhibitor cocktail (Sigma #P8340) (1:25 dilution)
10 mM activated sodium orthovanadate (Na_3VO_4, Sigma #S6508)

Solutions:
(all solutions make fresh, except PBS and Sucrose)
1X PBS : 500mL warm (37°C), 500mL cold (4°C)
2.5M Sucrose:
427.8g Sucrose
-Combine with water, heat to 60°C to dissolve, final volume to 500mL
-Store at 4°C

Buffer A : (stable for 1 week stored at 4°C) Final Conc:
20mL 2.5M Sucrose 0.25M
0.076g Na_4EDTA 1mM
0.716g tricine 20mM
-Combine with 170mL water, pH to 7.8, bring to final volume of 200mL

To 10 mL of Buffer A, add 400 µL of protease inhibitor cocktail and 100 µL Na_3VO_4 (final concentration 100 µM). Use this in step #11

2XA : (Stable for 1 week stored at 4°C)
13.32mL 2.5M Sucrose 0.5M
0.05g Na_4EDTA 2mM
0.48g tricine 40mM
-Combine with 40mL water, pH to 7.8, bring to final volume of 66.6mL

OptiPrep Diluent : (stable for 1 week stored at 4°C)
1mL 2.5M Sucrose 0.25M
0.022g Na_4EDTA 6mM

0.216g tricine 120mM

-Combine with 7mL water, pH to 7.8, bring to final volume of 10mL

30% Percoll : Don't make until ready for use!

30mL Percoll

50mL 2XA

20mL water

50% Opti-Prep (Gibco) :

36mL OptiPrep

7.2mL OptiPrep diluent

OptiPrep Solutions:

5% -0.4mL 50%OptiPrep+3.6mL Buffer A 10% -2.94mL 50%OptiPrep+11.74mL Buffer A

15%-1.5mL 50%OptiPrep+3.5mL Buffer A 20% -5.86mL 50%OptiPrep+8.8mL Buffer A

Dialysis buffer:

1 mM Na_4EDTA

20 mM tricine (pH 7.8)

Procedure:

1. Grow YAMC cells in T-175 flasks (need approximately 8 flasks of YAMC cells for n=1 per treatment).
2. Aspirate media from the flask and wash with 20 mL PBS.
3. Aspirate PBS and add 10 mL trypsin.
4. Place flask in 37^{o}C incubator for 3-5 min until all cells are lifted. Tap the bottom of the flask to help release cells. Stop trypsinization with 20 mL of media.
5. Place trypsinized cells into a 50 mL conical tube.
6. Count cells using hemacytometer.
7. Centrifuge cells at 200 x g for 5 min.
8. Aspirate trypsin/media from the tube without disturbing the pellet.
9. Wash the pellet with PBS and centrifuge at 200 x g for 5 min.
10. Aspirate PBS and repeat wash/centrifuge step.
11. Aspirate PBS and resuspend pellet in Buffer A with protease inhibitor cocktail and phosphatase inhibitor at 1.15-1.2 x 10^7 cells/mL. Put into cryovials.
12. Lyse cells by performing a rapid freeze (place in liquid nitrogen for 1 min) and thaw (place in a 37^{o}C water bath for 1 min) twice.

13. Combine cryovials of samples from the same group, save an aliquot (~100 µL) as Sample A, and spin at 1000 x *g*, for 10 min at 4°C.
    -During the spin, pre-cool ultracentrifuge and make 30% Percoll.
14. Collect supernatant (post-nuclear) and keep on ice.
15. Save an aliquot (~100 µL) and label as Sample B.
16. Load supernatants on top of 23 mL of 30% Percoll in 38.5 mL Beckman Ultra-clear centrifuge tube (Beckman #344059).
17. Centrifuge in Beckman SW28 at 84,000 x *g* (25,000 rpm) for 30 min, 4°C.
    -Meanwhile make remaining OptiPrep Solutions
18. Collect 2 mL plasma membrane fraction (visible band ~6 cm from the bottom of tube). Place in 15 mL Beckman tube (#343664). Save aliquot (~100 µL) as Sample C.
19. For sonication, use the Sonics & Materials sonicator (Model VC50T, Serial #344058).
    Set power output 90, J/w/s 50, pulser off.
    Tune probe in Buffer A before sonicating sample.
    To sonicate sample, place the sample on ice and place the sonicator probe in center of solution and sonicate 2X with rapid pulse.
    Sit on ice 2 min.
    Repeat rapid pulse 2X, sit on ice 2 min.
    Repeat rapid pulse 2X, put back on ice.
20. Prepare 23% Opti (2 mL Sample + 1.84mL 50%Opti + 0.16mL Buffer A) and add to 12 mL Beckman Ultra-clear centrifuge tubes (#344059). On top, layer a linear 20% to 10% Opti gradient (3 mL each) using a gradient maker connect to a peristaltic pump set at a flow rate of 1 mL/min.
21. Centrifuge at 52,000 x *g* (17,000 rpm) 90 min, 4°C in SW41 Ti rotor.
22. Collect top 5 mL into new tube. Save aliqot (~100 µL) as Sample D.
23. Collect visible cloudy band below and save as Sample E.
24. Add 4 mL 50% OptiPrep to sample and mix.

25. Overlay with 1 mL 15% OptiPrep followed by 0.5 mL 5% OptiPrep. Centrifuge at 52,000 x *g* (17,000 rpm) 90 min, 4^{o}C.
26. Collect top white band (500-700 µL) within 5% Opti layer, just above interface. Collect additional band below (Sample F).
27. After sample collection, dialyze using slide-a-lyzer cassettes using dialysis buffer. Dialyze overnight at 4^{o}C, change buffer, dialyze 1 h at 4^{o}C.
28. After dialysis, use Savant Automatic Environmental SpeedVac System (#AES1010) and speed-vac samples to between 1/3 and 1/4 original volume to concentrate. Follow SpeedVac settings given on the machine.
29. Perform Coomassie to determine protein assay.

APPENDIX F

COLOCALIZATION ANALYSIS

Purpose: To determine the colocalization of EGFR with a lipid raft marker (truncated H-Ras) in cells treated with DHA, LA, or control.

Materials:
Effectene transfection reagents (Qiagen #301425)
Lab-Tek chambered coverglass #1.0 (Thermo Scientific #155380)
RPMI 1640 (Cellgro #15-040-CV)
Gibco Leibovitz L-15 media, no phenol red (Life Technologies #21083-027)

Procedure:

1. Seed YAMC cells in Lab-Tek 2-well chambered coverglass at a density of 1.0 x 10^5 and incubate at 33^{o}C with 5% CO_2.
2. After 4 h (allow cells to adhere), change media and add FA to a final concentration of 50 µM and incubate O/N.
3. After 24 h, aspirate old media and replace with fresh (including FA).
4. Dilute stock of RFP-tH to 0.1 µg/µL with sterile TE.
5. After 12 h, transfect cells with 0.3 µg RFP-tH using Effectene according to the manufacturer's instructions. See HFT protocol "Lipofection of YAMC in 2-well slides" for detailed instructions. Use the amount of reagents specified for a 12-well plate in the manufacturer's protocol.
   Volume DNA: 3 µL (for 0.3 µg)
   Enhancer volume: 2.4 µL
   Buffer EC: 72 µL
   Effectene Reagent: 6 µL
   Volume of media to add to cells: 800 µL
   Volume of media to add to complexes: 400 µL
6. After 12 h, transfect cells again with 1.0 µg EGFR-GFP using Effectene according to the manufacturer's instructions
7. After 8 h, cells were washed once with PBS and placed in serum starvation (0.5% FBS) media at 33^{o}C with 5% CO_2.
8. After 16 h, bring cells to the Image Analysis Lab and placed in the incubator at 33^{o}C with 5% CO_2.
9. Immediately prior to imaging, wash cells once with PBS and then replace with Leibovitz media with no phenol red.
10. Collect images on the Zeiss 510 META NLO Multiphoton Microscope System consisting of an Axiovert 200 MOT microscope (Carl Zeiss Microimaging). For EGFR-mGFP, use excitation wavelength of 488 nm and emission of 530 nm. For RFP-tH, use excitation of 543 nm and emission of 590 nm. Collect images in confocal mode with the pinhole set at 1 AU using a 40x objective (1.3 NA oil

immersion lens) at room temperature. Identical acquisition parameters must be used for all images within the experiment.

11. Quantify colocalization at the plasma membrane using Mander's colocalization coefficient for green (EGFR-mGFP) with red (RFP-tH) using Nikon Elements AR 3.2. Perform analysis on **background-subtracted** 16-bit images.

    Tip for slide layout: Put different treatments on the same slides so that if a slide is lost or damaged, you do not lose 2 of the same group.

APPENDIX G

WESTERN BLOTTING

Purpose: To measure the amount of total or phosphorylated proteins

Preparation:

-Thaw samples on ice
-Label 0.6 mL eppy tubes
-Turn heating block on and set temperature to 98°C
-Prepare the western template sheet
- Cut PVDF membrane and filter papers ready

Procedure:

Sample preparation

1. Thaw the samples on ice while you turn on the heating block and set the temperature to 98°C (takes about 15 min).
2. Dye used for the sample dilution is 5X Pyronin. Use 1X of the dye based on the total volume of sample required (usually 25 mL total).
3. With the aid of western template sheet make the necessary dilution (if required) and add the calculated amount of dye and water to the samples and standard.
4. Quick spin.
5. Boil the samples for 5-10 min depending on the volume of the samples (25 mL volume boil for 10 min). Do not boil the marker.
6. Quick- spin of the samples on the tabletop.

Gel unit set up

7. Take the pre-made gel (usually 4-20%) and carefully rip off and discard the white tape and the comb. Mark the lanes on the plate.
8. Attach the gel to the gel rack align 3rd with the lower gasket and clamp the unit. (Note that the red clip should have the broad end facing you, broad ends face outside on all 4 clips). Either run a gel on each side or attach the white space holder on the empty side.
9. Pour running buffer to fill the stand and the trough up to the top mark.
10. Use gel-loading tips (or 10 mL XL tips) and load the complete sample volume.
11. Close the unit with the lid and check the leads and make sure black-to-black and red-to-red.
12. In the cold room run the gel at 125 V for as long as needed. Check after 10 minutes to make sure it is running.
13. After about 1 h check every 15 min.
14. Stop the gel when it has run as far as needed.

Gel transfer

15. Crack open the plate with a scalpel between the markings on the plate all around by keeping the large side of the gel down.
16. Cut the gel just above the bottom.
17. Carefully separate the gel from the plate and cut the gel at lane one to identify the side (left end).
18. Take the gel transfer unit in a staining tray and pour transfer buffer into it and the trough. Allow gel to equilibrate in transfer buffer for 15-30 min. Wet membrane with methanol then equilibrate in transfer buffer for ~5 min.
19. Take the cassette and lay it open.
20. Put a sponge on the black side of the cassette and place a filter paper on top of it.
21. Pour transfer buffer to keep it wet.
22. Take the gel plate out of the running trough and transfer the running buffer into the bottle for reuse.
23. Place the gel on the filter paper with lane one on the right (protein side facing the membrane.
24. Cut the right hand top corner of the membrane to identify the side.
25. Place the membrane on the gel and place the other filter paper on the membrane. Now, use a roller on the filter paper to eliminate any air bubbles in between.
26. Place the sponge and close the white side of the cassette and clip it.
27. Place the cassette in the transfer unit with the hinges facing the top and black side facing back.
28. Put a stir bar into the transfer trough.
29. Fill the trough with transfer buffer just enough to cover the hinges of the cassette. Check the terminals black to black correspond.
30. Place it on the cold room stir plate.
31. Connect black-to-black and red-to-red and set current to 400 milliamps and let it transfer for at least 90 min.

Blocking

32. At the end of 90 min- make 4% nonfat dry milk/ PBS/ Tween in a 50 mL tube (to 30 mL of PBS –Tween and add 1.2 gms of pre-weighted milk powder). Mix gently by inverting. If 5% BSA is required, add 1.5 g IgG free BSA to 30 mL PBS-T.
33. Pour the milk into a dish and keep ready to transfer the membrane into it.
34. After the transfer is complete- open the gel unit and transfer the transfer buffer into the bottle.
35. Use a pair of forceps to take the membrane and place the membrane into the milk dish (with the side facing gel-protein side now facing top)
36. Place it on the shaker for 1 hr at room temperature.

Primary antibody

37. Take a dish with 1.2 gm dry milk powder and 30 mL PBS- Tween. Mix and pour into a new dish.
38. Transfer the membrane from the blocking buffer into the dish with fresh milk.

39. Now, add the appropriate volume of the primary antibody (based on the dilution and add it into the dish).
40. Close the lid of the dish and shake it gently on the cold room shaker overnight.

Washing
41. The next day take the membrane and give a quick wash with PBS –Tween.
42. Then replace the membrane in fresh PBS- Tween in the dish and keep on the shaker at room temp for 10 min. Let it shake vigorously.
43. Repeat the wash 2 times at 5-10 min interval.

Secondary antibody
44. Make 30 mL milk/ PBS/ Tween and pour into the dish after the second wash.
45. Add the required volume of secondary antibody based on the dilution.
46. Set on shaker for 1 hr at room temperature.
47. Repeat washing with PBS –Tween 3 times.
48. While the 1 wash of 2° antibody is going on turn on the imager and set focus.

Developing
49. Cut an acetate sheet into 2 halves and remove the black sheet.
50. Mix equal parts of chemiluminescent super signal reagent A and reagent B in an ependroff tube. Mix gently by inversion.
51. Transfer the membrane between the layers of the acetate sheet and evenly disperse the developing solution across on the top of the membrane.
52. Slowly close the top layer so that the solution gets evenly distributed on the membrane.
53. Expose for 5 minutes and then transfer the membrane on to the clean acetate sheet .
54. Transfer it into the BioRad imager for imaging immediately.

Imaging
55. Turn on switch and make sure the lever on the hood is at chemiluminescence.
56. Select QuantityOne on program on desktop.
57. Select scanner – click on chemidoc.xrs.
58. Step 1- option is chemiluminescences.
59. Step 2 – live focus. Focus with a printed sheet and set the iris as you need for brightness. Zoom and focus, as you need for clarification.
60. Freeze. Put the gel in the imager and zoom and freeze again. Close the door.
61. Click on live acquire.
62. Set the Starting exposure time, Total exposure time, and Number of exposures as needed.

Special instructions if western blotting for p-EGFR
a. Perform blocking steps (#32-36) using Invitrogen Membrane Blocking Solution (MBS; 00-0105).
b. Following blocking, wash the membrane for 5 min with TBS-T.

c. Incubate membrane with antibody diluted 1:1000 in MBS O/N at 4°C with slow rotation.
d. Wash membrane according to protocol with TBS-T.
e. Incubate the membrane with secondary antibody diluted in 4% milk in TBS-T for 1 h at RT with slow rotation.
f. Finish protocol (#47-62) according to directions above using TBS-T.

APPENDIX H

IMMUNOPRECIPITATION

Purpose: To perform immunoprecipitation or co-immunoprecipitation of EGFR

Reference: Current protocols in protein science 19.4.5

Materials:
Immunoprecipitation Buffer (for 5 mL): 500 uL of 500 mM Tris-Cl (pH 7.5) (Fisher #BP153), 750 µL of 100 mM EGTA (Sigma #E4378), 1 mL of 500 mM NaCl (Sigma #S3014), 50 µL of 10% Triton X (Sigma #X-100), 250 µL of 10 mM activated sodium orthovanadate (Sigma #S6508), protease inhibitor cocktail (Sigma #P8340), 3.5 µL β-mercaptoethanol (Sigma #M6250). Add ingredients in red on the day of use.
Protein G Dynabeads (Invitrogen #100.04D)
Magnet (Invitrogen: DynaMag-2 #123.21D; Sample rack #123.22D)
Anti-EGFR antibody (Millipore #06-847)

Procedure:
1. Harvest YAMC cells according to the Total Cell Lysate preparation protocol, but use the Immunoprecipitation Buffer described above in place of the Homogenization Buffer from the protocol. Perform Coomassie protein assay to determine protein concentration.
2. Prepare samples on ice by combining 250 µg total cell lysate with 25 µL antibody. Add immunoprecipitation buffer to bring to a final volume of 500 µL.
3. Invert tube gently several (5-7) times followed by incubation on ice for 90 min with occasional tube inversion (~every 5 min).
4. Prepare Protein G Dynabeads by completely resuspending beads by rotating on orbital shaker for ~5 min. Transfer 50 µL Dynabeads to an eppy-tube. Separate on the magnet until the supernatant is clear and remove the supernatant.
5. Quick-spin the tube from step #3, and add the antibody-antigen (Ab-Ag) mixture to the tube with dynabeads.
6. Rotate tube at 4°C for 1 h.
7. Place tube on magnet and allow to separate until the supernatant is clear.
8. Save the supernatant as "flow through".
9. Wash the Dynabeads-Ab-Ag complex by adding 200 µL of lysis buffer to the tube and resuspending by gentle pipetting. Separate on the magnet and remove supernatant (discard). Repeat the wash 2 more times.
10. Resuspend the Dynabeads-Ab-Ag complex in 100 µL lysis buffer and transfer the bead suspension to a clean tube. This is recommended to avoid co-elution of proteins bound to the tube wall.
11. Place the tube on the magnet and remove the supernatant.

12. Add 50 µL 2X pyronin and gently pipette to resuspend the dynabeads-Ab-Ag complex.
13. Heat to 98°C for 10 min.
14. Place the tube on the magnet and remove the supernatant to a new tube.
15. Repeat elution step and combine the supernatant with that from step #12.
16. The sample is now ready to be loaded directly onto an SDS-polyacrylamide gel.

APPENDIX I

PROLIFERATION

Purpose: To measure proliferation of YAMC cells

Materials:

RPMI 1640 (Mediatech # 15040CV):

Complete: To a 500 mL bottle, add 532 µL ITS Premix (BD Biosciences #354351), 26.6 mL fetal bovine serum (FBS, Hyclone SH30070.01), and 5.3 mL Glutamax (Gibco 35050). Immediately prior to use, add 1 µL IFNγ (Gibco #13284-021) per 10 mL complete media.

CyQuant Cell Proliferation Assay (Invitrogen #C7026)

Procedure:

1. Grow YAMC cells in T-75 flasks for 24 h in complete RPMI 1640 at 33°C and 5% CO_2.
2. Treat YAMC cells for an additional 24 h with complete media supplemented with control (no fatty acid), LA, or DHA (50 µM). Culture at 33°C and 5% CO_2.
3. Wash cells 1X with PBS then trypsinize for 5 minutes at 37°C.
4. Neutralize the trypsin with complete RPMI 1640 and immediately spin down at 200 x g for 5 min.
5. Aspirate the media/trypsin and resuspend cells in 1 mL of complete media supplemented with the same fatty acid treatment as previously.
6. Count cells using a hemocytometer. Make the final concentration of cells to ~$1x10^5$ cells/200 µL.
7. Seed 200 µL of cell suspension into a 96-well plate and culture with complete media supplemented with fatty acids for an additional 48 h at 33°C and 5% CO_2. Change the media/fatty acid after 24 h.
8. After 48 h of growth in the 96-well plate, completely remove all media, wash 1X with PBS, and completely remove all PBS.
9. Wrap parafilm tape around the 96-well plate and the lid. Place the plate in a -80°C freezer until ready to process (up to 4 weeks).
10. When you are ready to quantitate the samples, start by preparing the reagent. Allow the CyQUANT® GR stock solution (Component A) to warm to room temperature.
11. Dilute the concentrated cell-lysis buffer stock solution (Component B) 20-fold in nuclease free distilled water.
12. Just prior to running the experiment, dilute the CyQUANT® GR stock solution (Component A) 400-fold into the 1X cell-lysis buffer. For example, to prepare 20 mL of CyQUANT® GR working solution (enough for ~100 assays), first make the 1X cell-lysis buffer by mixing 1 mL of the 20X stock with 19 mL of nuclease-free distilled water; next add 50 µL of the CyQUANT® GR stock

solution and mix thoroughly. It is recommended to prepare the diluted solution in a plastic container, rather than in glass because the CyQUANT® GR reagent may adsorb to glass surfaces. Protect the working solution from light by keeping it in an opaque bottle, covering it with foil, or placing it in the dark to prevent photodegradation of the CyQUANT® GR dye. For best results, the solution should be used within a few hours of its preparation.

13. Thaw the plates at room temperature, then add 200 µL of the CyQUANT® GR dye/cell-lysis buffer (prepared in Preparing the Reagent) to each sample well.
14. Incubate the samples for 2–5 minutes at room temperature, protected from light.
15. Measure the sample fluorescence using a fluorescence microplate reader with filters set at ~480 nm excitation and ~520 nm emission maxima.

APPENDIX J

ERK1/2 INHIBITION

Purpose: To inhibit ERK1/2 activation in YAMC cells

Materials:
U0126 (Invitrogen #PHZ1283)
EGF (Sigma #E1257)
Serum starvation media: RPMI 1640 supplemented with 0.5% FBS and IFN-γ
Serum free media: Plain, unsupplemented RPMI 1640 media
Antibodies:
Anti EGFR antibody Cell Signaling #2646 (1:2000)
Anti phospho-EGFR antibody Cell Signaling #3777 (1:1000)
Anti p44/42 MAPK (ERK1/2) antibody Cell Signaling #4695 (1:2000)
Anti phospho-ERK1/2 antibody Cell Signaling #4370 (1:2000)

Procedure:
1. Seed YAMC cells into 150 mm dishes in complete RPMI media with IFN-γ.
2. Incubate O/N at 33°C.
3. Change media, and incubate for 24 h at 33°C.
4. Replace complete media with 0.5% FBS serum starvation media. Incubate at 33°C O/N.
5. Prepare a stock of U0126 of 1 mM by adding 0.38 mg U0126 to 1 mL of sterile, plain serum free RPMI 1640 media (no supplements).
6. Add 150 µL of stock 1 mM U0126 to 15 mL of serum free media for each plate to be treated. Final concentration is 10 µM U0126.
7. Aspirate old media from the plates and add the serum free media with 10 µM U0126 and incubate at 33°C for 2 h.
8. Following treatment with inhibitor, aspirate media, wash 1X with room temperature PBS, and stimulate cells for 10 min with serum free media supplemented with 25 ng/mL EGF.
9. Harvest cells in homogenization buffer treated with protease and phosphatase inhibitors and isolate total cell lysate (see Total Cell Lysate protocol for details).
10. Determine concentration of protein using Coomassie assay.
11. Perform WB for total and phosphorylated ERK1/2 to determine inhibition of EGFR-induced activation of ERK1/2.
12. Perform WB for total and phosphorylated EGFR to determine the effect of ERK1/2 inhibition on EGFR activation.

APPENDIX K

DIMERIZATION

Purpose: To assess EGFR dimerization

Reference: Sorkin A, Carpenter G. Dimerization of internalized epidermal growth factor receptors. JBC 1991;266(34)23453-60.

Materials:
5 mL Homogenization buffer (for composition, see TCL protocol)
150 mm dishes
EGF (Sigma #E 1257)
BS^3 (bis sulfosuccinimidyl suberate, Thermo Scientific # 21586; MW=572.4)
Glycine (Fisher #BP381)

Procedure:
1. Seed YAMC cells onto 150 mm dishes at a density of 500,000 cells in 15 mL of complete RPMI media and incubate O/N at 33°C.
2. The next day, change media and incubate O/N at 33°C.
3. On the following day, replace media in dishes with low serum (0.5% FBS) and place at 33°C O/N (16-18 h).
4. Wash dishes with PBS and incubate for 1 h on ice with 15 mL serum free RPMI supplemented with 25 ng/mL EGF. Incubation on ice allows for ligand binding and dimerization but inhibits receptor endocytosis.
5. Wash dishes 3X with ice-cold PBS.
6. Crosslink dimers with 5 mL of 3 mM BS^3 in ice cold Ca^{2+}, Mg^{2+} free PBS for 20 min on ice. To make 3mM BS^3, add 8.60 mg BS^3 to 5 mL PBS.
7. Following crosslinking, quench with 10 mL of 250 mM glycine in PBS for 5 min at 4°C.
8. Wash with ice cold PBS 3X.
9. Add 300 µL of homogenization buffer to each plate and scrape. Collect scraped cells into eppy-tubes and place on ice.
10. Pass cell homogenates through a 29G needle once into the same set of eppy tubes. Flush the suspension very hard while keeping the tube on ice to sheer the cells.
11. Incubate the total cell suspension on ice for 30 min.
12. Centrifuge at 16,000 x *g* at 4°C for 20 min.
13. Transfer the supernatant (total cell lysate) to clean epi-tube (do not disturb the pellet) and mix by pipetting up and down a few times.

14. Aliquot the lysates and save the aliquots at -80°C for further protein estimation using Coomassie Plus and immunoblotting. Make aliquots of 30 µl plus one set of 10 µL for protein quantification.
15. Assess dimerization of EGFR by western blotting for EGFR according to the western blotting protocol (with the slight adjustments mentioned below).
16. Dimers on western blot should be twice the size of EGFR band. Serum starved, unstimulated cells should not have a dimer band and can be used for control.
17. SDS-PAGE should be run for approximately 4-5 h at 125 V, and transfer should be overnight at 400 mAmps. Make sure to incubate the gel in transfer buffer for ~15-30 minutes before beginning the transfer.

APPENDIX L

TOTAL INTERNAL REFLECTION FLUORESCENCE MICROSCOPY

Purpose: To assess recruitment of Grb2 to the plasma membrane following stimulation with EGF

Materials:
SH2-Grb2-YFP (1.5 µg protein/transfection) (Dr. Alexander Sorkin, University of Colorado)
Mouse EGF (Sigma #SRP3196; stock 10 ng/µL)
Round glass bottom dishes (Glass bottom dishes #P35G-1.5-20-C)
RPMI 1640 (Complete: supplemented with ITS, glutamine, 5% FBS, and IFN-γ; Serum-starvation: supplemented with 0.5% FBS)
Leibovitz media with no supplementation (Sigma #L5520)

Procedure:
1. Seed YAMC cells into T-75 flasks and culture in 15 mL complete media O/N at 33°C with 5% CO_2.
2. Aspirate media and replace with complete media (control) or complete media supplemented with treatment (50 µM BSA-complexed DHA or LA). Stock fatty acids are 2.5 mM, so add 14.7 mL media and 300 µL stock fatty acid. Leave fatty acid in the fridge and wrapped in foil until ready to add. Try to add fatty acid quickly and without creating bubbles to minimize oxidation.
3. Culture O/N at 33°C with 5% CO_2.
4. Transfect cells using Nucleofection protocol with 1.5 µg SH2-Grb2-YFP.
5. Place the round glass bottom dishes into the wells of a 6-well plate. The dishes will sit on top of the wells. This will prevent the bottom of the dishes from touching anything. Make sure that the bottoms of the dishes do not directly touch any surface. This can interfere with ability to perform TIRF.
6. Seed 25,000 cells into round glass bottom dishes in 1 mL of complete media supplemented with treatment as above.
7. Culture the cells for 24 h at 33°C with 5% CO_2.
8. Aspirate media and replace with low serum (0.5% FBS) media for 16-18 h at 33°C with 5% CO_2.
9. Bring cells to the Image Analysis Lab and place in the incubator.
10. Take 1 dish and wash 2X with plain Leibowitz media (without phenol red) to remove all phenol red. Add a final volume of 1 mL to the dish.
11. Additionally, in a 1.5 mL epi-tube, add 247 µL of Leibowitz plus 3 µL stock EGF for a final concentration of 25 ng/mL EGF.
12. Take dish and set it on the microscope.

13. Focus on a cell. The light angle works best from the right. Begin by using a critical angle of approximately 72-73. The best angle will result in even illumination of the cell.
14. Set the software to acquire an image every 5 seconds. Make sure to turn on the perfect focus.
15. All acquisition of ~5 images and then add the 250 µL Leibowitz + EGF to the dish. BE EXTREMELY CAREFUL while adding. Do not touch the dish at all or it will ruin the acquisition process.
16. Allow the software to continue capturing images every 5 seconds for up to 10 minutes.

Analysis:

1. Using Image J (free NIH software), File – Import – Image Sequence – Choose sequence you wish to analyze.
2. Once the image sequence has been imported, go to Image – Stacks – Plot Z-axis profile. This will give you a graph of the mean intensity for each of the time points as well as a table with the area and min, max, and mean intensity.
3. In Excel, input the initial mean intensity and the mean intensity of the time point with the highest mean intensity (peak of Grb2 recruitment to the plasma membrane).
4. Calculate the change in intensity.
5. Analyze the mean change in intensity per treatment group (Control (untreated), DHA, or LA). Graph in excel using the mean for each treatment and the standard error of the mean (SEM).
6. Perform statistical analysis using SPSS and a one-way ANOVA. Check for normality and equality of variance.

APPENDIX M

RAS ACTIVATION ASSAY

Purpose: To assess EGF-stimulated activation of Ras

Materials:

RPMI 1640 (Mediatech # 15040CV) *complete and serum starvation*:

Complete: To a 500 mL bottle, add 532 µL ITS Premix (BD Biosciences #354351), 26.6 mL fetal bovine serum (FBS, Hyclone SH30070.01), and 5.3 mL Glutamax (Gibco 35050). Immediately prior to use, add 1 µL IFNγ (Gibco #13284-021) per 10 mL complete media.

Serum starvation: Immediately prior to use, to plain unsupplemented RPMI 1640 add FBS to a final concentration of 0.5%. Also add 1 µL IFNγ (Gibco #13284-021) per 10 mL complete media

Ice cold PBS (Gibco #14190)

Ras activation assay kit (Pierce #16117)

EGF (Sigma #E1257)

Antibodies: pan-Ras (comes with kit), H-Ras (Santa Cruz #sc-520), K-Ras (Santa Cruz # sc-521), N-Ras (Santa Cruz #sc-519)

Procedure:

Cell treatment

1. Seed YAMC cells into 12 of 150-mm sterile plastic dishes in 17 mL complete media. Incubate cells O/N at 33°C with 5% CO_2.
2. Aspirate media and replace with complete media (control) or complete media with 50 µM BSA-complexed fatty acids (LA or DHA). Stock fatty acid is 2.5 mm, so add 340 µL stock fatty acid to 16.66 mL media. Use 4 dishes per treatment. Incubate cells O/N at 33°C with 5% CO_2.
3. Replace media with fresh media containing the same treatments after ~24 h and continue incubation.
4. After ~54-56 h of treatment, aspirate complete media from the dishes, wash 1X with PBS, and add serum-starvation media containing the same treatments as above. Incubate cells for 16-18 h at 33°C with 5% CO_2.

Harvest

5. Prepare 5 mL lysis buffer (LB) from kit by adding sodium orthovanadate and protease inhibitor cocktail. Keep on ice.
6. For each treatment, leave 1 plate unstimulated and stimulate 3 plates with 25 ng/mL EGF for 2 min at 33°C with 5% CO_2.
7. Wash plates 3X with ice-cold PBS.

8. Add 300 µL LB per plate and scrape the plate with a rubber policeman.
9. Place cells + LB into a 1.5 mL epi-tube on ice and shear cells using a 29 G-needle.
10. Incubate on ice for 30 minutes. Clarify lysates by spinning at 16,000xg for 20 minutes at 4°C.
11. Collect the supernatant into a new epi-tube and discard the pellet.
12. Measure the protein concentration using a Coomassie assay.
13. Aliquot the lysates and store at -80°C.

Immunoprecipitation

Perform Ras IP by following the manufacturer's instructions:

1. Set up and label a spin cup in a collection tube for each sample.
2. Thaw 500 µg of lysate from each sample. Bring all samples to the same final volume (must be less than 700 µL)
3. Swirl the bottle of Glutathione Resin to thoroughly resuspend the agarose beads. Add 100 µL of the 50% resin slurry to the spin cup with collection tube. Centrifuge the tubes at 6,000x*g* at 4°C for 30 seconds.
4. Discard the flow-through. Add 400µL of Lysis/Binding/Wash Buffer to each tube with resin. Invert the tubes gently several times. Centrifuge the tubes at 6,000x*g* for 30 seconds at 4°C. Discard the flow-through.
5. Thaw the GST-Raf1-RBD on ice and immediately make 80 µg aliquots. Store aliquots for later use at -70°C.
6. Add 80 µg of GST-Raf1-RBD to each spin cup containing the glutathione resin.
7. Immediately transfer up to 700 µL of the cell lysate (containing 500 µg of total proteins) to the spin cup.
8. Seal cap of the collection tube with parafilm to prevent leakage, which may result from the presence of detergent in the lysate, and vortex the sample.
9. Incubate the reaction mixture on a tube rotator at 4°C for 1 hour.
10. Centrifuge the spin cup with collection tube at 6,000x*g* for 30 seconds.
11. Remove the laboratory film and transfer the spin cup to a new collection tube. Keep the flow throw and store at -80°C
12. Wash resin by adding 400 µL of Lysis/Binding/Wash Buffer. Invert the tube three times, and centrifuge at 6,000x*g* for 30 seconds. Remove the spin cup and decant the buffer from the collection tube. Replace the spin cup in the tube and repeat this wash step two additional times.
13. Transfer the spin cup to a new collection tube.
14. Prepare 50µL of elution buffer by diluting stock 5X pyronin to 2X using ddH_2O.
15. Add 50 µL 2X elution buffer to the resin. Vortex the sample and incubate at room temperature for 2 minutes.
16. Centrifuge the tube at 6,000x*g* for 2 minutes. Remove and discard the spin cup containing the resin.
17. Heat the eluted samples for 5 minutes at 98°C.
18. Samples may be electrophoresed on a gel or stored at -80°C until use.

19. Apply 25 μL per lane for a 10x10cm mini-gel (4-20% Tris-Glycine gel).
20. Perform western blotting to determine activation of pan-Ras, H-Ras, N-Ras, and K-Ras.

APPENDIX N

BIOTINYLATION

Purpose: To determine cell surface localization and internalization of EGFR

Hypothesis: EGF stimulation will lead to increased EGFR internalization. DHA may alter EGFR internalization due to its effects on EGFR localization and activation.

Reference: Vassilieva EV, et al. Am J Physiol Gastrointest Liver Physiol. 2008;295(5)G965-76.

Materials:
EZ-Link Sulfo-NHS-SS-Biotin (Pierce # 21331)
NUNC Immobilizer Streptavidin C8 ELISA plates (Thermo Scientific #436022)
Reducing buffer: 100 mM sodium-2-mercaptoethane sulfonate (MESNA; Sigma #M1511-5G), 50 mM Tris (pH 8.6), 100 mM NaCl, 1 mM EDTA, and 0.2% BSA
RIPA buffer: 20 mM Tris, 150 mM NaCl, 2 mM EDTA, 2 mM EGTA, 1% sodium deoxycholate, 1% SDS, and 1% Triton X-100, protease inhibitor cocktail (Sigma #P8340) (1:25 dilution), and 100 µM sodium orthovanadate
Iodoacetamide (Sigma #I1149)
PBS
EGF (Sigma #E 1257)
Anti-EGFR antibody (Santa Cruz #sc-03)
Goat anti-rabbit IgG HRP (KPL #074-1506)
TMB High Sensitivity Substrate Solution (Biolegend #421501)

Procedure:
1. Seed YAMC cells into 150 mm dishes. Allow to grow to ~ 80% confluence. Culture at 33°C at 5% CO_2.
2. Prepare EZ-Link Sulfo-NHS-SS-Biotin (Pierce # 21331)(0.5 mg/ml) dissolved in PBS.
3. Wash cells 2X with ice cold PBS.
4. Treat cells with 5 mL biotin for 30 min on ice (leave 1 plate w/o biotin as a control). Make sure that the biotin solution completely covers the surface of the plate. Make sure the plate is flat on the ice and the biotin solution does not collect in one side of the plate.
5. Wash cells 3X with ice cold PBS.
6. Replace PBS with 15 mL warm, serum-free media supplemented with 25 ng/mL EGF for 10 min (leave 2 plates unstimulated).

7. Cleave biotin remaining on cell surface by washing 3X for 20 min with 5 mL reducing buffer containing reducing agent (100 mM MESNA Sigma #M1511-5G) at 4°C. Make sure the entire plate surface is covered with buffer.
8. Rinse cells 2X with PBS.
9. Quench excess biotin with 60 mM iodoacetamide (Sigma #I1149) in PBS for 5 min at 4°C
10. Wash plates 3X with PBS. Add 300 µL of RIPA buffer to each plate. Use a cell scraper to scrape the entire plate. Collect the cells and buffer into an epi-tube. Shear cells using a 29 G needle. Incubate on ice for 30 minutes.
11. Clarify lysate by centrifugation at 14000xg for 20 min at 4°C. Place supernatant (cell lysate) into a new tube, aliquot, and store at -80°C until ready to process.
12. Measure protein concentration using Bradford Protein Assay.
    RIPA buffer is not compatible with Coomassie Protein Plus Assay.
13. Dilute samples to be used to 10 µg/mL using PBS containing 0.5% Tween 20 (pH 7.3).
14. Capture biotinylated EGFR using 96-well NUNC Immobilizer Streptavidin C8 ELISA plates (Thermo Scientific #436022) by incubating 200 µL of diluted cell lysates per well.
15. Place 1 µL RIPA buffer into 200 µL PBS containing 0.5% Tween 20 (pH 7.3) as a background well. Additionally, use cell lysate from unbiotinylated sample as an additional control.
16. A relative standard curve can be generated by incubating 0.5, 0.75, 1, 2, 3, 4, 5 µg of any sample into 7 wells. *Choose any sample to create the standard curve. If multiple plates are being run at the same time, use the same sample to create the standard curve on all plates.*
17. Wash plate 3X with PBST (0.5% Tween 20).
18. Incubate with 100 µL anti-EGFR antibody (1:20 dilution in PBST) at 200 RPM on plate shaker for 2 h at RT.
19. Wash 3X with PBST.
20. Incubate with 100 µL HRP-conjugated secondary ab (1:250 dilution in PBST) at 200 RPM on plate shaker for 1 h at RT.
21. Wash plate 3X with PBST.
22. Add 100 µL TMB substrate and allow to develop for 10 min.
23. Stop color development by adding 100 µL of 4 M H_2SO_4.
24. Analyze on SpectraMax with wavelength set at 450 nm.

APPENDIX O

EXTENSIVE WOUNDING OF YAMC

Purpose: To stimulate signaling in YAMC by injury

Materials:

RPMI 1640 (Mediatech # 15040CV) *complete and serum starvation*:

Complete: To a 500 mL bottle, add 532 µL ITS Premix (BD Biosciences #354351), 26.6 mL fetal bovine serum (FBS, Hyclone SH30070.01), and 5.3 mL Glutamax (Gibco 35050). Immediately prior to use, add 1 µL IFNγ (Gibco #13284-021) per 10 mL complete media.

Serum starvation: Immediately prior to use, to plain unsupplemented RPMI 1640 add FBS to a final concentration of 0.5%. Also add 1 µL IFNγ (Gibco #13284-021) per 10 mL complete media.

Procedure:

1. Culture YAMC cells in 150 mm dishes in complete media (plus any treatment) at 33°C and 5% CO_2 until they become ~95% confluent.
2. Aspirate complete media and wash cells 2X with PBS.
3. Add serum starvation (0.5% FBS) media and incubate overnight (16-18 h) at 33°C and 5% CO_2.
4. Using a p-1000 pipette tip, as quickly as possible, scratch the cell monolayer in 25 vertical lines progressively from left to right. Turn the dish 45 degrees, and repeat scratching in the same way. Repeat the turn and scratch process 2 more times until the dish has been scratched a total of 100 times in 4 directions. The entire process should take less than 1 minute.
5. Incubate cells 33°C and 5% CO_2 for 2 minutes.
6. Aspirate media from the cells and wash with ice-cold PBS 3 times.
7. Harvest cell lysates according to the Total Cell Lysate Isolation protocol.

APPENDIX P

SCRATCH ASSAY

Purpose: To observe wound healing following a scratch wound of YAMC

Materials:

35 mm dishes with glass bottom (Glass bottom dishes #P35G-1.5-20-C)
EGF (Sigma #E 1257)
RPMI 1640 (Mediatech # 15040CV) *complete and serum starvation*:

Complete: To a 500 mL bottle, add 532 µL ITS Premix (BD Biosciences #354351), 26.6 mL fetal bovine serum (FBS, Hyclone SH30070.01), and 5.3 mL Glutamax (Gibco 35050). Immediately prior to use, add 1 µL IFNγ (Gibco #13284-021) per 10 mL complete media.

Serum starvation: Immediately prior to use, to plain unsupplemented RPMI 1640 add FBS to a final concentration of 0.5%. Also add 1 µL IFNγ (Gibco #13284-021) per 10 mL complete media.

Procedure:

1. Culture YAMC cells in 4 of T-75 flasks. Treat for 48 h with 50 µM DHA, LA, EPA or control (no fatty acid). Change media after 24 h. Incubate at 33°C and 5% CO_2.
2. After 48 h of treatment, trypsinize cells in each flask, spin down, and resuspend. Count cells using a hemocytometer.
3. Seed cells into 35 mm dishes at a density of ~100K cells/dish.
4. Incubate in complete media supplemented with the same treatment for ~8 h at 33°C and 5% CO_2.
5. Replace the media with serum starvation (0.5% FBS) media supplemented with the same treatment as above. Incubate for 16 h at 33°C and 5% CO_2.
6. On the morning of the scratch assay, turn on the microscope. Set up the incubation chamber on the scope with the insert for 35 mm dishes, and set the temperature to 33°C and 5% CO_2.
7. Following serum starvation, use a sterile p-200 pipette tip to scratch the monolayer of cells in each dish in a straight line down the center. On the bottom of the dish, mark the ends of the scratch with a sharpie so you know where the scratch was made. Make sure to use a new tip for each well. Try to make the scratch as straight as possible. Also, do not scratch too hard or it will scratch the dish.
8. Wash each dish 1X with PBS, then add 1 mL plain, unsupplemented media (with IFN-γ) treated with the same fatty acid treatment as before plus 25 ng/mL EGF (stock is 10 ng/µL).
9. Immediately place on the microscope, and open NIS elements. Try to orient the dish so that the scratch runs either vertically or horizontally (not on an angle).

10. Set the time-lapse to take an image every 15 minutes for 48 h.
11. Use the 10X phase objective, and turn on the PFS (perfect focus system).
12. Using the "live" image, find the end of the scratch. Use the PFS to focus on the spot, and then on the multipoint analysis, set this to be position #1. This will remember the x-y location as well as the z.
13. Repeat this for multiple positions within the scratch of the first dish. Then continue to the next dish and repeat the same process. The insert can hold up to 4 dishes.
14. Once you have chosen all of fields of interest, hit "Run".
15. The computer will acquire images.
16. To analyze the image, at time 0 (first time-point), use the polygon tool to determine the size of the wounded area. Then, at the 12 and 24 h time points, count the number of cells that have migrated into the wounded area.
17. Graph the cells/mm wounded area. Try to choose areas that are approximately the same width (i.e. the initial wounded gap is the same distance). This will make comparisons more accurate. Also, try to use areas that did not have very much cell debris following wounding.

APPENDIX Q

TRANSWELL MIGRATION ASSAY

Purpose: To assess migration of YAMC cells in response to EGF

Materials:

QCM 24-well colorimetric cell migration assay (Millipore #ECM 508)
EGF (Sigma # E1257)
RPMI 1640 (Mediatech # 15040CV) *complete and serum starvation*:

Complete: To a 500 mL bottle, add 532 µL ITS Premix (BD Biosciences #354351), 26.6 mL fetal bovine serum (FBS, Hyclone SH30070.01), and 5.3 mL Glutamax (Gibco 35050). Immediately prior to use, add 1 µL IFNγ (Gibco #13284-021) per 10 mL complete media.

Serum starvation: Immediately prior to use, to plain unsupplemented RPMI 1640 add FBS to a final concentration of 0.5%. Also add 1 µL IFNγ (Gibco #13284-021) per 10 mL complete media

Procedure:

1. Grow cells until ~80% confluent in a T-75 flask.
2. Starve cells by incubating 16-18 hours prior to assay in serum starvation (0.5% FBS) media with IFN-γ.
3. For optimal results, bring plates and reagents to room temperature (23-25°C) prior to initiating assay. Sterilize forceps (provided with kit) with 70% ethanol and handle inserts with forceps.
4. Following starvation, wash cells with PBS then trypsinize for 5 minutes.
5. Neutralize the trypsin with complete RPMI 1640 and immediately spin down at 200 x g for 5 min.
6. Aspirate the media/trypsin and resuspend cells in 1 mL of serum free media with IFN-γ.
7. Count cells using a hemocytometer. Make the final concentration of cells to ~1 x 10^6 cells/mL.
8. Add 300 mL of prepared cell suspension to each insert supplied in the kit.
9. Add 500 mL of serum free media with 25 ng/mL EGF to the lower chamber.
10. Ensure the bottom of the insert membrane contacts the media. Air may get trapped at the interface.
11. Cover plate and incubate for 12-24 hours at 33°C and 5% CO_2.
12. Carefully remove the cells/media from the top side of the insert by pipetting out the remaining cell suspension, and place the migration insert into a clean well containing 400 µL of Cell Stain. Incubate for 20 minutes at room temperature.
13. Dip insert into a beaker of water several times to rinse.
14. While the insert is still moist, use a cotton-tipped swab (provided with kit) to gently remove non-migratory cells layer from the interior of the insert. Take care

not to puncture the polycarbonate membrane. Be sure to remove all cells on the inside perimeter, as any remaining cells inside the insert will contribute to background staining. Repeat procedure with a second, clean cotton-tipped swab.

15. Allow insert to air dry.
16. Transfer the stained insert to a clean well containing 200 µL of Extraction Buffer for 15 minutes at room temperature. Extract the stain from the underside by gently tilting the insert back and forth several times during incubation. Remove the insert from the well.

    Note: Alternatively, cells can be counted manually through a microscope.
17. Transfer 100 µL of the dye mixture to a 96-well microtiter plate suitable for colorimetric measurement.
18. Measure the Optical Density at 560 nm.